TECHNISCHE UNIVERSITÄT MÜNCHEN

Wissenschaftszentrum Weihenstephan für Ernährung, Landnutzung und Umwelt

Lehrstuhl für biochemische Pflanzenpathologie

NO-induced modulation of chromatin structure: S-nitrosothiols affect light-dependent histone acetylation

Alexandra Ageeva-Kieferle

Vollständiger Abdruck der von der Fakultät Wissenschaftszentrum Weihenstephan für Ernährung, Landnutzung und Umwelt der Technischen Universität München zur Erlangung des akademischen Grades eines

Doktors der Naturwissenschaften

genehmigten Dissertation.

Vorsitzender:	Prof. Dr. Aurélien Tellier
Prüfer der Dissertation:	1. Prof. Dr. Jörg Durner
	2. Prof. Dr. Frank Johannes

Die Dissertation wurde am 24.06.2019 bei der Technischen Universität München eingereicht und durch die Fakultät Wissenschaftszentrum Weihenstephan für Ernährung, Landnutzung und Umwelt am 06.10.2019 angenommen.

Publications and Talks

Parts of this thesis were published in:

Ageeva-Kieferle A., Rudolf E., Lindermayr C. Redox-dependent chromatin remodeling: A new function of nitric oxide as architect of chromatin structure in plants. Frontiers Plant Science accepted 2019 Apr.

Mengel A, **Ageeva A**, Georgii E, Bernhardt J, Wu K, Durner J, Lindermayr C. *Nitric oxide modulates histone acetylation at stress genes by inhibition of histone deacetylases*. Plant Physiology 2017 Feb, Volume 173 (2), Pages 1434-1452.

Kovacs I, **Ageeva A**, Konig E, Lindermayr C. *S-Nitrosylation of Nuclear Proteins: New Pathways in Regulation of Gene Expression*. Advances in Botanical Research 2016. Volume 77, Pages 15–39.

Ageeva-Kieferle, A. *Effect of nitric oxide on histone acetylation in Arabidopsis thaliana*. Poster and brief talk at the International Meeting Botanikertagung in Kiel, Germany, 2017.

Ageeva, A. *Effect of nitric oxide on histone acetylation in Arabidopsis thaliana.* Talk at the 6th Plant Nitric Oxide International Meeting in Granada, Spain, 2016.

Table of Contents

PUBLICATIONS AND TALKS I
TABLE OF CONTENTS II
ABBREVIATIONS IV
LIST OF FIGURES AND TABLES VI
SUMMARY IX
1 INTRODUCTION 1

1.1 Nitric oxide signaling in plants 1
1.1.1 Physicochemical properties of NO 1
1.1.2 NO generation in plants 3
1.1.3 Physiological functions of NO 6
1.1.4 NO mode of action 7
1.1.5 Regulation of gene expression by NO 9

1.2 Aim of this study 17

2 RESULTS 19

2.1 Effect of NO on chromatin remodeling 19
2.1.1 Tendency towards induced histone acetylation by exogenously applied NO 19
2.1.2 Tendency towards enhanced histone acetylation by endogenously produced NO 25
2.1.3 Correlation between histone acetylation and gene expression 27
2.1.4 NO-dependent modulation of chromatin structure 28

2.2 Interaction between NO and light/temperature 33
2.2.1 Effect of enhanced endogenous SNO/NO on photosynthetic apparatus 33
2.2.2 Light-dependent production of NO 34
2.2.3 Tendency towards light/NO-induced histone acetylation 38
2.2.4 Light/NO-dependent histone acetylation and expression of photosynthesis related genes 41
2.2.5 Light/NO-dependent H3K9 acetylation of photosynthesis-related genes 44

3 DISCUSSION 53

3.1 NO-dependent histone acetylation 53
3.1.1 Redox-regulation of HDA6 55

3.2 NO regulates gene transcription via modulation of chromatin structure 58
3.3 Function of NO in photosynthesis 59
3.3.1 Effect of light on NO production 61

3.3.2 Light-induced SNOs formation seems to affect histone acetylation 62

4 OUTLOOK 69

5 MATERIAL AND METHODS 71

5.1 Materials 71

5.1.1 Plant Material and Soil 71

5.1.2 Bacterial strains 71

5.1.3 Plasmids and vectors 72

5.1.4 Primer 73

5.1.5 Chemicals 75

5.1.6 Enzymes 75

5.1.7 Antibiotics 76

5.1.8 Antibodies 76

5.1.9 Solutions and media 77

5.1.10 Kits 81

5.1.11 Other working materials 81

5.2 Methods 83

5.2.1 Plant cultivation 83

5.2.2 Molecular biology techniques 83

5.2.3 Generation of transgenic lines 87

5.2.4 Protein methodologies 88

5.2.5 Recombinant expression and purification 90

5.2.6 Measurement of HDA activity 91

5.2.7 NO measurements 91

5.2.8 LC-MS/MS 92

5.2.9 Chromatin immunoprecipitation followed by qPCR (ChIP-qPCR) or deep sequencing (ChIP-seq) 94

5.2.10 Programs and databases 97

6 LITERATURE 99

7 SUPPLEMENT 115

ACKNOWLEDGEMENTS 126

Abbreviations

ANOVA	Analysis of variance
ChIP	Chromatin immunoprecipitation
ChIP-qPCR	Chromatin immunoprecipitation followed by quantitative PCR
ChIP-seq	Chromatin immunoprecipitation followed by deep-sequencing
cPTIO	2-(4-Carboxyphenyl)-4,4,5,5-tetramethylimidazoline-1-oxyl-3-oxide
Cys	Cysteine
DF	Degree of freedom
DMSO	Dimethylsulfoxide
DNA	Deoxyribonucleic acid
DTT	Dithiothreitol
EDTA	Ethylenediaminetetraacetic acid
Flg22	Flagellin 22
GSH	Glutathione
GSNO	S-Nitrosoglutathione
H1,2,3,4	Histone 1, 2, 3, 4
H3K9ac	Histone 3 lysine 9 acetylation
HAT	Histone acetyltransferase
HDA	Histone deacetylase
HDT	Plant specific histone deacetylase family
INA	2, 6-Dichloro-isonicotinic acid
ko	knock-out
LC-MS/MS	Liquid chromatography coupled to mass spectrometry
MES	2-(N-morpholino)ethanesulfonic acid
mRNA	Messenger ribonucleic acid
MS-medium	Murashige-Skoog medium
NADPH	Nicotinamide adenine dinucleotide phosphate
NO	Nitric oxide
NOS	Nitric oxide synthase
NR	Nitrate reductase
NRBT	Nuclei resuspension buffer with Triton-X100
N-terminal	Amino-terminal
PAGE	Polyacrylamide gel electrophoresis
PBS	Phosphate buffered saline
PCR	Polymerase chain reaction
PR-gene	Pathogenesis related gene

PS I	Photosystem I
PS II	Photosystem II
PTM	Posttranslational modification
qPCR	Real time quantitative PCR
RNS	Reactive nitrogen species
ROS	Reactive oxygen species
RPD3-like	Reduced potassium deficiency 3 like
SA	Salicylic acid
SDS	Sodium dodecyl sulfate
SE	Standard error of the mean
SNAP	S-Nitroso-N-acetylpenicillamine
SNO	S-Nitrosothiol
TSA	Trichostatin A
wt	Wild type

List of Figures and Tables

Figures

Figure 1: Formation of NO intermediates and transduction of their biochemistry 2
Figure 2: Overview of NO biosynthesis in plants 4
Figure 3: NO-mediated gene expression. 11
Figure 4: Epigenetic modifications of chromatin structure 14
Figure 5: No changes in global protein acetylation level after GSNO and INA treatment in wt suspension cells. 19
Figure 6: Enhanced H3 acetylation in wt suspension cells after GSNO and TSA treatment 20
Figure 7: Mass spectrometry workflow 21
Figure 8: LC-MS/MS analysis revealed a slight but not significant increase of H3 and H4 acetylation level after GSNO treatment in seedlings 22
Figure 9: Treatment of seedlings with GSNO and TSA results in a triple acetylation motif on H4. 23
Figure 10: GSNO and TSA treatments of *Arabidopsis* seedlings result in H3 and H4 acetylation. 25
Figure 11: Treatment of *Arabidopsis* seedlings with INA might stimulate H3 and H4 acetylation 26
Figure 12: GSNO-altered H3K9/14ac of some genes does not necessarily lead their gene expression. 28
Figure 13: GSNO and GSH treatments do not change transcriptional level of HDAs 29
Figure 14: *Arabidopsis thaliana* HDA6 and HDA19 show a high amino acid sequence homology to mouse HDA2 30
Figure 15: *Arabidopsis thaliana* HDA6 and HDA19 demonstrate a similar protein folding as mouse HDA2. 30
Figure 16: GSNO and TSA treatments do not induce H3 acetylation in *hda6* suspension cells 31
Figure 17: GSNO inhibits an activity of recombinant 35S:Flag-HDA6. 32
Figure 18: SNOs seems to induce changes in some photosynthetic parameters 34
Figure 19: NO emission and SNO content of 4 weeks old plants in light and dark conditions 35
Figure 20: Enhanced light intensity induces NO emission of 4-weeks old plants 36
Figure 21: Different light and temperature conditions induce changes in S-nitrosothiol and nitrite concentration of *Arabidopsis* plants 37
Figure 22: Different light conditions lead to altered H3 acetylation in wild type and *hot5-2* plants. 39
Figure 23: Different light and temperature conditions induce changes in H3 acetylation of *Arabidopsis* wt, *hda6* and *hda19* knockout mutant plants 40
Figure 24: Light leads to a slight increase in H3K9/14 acetylation of some photosynthesis-related genes. 42
Figure 25: Different light and temperature conditions change transcriptional level of photosynthesis-related genes 43
Figure 26: H3K9ac is located along chromosome arms in *Arabidopsis* genome. 45
Figure 27: Genomic distribution of H3K9ac among *Arabidopsis* genome 46
Figure 28: H3K9ac depends on light and dark condition 47
Figure 29: H3K9ac level dependent on genotype 48
Figure 30: Step-wise induction of peaks at chloroplast genes. 49
Figure 31: Chloroplast genes are enriched in H3K9ac 50
Figure 32: A possible NO mode of action in regulating histone acetylation. 56
Figure 33: Schematic presentation of NO binding sites in photosynthetic apparatus. 60
Figure 34: A model of NO regulation of photosynthetic machinery 69

Tables

Table 1: NO-induced hyperacetylation and upregulation of photosynthesis-related genes 33
Table 2: List of selected significantly changed H3K9ac sites identified in both mutants 52
Table 3: Plant Material 71
Table 4: Cell lines 71
Table 5: Bacteria strains 72
Table 6: Plasmids used for Gateway® cloning 72
Table 7: Vectors 73
Table 8: Primer used for cloning and mutagenesis 73
Table 9: Primer used for sequencing 73
Table 10: Primer used for qPCR 74
Table 11: Selected chemicals 75
Table 12: Enzymes 75
Table 13: Antibiotic selection of bacteria 76
Table 14: Antibodies 76
Table 15: Media used for plant cultivation 77
Table 16: Media used for bacterial cultivation 77
Table 17: Buffer for nucleic acid agarose gel 77
Table 18: Glycin-SDS-Polyacrylamidgelelektrophoresis 77
Table 19: 2 x Glycin-SDS gel 78
Table 20: Buffers for transfer and immunodetection of proteins (Western Blot) 78
Table 21: Buffers for protein staining 78
Table 22: Buffers for plant transformation 79
Table 23: Buffers for protein extraction 79
Table 24: Buffers for HDA activity assay 80
Table 25: Buffers for chromatin immunoprecipitation 80
Table 26: Applied Kits 81
Table 27:Working materials 81
Table 28: Devices and accessories 82
Table 29:Cycler program for qPCR 84
Table 30: Cycler program for site mutation 85
Table 31: Cycler program for ChIP-qPCR 97

Supplemental Figures

Supplemental Figure 1: Possible acetylation motifs at H3 and H4 115
Supplemental Figure 2: 35S:Flag-HDA6 transgenic line 116
Supplemental Figure 3: Immunoblot analysis of acetylated H3 and H4 in 4 weeks old plants and 7 days old seedlings 116
Supplemental Figure 4: Shearing efficiency of leaves chromatin using Bioruptor® Pico 117
Supplemental Figure 5: Shearing efficiency of leaves chromatin using Covaris E220 evolution 117
Supplemental Figure 6: Transcriptional level of photosynthesis related genes within a day. 118
Supplemental Figure 7: Phenotype of *hda6* mutant plants (53 days after sowing). 118
Supplemental Figure 8: Quality of ChIP-seq samples 119
Supplemental Figure 9: GO enrichment analysis of H3K9 hyperacetylated loci depending on the condition effect. 120
Supplemental Figure 10:GO enrichment analysis of H3K9 hyperacetylated loci depending on the genotyping effect. 121

Supplemental Tables

Supplemental Table 1: Alignment of ChIP-seq results. 119
Supplemental Table 2: List of significantly H3K9 hyperacetylated sites associated with chloroplast. 122

Summary

Nitric oxide (NO) is a small gaseous molecule with a wide range of functions. Due to its highly reactive nature and rich chemistry, it is categorized as a signaling molecule, which is involved in varies physiological processes in human and animals. Loss of its functions is considered as one of the earliest indicators of disease. In plants NO plays an important role in response to biotic and abiotic stress. S-Nitrosylation was identified as a possible mechanism which describes how NO might contribute to plant development and stress-related responses. In this context, it was investigated whether and how NO might be involved in regulation of histone acetylation and which physiological meaning this process has in *A. thaliana*.

An LC-MS/MS analysis in combination with an immunoblotting approach revealed that treatment of *Arabidopsis* seedlings with a physiological NO donor (GSNO) demonstrate a trend of induced histone 3 and 4 acetylation. Treatment of seedlings with a 2,6-Dichloro-isonicotinic acid (INA), which is known to induce endogenous NO production, also resulted in a tendency towards enhanced histone acetylation. Moreover, it was found that the NO-dependent modulation of chromatin structure is mainly based on the inhibition of HDAs activity rather than on the transcriptional regulation of these proteins by NO. Furthermore, a comparative analysis of S-nitrosylated mammalian HDA2 with plants HDAs identified *Arabidopsis'* HDA6 and HDA19 as the main candidates to be redox-regulated. Indeed, a recombinant HDA6 was demonstrated to be sensitive to NO and partially lost its activity upon GSNO treatment. Aside from this, no changes in histone 3 acetylation were observed in GSNO-treated *hda6* cell culture, while a significant increase in histone 3 acetylation was detected in a wild type suspension culture.

Additionally, a strong correlation between light-induced NO production and light-induced histone acetylation supports the hypothesis that NO might control histone acetylation and therefore regulate gene transcription in a light-dependent manner. Using ChIP-seq analyses, changes in H3K9ac were observed between plants transferred to the dark and those exposed to light. An overlap of hundreds of genes was found hyperacetylated in both mutants, *hda6* and *hot5-2*, under dark and light conditions, indicating that these loci might be regulated by NO-induced inhibition of HDA6 activity. Moreover, a potential role of NO in the regulation of the photosynthetic processes was identified in this study.

In summary, this study suggests a new role of NO in the regulation of chromatin structure, probably related to the direct inhibition of HDAs activity. Evidence was found indicating that NO may participate in the photosynthetic performance and the assembly of photosynthetic complexes through the regulation of histone acetylation of some of its subunits.

1 Introduction

1.1 Nitric oxide signaling in plants

At least six gaseous molecules have been identified as intra- and intercellular messengers with similar functions across almost every kingdom. They can be endogenously produced and influence cellular processes. Four of these molecules (excluding oxygen and carbon dioxide) have attracted the attention of many researchers, who extol them as being true signaling messengers. These are ethylene (C_2H_4), carbon monoxide (CO), hydrogen sulfide (H_2S) and nitric oxide (NO) [1].

NO seems to possess the greatest potential as a signaling molecule, with more than 22,000 articles being published on the subject by the end of 2016 [2]. NO first rose to prevalence in 1979, when it was demonstrated that it has an important role in relaxation of vascular smooth muscles [3]. Later, in 1987 NO was identified as having an important role in regulating blood pressure and relieving heart conditions. By 1992, Science magazine had pronounced NO as "molecule of the year", and in 1998, it received worldwide recognition, when three scientists, Robert F. Fuschgott, Louis J. Ignarro and Ferid Murad, obtained the Nobel Prize in Physiology and Medicine by demonstrating the signaling properties of this gaseous molecule [4][1].

NO is a very ancient molecule that seems to have been preserved over millions of years of evolution [5]. It is essential for many biological processes throughout entire organisms. However, the chemistry of NO is highly diverse, making it challenging to identify its molecular function within a single cell.

1.1.1 Physicochemical properties of NO

NO is a heteronuclear diatomic molecule, with one unpaired electron on the nitrogen atom. The half-life of NO is in the order of 3-5 seconds in biological systems, which is extremely short in relation to other signaling molecules. On the other hand, when compared to many other free radicals which life-span averages often only several milliseconds, this is a relatively long time. NO exhibits hydrophobic characteristics and therefore can easily diffuse and accumulate in the lipid phase of the membranes [6][4][7].

In the presence of oxygen, NO can form other oxides, such as nitrogen dioxide (NO_2), dinitrogen trioxide (N_2O_3), and dinitrogen tetroxide (N_2O_4), that can undergo further reactions

with cellular amines or thiols. These nitrogen species can also be hydrolyzed to the main products of NO metabolism: nitrate (NO_3^-) and nitrite (NO_2^-) [8].

NO can rapidly react with superoxide ($O_2\cdot^-$) to form a highly reactive species, peroxynitrite ($ONOO^-$). Although it is unstable under physiological pH, ONOO- can still move considerable distances within a cell and further react with proteins, lipids, carbohydrates and DNA, inducing serious damage of a cell's structure [9][10].

Loss of one of the unpaired electrons of NO results in the formation of a nitrosonium cation (NO^+), while a one - electron reduction of NO leads to the production of a nitroxyl radical (NO^-) that was identified as a potential agent for the treatment of cardiovascular diseases [11]. An overview of NO intermediates is illustrated in **Figure 1A**.

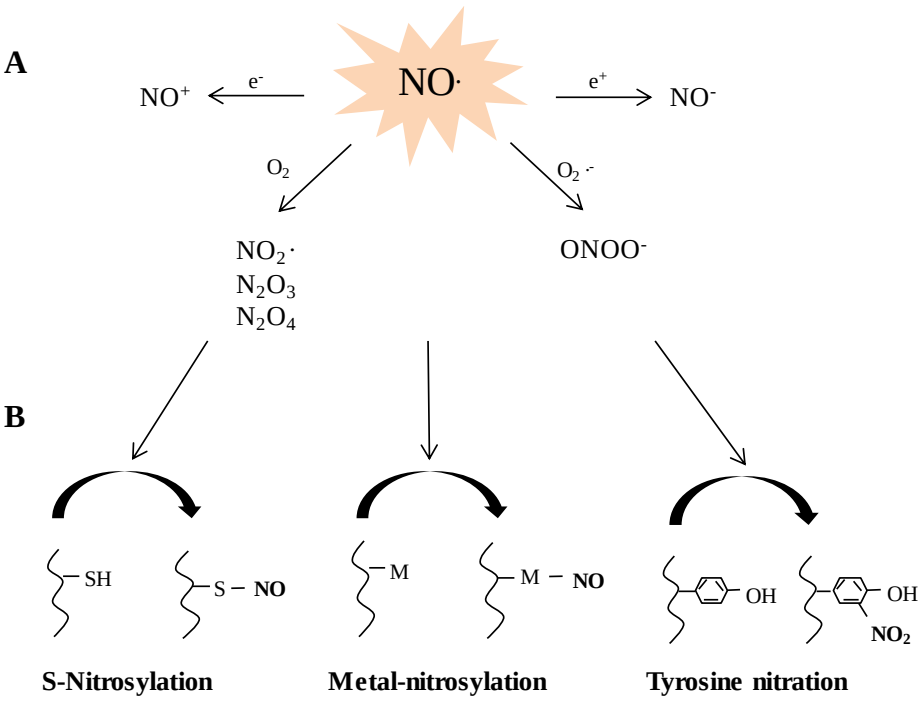

Figure 1: Formation of NO intermediates and transduction of their biochemistry.
Modified from [12]. When exposed to oxygen NO may form nitrogen dioxide (NO_2), dinitrogen trioxide (N_2O_3) and dinitrogen tetroxide (N_2O_4). Peroxynitrite ($ONOO^-$) occurs through the reaction of superoxide ($O2^-$) with NO. Nitroxyl anion (NO^-) is a one-electron reduction product, whereas nitrosonium cation (NO^+) results from oxidation of NO. B) Posttranslational protein modifications by NO in a living cell. Binding of NO to a cysteine residue of proteins results in the reversible formation of S-nitrosothiol and can promote or inhibit the formation of disulfide bonds within neighboring thiols. NO can react with transition metals. The covalent interaction of NO with the centers of iron sulfur clusters, heme, and zinc-finger proteins (M) leads to the formation of nitrosylated metalloproteins (M-NO). Tyrosine nitration is mediated by a NO-derived specie, peroxynitrite (ONOO–). Nitration occurs in one of the two equivalent carbons in the aromatic ring of Tyr residues, which results in the formation of 3-nitrotyrosine residues (3-NO2-Tyr).

Moreover, NO and its intermediates react with cellular nucleophiles, e.g. cysteines' thiols and the phenolic ring of tyrosine (**Figure 1B**). Through the oxidation of these two compounds

nitrosothiols (R-S-N=O) and nitrotyrosines ($R\text{-}NO_2$) are generated, respectively [13]. The formation of both adducts plays an important role in understanding of NO functions in different physiological processes and stress induced responses. Furthermore, NO can undergo reactions with transition metals, such as iron or iron-sulphur clusters [9].

All in all, the behavior and biological functions of NO in a cell depends on the chemical microenvironment, such as NO location, redox status, and oxygen concentration [1].

1.1.2 NO generation in plants

Since 1998, when NO was recognized as important signaling molecule in plants, scientists have been faced with the problem of finding the source of NO production in plant cells. As the mechanism of NO production has been described in detail in mammalian cells, it was suggested that plants could have a homologous system. However, despite the full sequencing of the *Arabidopsis* genome, no enzymes have been identified in higher plants that are similar to those found in mammals.

In plants, NO is formed by two major pathways: reductive (nitrate-dependent) and oxidative (arginine-dependent), which are depicted in **Figure 2** [14]. The first pathway is based on nitrate reductase (NR). NR is a molybdenum-containing enzyme that catalyzes the reaction of nitrate to nitrite, and can further reduce nitrite to NO. NR is only one enzyme that has been shown to function in NO production both *in-vivo* and *in-vitro* [15]–[17]. There are two NR genes in Arabidopsis, NIA1 and NIA2, that exhibit a high amino acid sequence identity to each other (83.5 %) [18]. Therefore, the question is often posed which of the isoforms is more relevant for NO production. Many scientists take an advantage of double mutant, *nia1nia2*, in which both isoforms are affected. Using this, it was found that NR dependent NO production is involved in cold responses [19][20], osmotic stress [21] and pathogen attack [22]. The role of NIA1 in NO synthesis, on the other hand, was identified as being crucial for ABA-induced stomata closure [23]. Moreover, NIA1 might contribute to increased NR activity in response to fungal elicitor [24]. It appears that NR-dependent NO production might be affected through the posttranslational modification of this enzyme. Phosphorylation of NR on a serine residue and binding of 14-3-3 proteins results in loss of its enzymatic activity [9][18]. Moreover, this posttranslational modification of NR can even promote its degradation [26]. Nevertheless, by the removal of posttranslational modifications from NR, NO emission could be detected from leaves and roots [27].

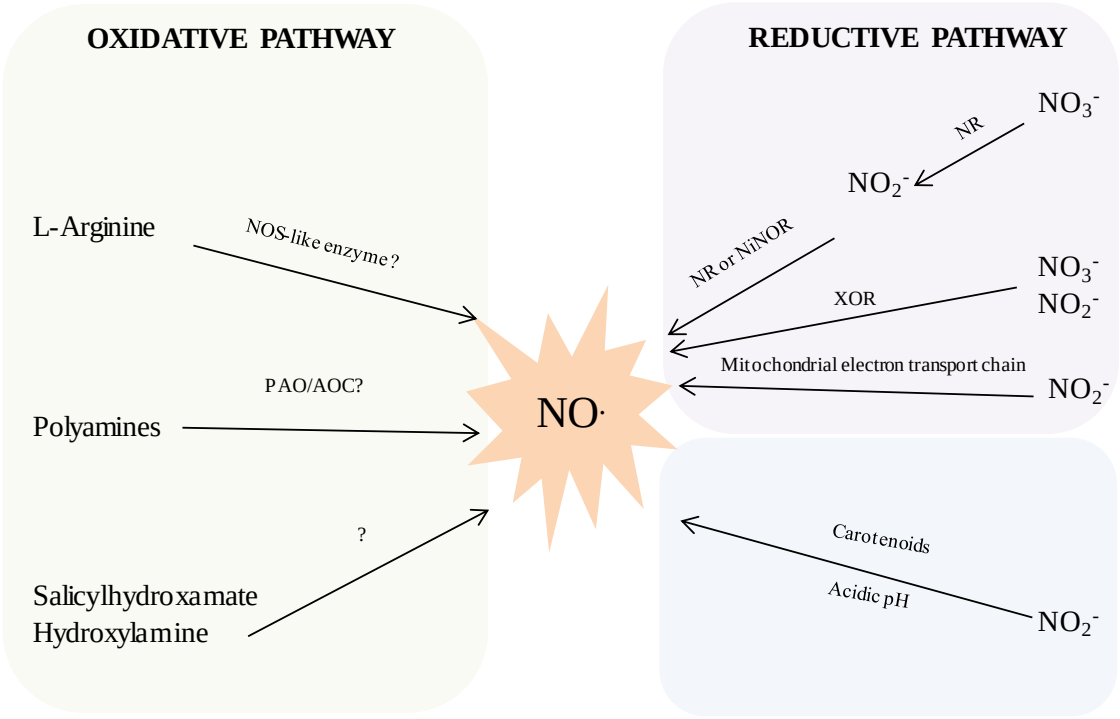

Figure 2: Overview of NO biosynthesis in plants.
Modified from [28]. An oxidative pathway involves a nitric oxide synthase (NOS)-like enzyme and two other ways of NO production using polyamines and hydroxylamines as substrates. A reductive pathway of NO synthesis includes: a non-enzymatic way of NO formation under acidic pH or through the reduction of NO_2^- by carotenoids as well as an enzymatic way which involves cytosolic and plasma membrane nitrate reductase (NR), nitrite-NO reductase (NiNOR), mitochondrial electron transport chain and xanthine oxidoreductase (XOR).

In contrast, although plasma membrane-bound nitrate reductase (PM-NR) is considered to be involved in nitrate uptake, it is not known whether PM-NR itself can form NO. However, after reduction of nitrate by PM-NR, produced nitrite can be further utilized to NO by associated plasma-membrane bound nitrite/NO reductase (NI-NOR) [29]. The amount of NO produced by this reaction is mainly dependent on nitrite and oxygen content. It is suggested that NO here plays a role in symbiotic interaction at the root surface [30].

Xanthine oxidoreductase (XOR) is also involved in NO formation. In mammals, this enzyme can reduce nitrite under anaerobic conditions, in the presence of electron donors such as NADH (pH 7) or xanthine (pH 6). XOR consists of two subunits with the mass of 145 kDa. Each subunit includes one molybdenum atom, one FAD, and two nonidentical iron-sulfur redox centers [31]. In plants, XOR was found in pea leaf peroxisomes [32]. However, no evidence of NO production by XOR in plants has yet been published.

Another source of NO in plants was found in mitochondria. It was demonstrated that when nitrite and NADH were applied to mitochondria, NO was formed, probably via cytochrome c oxidase and/or reductase. However, NO production was only possible under anoxia [33].

Under this condition a mitochondrial nitrite reduction also results in a synthesis of a small amount of ATP.

NO can also be produced nonenzymatically. For example, an increase in NO levels was demonstrated under acidic conditions in apoplast [34], and light-mediated reduction of nitrite to NO by carotenoids has been described [35].

Production of NO via an oxidative route is based on the existence of NOS-like activity in plants, which was primarily found in mammals. In animals, NO is synthesized predominantly by nitric oxide synthase (NOS) that oxidizes L-arginine in the presence of O_2 and NADPH to citrulline. There are three isoforms of NOS known: endothelial NOS (eNOS) and neuronal NOS (nNOS) which are present constitutively and the activity of these enzymes is Ca^{2+} dependent. The third isoform is an inducible NOS (iNOS or mNOS) which is expressed as part of an immune response mechanism and is Ca^{2+} independent [36].

The existence of NOS activity in plants has been discussed for many years. It was suggested that AtNOS1 is a crucial player in NO synthesis since it was demonstrated to convert L-arginine to L-citrulline and the activity of this protein was dependent on NADPH, Ca^{2+} and calmodulin, as seen like in the case of mammalian eNOS and nNOS. Additionally, *atnos1* mutant plants exhibit a lower level of NO accumulation than wild type plants [37]. Later this results were confirmed by other groups [38][39]. However, several other scientists have expressed doubt about the reproducibility of earlier results and questioned the true function of AtNOS1 [40][41]. Therefore, it was suggested to rename this protein to *Arabidopsis thaliana* NO-associated 1 (AtNOA1). Later it was found that AtNOA1 is a member of the cGTPase family and thus exhibits GTPase activity [42].

However, researchers are still optimistic about finding NOS in plants. L-arginine-dependent NOS activity has been reported in 11 plant species [43]. A homolog of the human NOS gene was found in green algae *Ostreococcus tauri*. *E. coli* cell cultures transformed with algae NOS were able to produce NO *in-vivo* and displayed enhanced cell viability [44]. This finding reignited speculation as to whether higher plants indeed contain NOS-like enzymes. Recently, another publication demonstrated a role of NOS-produced NO in plant response to Fe-deficiency. However, again no NOS related enzyme was identified [45]. The fact that different NOS isoforms are present in animals could indicate that NOS in plants also consists of different enzymes or complexes, where each subunit is a part of the redox machinery. For instance, AtNOA1 might contribute to or be a part of this system [18].

It was also suggested that polyamine oxidases and copper containing amine oxidases participate in oxidative NO production. The polyamines spermine and spermidine triggered

NO biosynthesis in *Arabidopsis* seedlings [46], while CuAO8 was demonstrated to be involved in arginine-dependent NO production by manipulation of arginine availability [47]. Incubation of tobacco cell cultures with hydroxylamine or salicylhydroxamate also resulted in NO accumulation [48], although the significance of this pathway is still unclear, since the existence of hydroxylamines in plants has not be confirmed [49].

1.1.3 Physiological functions of NO

The chemical properties of NO make it multifunctional. Whereas some studies report toxic and harmful action of NO species, such as cell death [50], damage of proteins, membranes, and nucleic acids or photosynthetic inhibition [51], others demonstrate that NO shows protective actions. In fact, the dual function of NO is often dependent on its concentration and environment. For instance, low NO concentration promoted an expansion of pea leaves, whereas an opposite effect was observed using a higher NO amount [52]. Similar results were also obtained in monitoring of maize root growth which was induced by very low NO concentration and reduced with the increasing of the amount of NO [53].

Based on NO functions it has been proposed as a stress-responding agent. It can counteract toxic processes induced by ROS [54][55]. It was shown that NO is involved in abiotic stress responses such as those to salinity, drought, UV-B radiation, temperature and heavy metal toxicity [56][57][58][59][60][61][62][63]. The role of NO in biotic stress is essential. It plays a key role in disease resistance against *Pseudomonas syringae* in *Arabidopsis* leaves, and is required for SAR induction in tobacco [64][65][66]. Moreover, NO participates in plant development and physiological processes such as germination, gravitropism, root development and flowering [38][67][68][69][70].

Although there is no doubt that NO is crucial for plant development and survival, the mechanism by which NO activates signaling function and the genes underlying this process remain to be elucidated.

Light is essential for plant growth and development, whereas photosynthesis plays a central role here by converting the light energy into complex compounds which are crucial for a cell living. A number of studies have been performed demonstrating the involvement of NO on photosynthesis, indicating that there should be a link between NO and light-induced processes. It was found that NO donors or NO fumigation can affect photosynthetic performance, chlorophyll fluorescence parameters as well as metabolic process related to photosynthesis [71]. Dependent on NO donor, it is able to reduce or stimulate the electron

transfer through PSII [72][73]. Inhibition of ΔpH formation by SNAP as well as the suppression of ATP synthesis was demonstrated in spinach [74]. A protective role of NO in plants has also been described. It was shown that NO is able to prevent chlorophyll (Chl) loss under stress conditions, e.g. induced by Cd [75]. It was also found that SNP effects the gene transcription of photosynthetic enzymes and decreases the amount of glucose in mung beans [76]. The influence of NO on transcription of photosynthesis-related genes was also found in a transcriptomic analysis of *Arabidopsis* plants fumigated with NO [77]. At the same time, light is also known to induce gene transcription by controlling histone acetylation [78].

1.1.4 NO mode of action

NO chemical properties contribute to its role in signal transduction in a living cell. It can rapidly undergo multiple chemical reactions with proteins, transcription factors or second messengers. NO and its related species are able to modulate protein activity and biological function through covalent post-translational modifications (PTM) by binding to the metal centers of proteins and by affecting their cysteine and tyrosine residues (**Figure 1B**). The major three NO-dependent PTMs are discussed in this chapter.

Tyrosine nitration is a post-translational modification that arises through the binding of a NO_2 into ortho carbons of aromatic ring of tyrosine residues that leads to the formation of 3-nitrotyrosine. At the same time this reaction induces changes in the neighboring amino acids, such as inducing a drop in the p*Ka* of the –OH group, causing steric restriction, or inhibiting tyrosine phosphorylation. Formation of nitrotyrosines is a marker for "nitroxidative stress" [79][80]. In plants, tyrosine nitration was detected under different stress conditions such as pathogen infection, salt stress, or high temperature [81][82][83][84]. Usually, tyrosine nitration is associated with loss of protein functions. For example, O-acetylserine(thiol)lyase A1 is an enzyme which is crucial for cysteine homeostasis, is inactivated upon nitration at Tyr-302 [85]. Another enzyme, glutamine synthetase is nitrated at Tyr-167 and subsequently loses its activity [86]. Ferredoxin-NADP reductase was also shown to be inhibited via a $ONOO^-$ donor, 3-morpholinosydnonimine [84]. *Arabidopsis* superoxide dismutases MSD1, FSD3 and CSD3 were demonstrated to lose their activity to different degree by $ONOO^-$. This inhibition was correlated with Tyr nitration and could be prevented by the $ONOO^-$ scavenger urate. Site-directed mutagenesis revealed that Tyr-63 is the main target of MSD1 nitration which is responsible for the activity of this protein [87].

In a direct reaction termed metal nitrosylation, NO binds to transition metals, resulting in formation of metal nitrosyl complexes. In this way, activity and function of proteins can be

regulated. Well studied targets for NO interaction are iron-sulphur clusters, as well as haeme groups and zinc ions of proteins [88].

The most common example of a metal nitrosyl complex is an interaction of NO with the haeme iron of mammalian soluble guanylate cyclase (sGC). This reaction leads to a conformational change and activation of sGC to catalyse cyclic guanosine monophosphate (cGMP) which activates a number of downstream processes [89][90].

Similar mechanisms may also be present in plants. NO-dependent accumulation of cGMP, cADRP as well as Ca^{2+} was measured after pathogen attack and ABA-induced stomata closure [91][92][93]. However, no plant homolog of mammalian sGC has yet been identified.

Examples of NO binding to iron present in haeme proteins have also been observed in plants. It was suggested that two major H_2O_2-scavenging enzymes in tobacco, ascorbate peroxidase and catalase are reversible inhibited by NO donors through the formation of an iron-nitrosyl complex [94]. The enzymatic activity of tobacco aconitase, which contains an iron-sulfur cluster, is also reduced after NO donor treatment with NOC-9 [95]. A non-heme iron enzyme lipoxygenase-1 in soybean forms a ferrous-nitrosyl complex after exposure to NO. Moreover, a substrate linoleic acid competes with NO for binding at pH 9 [96]. Plants hemoglobins were also identified as a target for NO. It was shown that *Arabidopsis* nonsymbiotic hemoglobin AHb1 binds NO and oxidizes it to nitrate, suggesting a role of hemoglobins in detoxification of NO [97].

S-Nitrosylation is the most studied redox-based post-translational modification. This modification results in the formation of S-nitrosothiols (SNO). S-Nitrosylation enables a living organism to directly respond to environmental stimulus through the regulation of protein activity, protein-protein interaction or protein localization [98][99]. The release of the NO moiety from proteins and therefore the control of SNO homeostasis in a cell is maintained by two enzymes: GSNOR reductase (GSNOR) which metabolizes GSNO to a mixture of intermediates, and thioredoxins which mediate denitrosylation [100][101].

The list of potential candidates which can be S-nitrosylated in plants is growing continuously. 63 candidates were found in *Arabidopsis* cell culture after GSNO treatment, as well as 52 proteins which were identified being S-nitrosylated in leaves after fumigation with NO [102]. S-Nitrosylated targets were also found in leaves and cell cultures of *Arabidopsis* after inoculation with virulent or avirulent *Pseudomonas syringae* [103][104], or under salt stress conditions in the mitochondria of pea plants [105]. Although a high number of candidates for S-nitrosylation were identified, only a few of them were experimentally confirmed and their functions in response to NO demonstrated [106]. Most of the studies are based on biotin

switch technique (BST), where S-nitrosylated cysteines are labeled with a biotinylating agent, allowing easy detection by immunoblotting using a specific antibody, or by mass spectrometry. Despite of the high specificity of the assay, false-positive candidates for S-nitrosylation can still be identified. It was demonstrated that BST includes several critical steps. For instance, effective blocking of free thiols is very important to avoid unspecific biotinylation [107]. It was also reported that the reduction of S-NO bonds to free thiols with ascorbate is inefficient. However, this step could be improved by using higher concentration of reducing agent (ascorbate) and longer incubation time [108]. Others noticed that ascorbate treatment increases the rate of biotinylation reactions, leading to false-positive signals and therefore to a misinterpretation of the results [109]. Another disadvantage of BST is that it detects mostly highly abundant proteins, making it difficult to find regulators with a low abundance [110].

S-Nitrosylated sites can be predicted by various computer programs that were developed in recent years. A comparison of different computational predictors was presented in [111]. All these programs are based on searching for specific NO-binding motives that were initially identified in animal proteins. A potential GSNO binding motif, which is composed of a combination of specific amino acids (HKR-C-hydrophobic-X-DE), was suggested to be necessary for NO "docking" to a cysteine residue [112]. Using a site-specific proteomics approach on breast cancer cells, DE-IC-RK motif was found to be important for S-nitrosylation, supporting the idea that a base-acid motif (KRHDE-C-DE) is necessary for formation of SNOs [113][114]. In proteomics studies from *Arabidopsis* cell cultures, 53 endogenous S-nitrosylated cysteines were identified. Notably, only three apolar amino acid residues (Ala, Gly, Ile), which were not located in close vicinity of cysteines, were found in all the proteins, suggesting that the enrichment of these may be important for cysteine modification [115]. Furthermore, several other features which control thiol accessibility and reactivity, e.g. redox state of a cell, pH, presence of Mg^{2+} and Ca^{2+} as well as cysteine hydrophobicity and pK_a define specificity of protein S-nitrosylation [116]. However, these findings were declaimed, suggesting that a distant localization of the charged amino acids from Cys is more important for the formation of S-nitrosothiols than all other features [117].

1.1.5 Regulation of gene expression by NO

In the recent years it has become more and more clear that NO can control physiological processes through the regulation of gene expression *via* activation of signaling pathways (described above) or through a direct interaction with transcription factors or chromatin

modulators. Studies that monitored expression profiles upon NO treatment in *Arabidopsis* are mostly based on large scale transcriptional analysis [118][119][120][121]. Using a cDNA-amplification fragment length polymorphism method, 120 genes were demonstrated to have altered expression patterns in response to infiltration of *Arabidopsis* leaves with 1 mM of the NO donor, SNP [122]. In microarray analysis 342 genes were found to be regulated in a dose-dependent manner upon SNP treatment. In total, 124 and 261 genes were induced after 0.1 mM and 1mM SNP treatment, respectively [123]. With the development of high-throughput sequencing, NO-responsive genes were also analyzed using RNA-seq technology. In total, 3263 genes were found to be differently regulated upon treatment with 1 mM GSNO, and among those 1945 genes were showed different expression patterns in leaves and roots [124].

In general, NO mediates changes in expression of genes involved in a wide range of physiological functions, such as disease resistance, defense, photosynthesis, signaling transduction and more. For instance, application of NO donors (GSNO and SNAP) or recombinant mammalian NOS to tobacco plants or tobacco suspension cells triggers the induction of defense-related genes such as pathogenesis related protein and phenylalanine ammonia lyase [91]. Moreover, treatment of soybean cells with SNP resulted in enhanced transcript levels of PAL and chalcone synthase, which levels were reduced by cPTIO [64]. NO-dependent activation of defense- and stress-related genes, including glutathione S-transferases, cytochrome P450, and other genes encoding PR proteins was also reported [39]. The function of endogenous NO/SNO on gene transcription was analyzed using a GSNOR null mutant (*hot5-2*), which exhibits higher SNO content than wild type plants. 99 up- and 170 downregulated genes were observed in *hot5-2* in comparison to wild type which were closely related to genes involved in pathogen response, redox regulation and signaling [125]. Microarray data of *hot5-2* and wild type plants fumigated with 3 ppm of NO revealed that pathways associated with photosystem, flavonoids and phenylpropanoids as well as genes involved in amino acid and protein synthesis are highly upregulated [100][101].

Transcriptomic data gives a clear answer about the impact of NO on gene expression. However, gene induction alone does not necessarily result in metabolomic changes and a physiological response of the cell. Therefore, additional studies are required to reveal the exact mechanism of NO functions/signaling and to avoid misinterpretation of transcript data [127]. An overview of NO-mediated regulation of gene expression is illustrated in **Figure 3**.

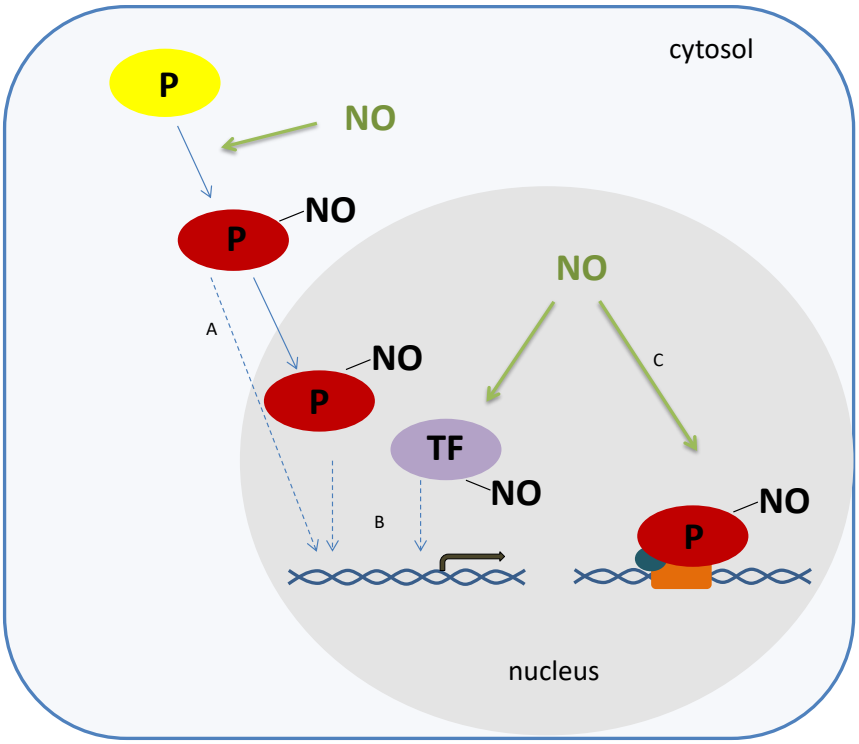

Figure 3: NO-mediated gene expression.
Modified from [128]. A and B) NO-dependent interaction with proteins (P) and transcription factors (TF) can result in changes of protein activity and translocation and therefore modulate a signaling pathway. C) NO may directly affect DNA-binding proteins and induce epigenetic modifications of chromatin structure. All these events may result in transcriptional changes. Dashed arrow, signaling pathway.

1.1.5.1 Via modification of transcription factors

It was demonstrated that transcription factor SoxR of *E. coli*, which is responsible for regulation of oxidation responses in bacteria, is only activated by oxidation of its iron –sulfur cluster (2Fe-2S) [129]. Later on, it was found that SoxR became activated after exposure to NO gas as well. Activation of SoxR was induced by formation of a dinitrosyl-iron-dithiol complex, in which the sulfide ligands were displayed through Fe-NO bonds. It was also shown that nitrosylated SoxR exhibits similar binding affinity and structural effects as its oxidized form [130]. A bacterial transcription factor OxyR regulates expression of genes involved in H_2O_2 detoxification through the redox modification at cysteine residues [131]. More evidence for direct NO-dependent modification of transcription factors was reported in mammals. It was demonstrated that S-nitrosylation of several transcription factors, such as multiple zinc finger transcription factors, tumor suppressor protein, etc., results in regulation of gene expression [132][133].

Using a bioinformatics approach, promoter regions of NO-regulated genes in plants were analyzed to identify their transcription binding sites. Several families of transcription factors appeared in this screen, including WRKY, GBOX, OCSE, OPAC and MYCL motifs that are

highly present in upregulated genes, while TBPF and MIIG elements were found in downregulated genes [121]. Nevertheless, less is known about direct regulation of plant transcription factors by NO. MYB domain proteins are a large family of transcription factors which control a wide range of physiological processes, e.g. response to biotic and abiotic stress, development, metabolic pathway, differentiation and so on. [134]. It was reported that R2R3 MYB proteins consist of two cysteines residues that need to be reduced to enable DNA-binding activity [135]. AtMYB2 has been shown to undergo NO-dependent posttranslational modification. Reversible S-Nitrosylation of Cys-53 was detected using biotin switch technique. This result provided evidence for the first time that transcriptional activity of plant MYB proteins is regulated by NO [136]. Another MYB member, AtMYB30, is a positive regulator of a hypersensitive response, and was also shown to be reversibly S-nitrosylated by NO. The authors speculated that during hypersensitive response, which is accompanied by oxidative burst, S-nitrosylation of AtMYB30 and subsequent loss of its DNA-binding activity is mediated by nitrogen species to prevent uncontrolled cell death initiated by a hyperactive AtMYB30 [137]. The transcriptional coregulatory non-expressor of PR1 (NPR1) plays a key role in activation of systemic acquired resistance by interacting with salicylic acid (SA) [138]. Usually, after pathogen infection, SA accumulates in the cell, which leads to changes in the redox state and consequently to the reduction of disulfide bonds of NPR1. Reduction of NPR1 results in its active monomeric form, which is further translocated to the nucleus where it interacts with TGA1 transcription factor and stimulates the expression of pathogenesis-related genes [139]. S-Nitrosylation of NPR1 leads to its oligomerization and keeps NPR1 in the cytosol. This process seems to be important for NPR1 homeostasis upon SA induction. Monomerization of NPR1 is catalyzed by thioredoxins, which reduce NPR1 and allow its migration into the nucleus [140]. Surprisingly, NO can also promote nuclear translocation of NPR1, suggesting that S-nitrosylation is rather an intermediate prior to monomerization and therefore, does not have an inhibitory effect on NPR1 signaling. Furthermore, in the presence of GSNO, TGA1 and NPR1 are both S-nitrosylated resulting in the enhanced DNA-binding affinity of TGA1. It was suggested that GSNO mediates conformational changes of TGA and/or NPR1, which result in more efficient TGA1-NPR1 interaction [141]. Another example of NO-dependent regulation of transcription factors is a fer-like Fe deficiency-induced transcription factor (FIT). It is not only activated and stabilized by NO, but it is also protected from proteasomal degradation in the presence of NO. FIT is required for regulation of controlled iron uptake in *Arabidopsis*. It was proposed that NO functions in parallel with

another signaling molecules, e.g. ethylene and jasmonate, which are also necessary for regulation of iron deficiency responses [142][143].

1.1.5.2 Via chromatin modification

On the genome level, cells of multicellular organisms are very similar. However, each cell differs from others through the differences in gene expression pattern that might occur in a temporally and spatially-dependent manner. Genes might be silenced/switched off and switched on again only when they are required. Over the last few decades it was found that chromatin is an important regulator of transcription.

Genetic material of all eukaryotic organisms has to be packed into the nucleus to protect it from becoming damaged. Since the length of eukaryotic DNA is far greater than the diameter of a nucleus, it has to be organized in a very tightly packaged structure, known as chromatin. The core subunit of chromatin is an octamer which is composed of two copies of the histone proteins, H2A, H2B, H3 and H4, which are positively charged and enable an electrostatic interaction with negatively charged DNA. Around 145-147 bp of DNA are wrapped around a histone complex forming repeating nucleosomal units, which are connected with each other by short DNA fragments (also called 'linker DNA'). Linker histone H1 is located between the nucleosomes and stabilizes chromatin structure, resulting in highly condensed 30 nm fibers [144].

Chromatin structure in eukaryotic organisms is very dynamic, and can be changed in response to environmentally stimuli. Chromatin marks are able to induce chromatin remodeling and therefore to control important molecular processes such as gene transcription, replication, repair and recombination [145]. DNA methylation and histone modifications are the key mediators of epigenetic modifications. DNA methylation is usually associated with long-term silencing of genes, whereas histone modifications contribute to both activation and repression of gene transcription and can be removed after several cell cycles (**Figure 4**) [146][147].

Histones play an important role in the regulation of chromatin structure and in subsequent gene transcription. N-terminal histone tails which are exposed outside the nucleosome may interact with neighboring nucleosomes and therefore manipulate the chromatin structure [145]. Histone tails can also undergo different posttranslational modifications (PTMs) such as acetylation, methylation, phosphorylation, and ubiquitination, resulting in different molecular changes that effect DNA accessibility. Meaning, that if the way of how DNA is wrapped around histone proteins changes, then gene transcription can change as well [148].

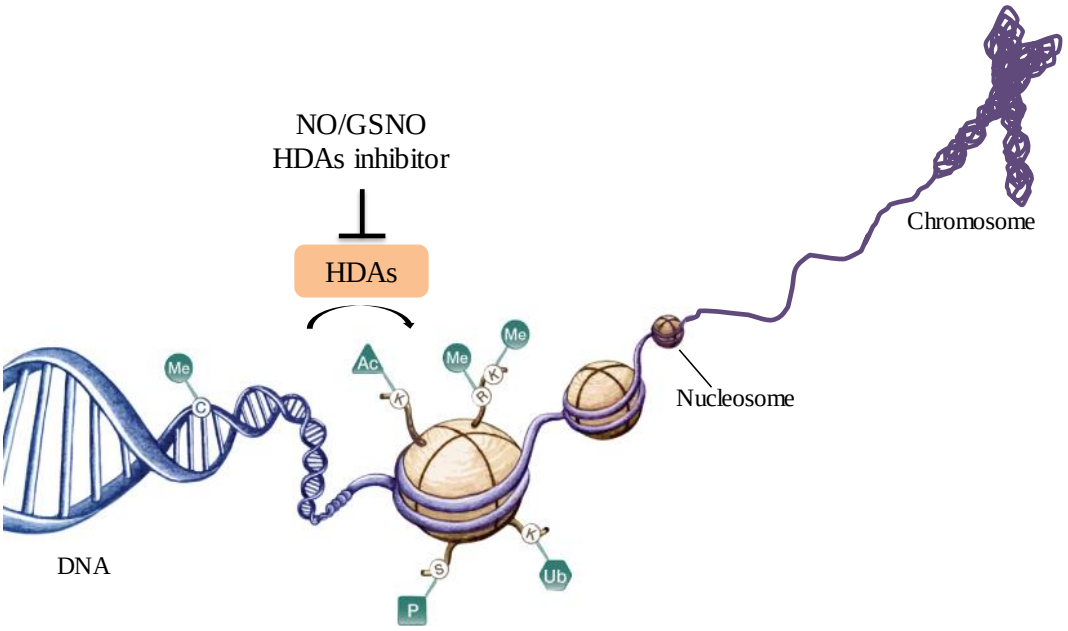

Figure 4: Epigenetic modifications of chromatin structure.
Modified from [149]. Epigenetic modifications of chromatin structure play an important role in regulation of gene expression and consist of two main pathways: DNA methylation and histone modifications. Adding a methyl group to the DNA molecule might lead to gene repression, especially if it binds to the promoter region of a gene. Posttranslational histone modifications such as acetylation (Ac), methylation (Me), phosphorylation (P) and ubiquitination (Ub) might affect physiological properties of chromatin and DNA accessibility. There is evidence demonstrating that inhibition of HDAs by NO/GSNO might result in acetylation of histone tails and therefore in activation of gene transcription.

In studies in the human field, a direct link between NO-induced inhibition of JmjC-domain containing histone demethylases and enhanced histone methylation was demonstrated [150]. Fifteen critical lysine residues on the core histones (H3 and H4) were found to be post-translationally modified after the treatment of human triple-negative breast cancer cells (MSA-MB-231) with NO donor DETA/NO. Moreover, NO-dependent changes in H3K9me2 correlated with changes in gene expression [151]. In *Arabidopsis*, arginine methyltransferase PRMT5 was found to be S-nitrosylated and activated in response to salt stress. Salt stress-induced arginine (Arg) demethylation was abolished and correlated with aberrant splicing of pre-mRNA when the NO-sensitive cysteine was replaced by serine (Ser) [152].

Histone acetylation plays a key role in regulation of gene transcription. This modification is very dynamic and is catalyzed by two families of enzymes: histone acetyltransferases (HATs) and histone deacetylases (HDAs). Histone acetylation removes a positive charge from histone tails and therefore decreases histone-DNA interaction. Loss of electrostatic interaction between DNA and histone proteins results in "opening" of chromatin making it more accessible for the transcriptional machinery. Therefore, acetylation is usually associated with gene transcription. For instance, acetylation of histone 4 at lysine 16 (H4K16ac) induced by

MOF (Males absent On the First) results in transcriptional activation of many genes during dosage compensation in *Drosophila* [153]. In turn, acetylation can be removed by HDAs maintaining chromatin in "closed" and inactivated state [154].

There is increasing evidence that the catalytic activity of some HDAs is regulated by redox modifications, which are further involved in the regulation of unwinding and wrapping of chromatin (**Figure 4**). Most studies of redox regulation of HDAs have been done in human and animal cells. It was reported that HDA2 in neurons gets S-nitrosylated upon NO signaling triggered by brain-derived neurotrophic factor. S-Nitrosylation of HDA2 results in chromatin acetylation and activation of gene expression that are involved in neuronal development. Notably, S-nitrosylation does not affect the enzymatic activity of HDA2 but stimulates its release from chromatin. The effect of NO on HDA2-cromatin interaction was confirmed, when redox-sensitive cysteines were mutated to alanine. It was shown that mutated HDA2 could not dissociate from chromatin [155]. S-Nitrosylation of HDA2 was also demonstrated in muscles of dystrophin-deficient MDX mice. The catalytic activity of this enzyme was impaired by NO *in-vivo* and *in-vitro* [156]. Human HDA8 was also identified as potential target for NO. It was shown *in-vitro* that HDA8 is S-nitrosylated by GSNO. Moreover, the protein activity was significantly reduced by GSNO and another NO donor, S-nitrosocystein (Cys-NO), in time- and concentration-dependent manner. Interestingly, application of SNP to HDA8 had no effect on the catalytic activity of this protein, indicating that a special structure for transferring NO might be present [157]. NO-dependent inhibition of gene expression was measured in human umbilical vein endothelial cells (HUVECs). It was demonstrated that upon NO production, protein phosphatase becomes activated and associates with a histone deacetylase complex pCamkIV/HDACs, promoting its dephosphorylation. This process leads to the shuttling of HDA4 and HDA5 (members of pCamkIV/HDACs complex) into the nucleus and deacetylation of histones. As a consequence, gene expression is inhibited. Under non-stressed conditions, when the NO level in the cell is low, HDA4 and HDA5 remain in the cytosol, allowing hyperacetylation of chromatin [158]. In sum, NO-dependent regulation of HDAs can be considered as a key mechanism in regulation of histone acetylation and gene expression.

In *Arabidopsis* there are 18 members of HDAs which are divided into 3 families: RPD3-like, HD-tuins and sirtuins. The first family is the largest one and is composed of 12 putative members (HDA2, HDA5-10, HDA14-15, HDA17-19), which, based on their structure, can be further divided into 3 classes. This type of HDAs is homologous to yeast reduced potassium deficiency 3 (RPD3) proteins that are present across all eukaryotes. All members of this

family contain a specific deacetylase domain that is required for their catalytic activity. It should be highlighted that this class of HDAs is able to deacetylate more targets than just histones. Lysine acetylome profiling uncovered 91 acetylated proteins in *Arabidopsis* leaves after the treatment with deacetylase inhibitors apicidin and trichostatin A. Of these, only 14 were histone-like proteins [159]. The second family contains the HD-tuins (HD2) and was originally found in maize. This type of proteins is only present in plants, although their homologue cis-trans prolyl isomerases are also present in other eukaryotes [160]. HD2s are structurally distinct from RPD3-like members, but display a sequence similarity with FK506-binding proteins. In total 4 members of HD-tuins have been identified in *Arabidopsis*: HDT1 (HD2A), HDT2 (HD2B), HDT3 (HD2C) and HDT4 (HD2D). These consist of a N-terminal domain that has a conserved pentapeptide MEFWG region, which is required for gene repression activity. This region is followed by a high-charged acidic motif that is rich in glutamic and/or aspartic acid and a variable C-terminal region [161]. Moreover, HDT1 and HDT3 possess a zinc-finger motif that probably is involved in protein-protein interaction and DNA-binding. The third family of plants HDAs is represented by sirtuins (SIR2-like proteins) which are homologues to yeast silent information regulator 2 (SIR2). These HDAs are unique because they require a NAD cofactor for their function and unlike RPD3 proteins, they are not inhibited by trichostatin A (TSA) or sodium butyrate. Moreover, sirtuins use a wide variety of substrates beyond histones. For instance, human SIRT1 deacetylates nuclear factor-kB, p53 protein and peroxisome proliferator-activated receptor γ coactivator1-α [162]. So far, 2 members of SIR2 are known in plants: SRT1 and SRT2 [163]. Notably, SRT2 is a NAD^+ - dependent lysine deacetylase, which is mainly located at the inner mitochondrial membrane and is involved in energy metabolism and metabolite transport [164]. Recently, it became possible to measure the activity of durum wheat (WM) sirturin, offering a new tool for studying physiological roles of plant sirtuins [165].

Biological functions of HDAs are very diverse. It was demonstrated that HDA19 is an important player in transcriptional regulation. More than 7% of *Arabidopsis* transcriptome were either up- or downregulated in T-DNA insertion line of HDA19 (*athd1-t1*) [166]. Via the interaction with HATs (GCN5 and TAF1/HAF2) HDA19 is part of a complex that is required for expression of light-regulated genes [167]. Plants overproducing HDA19 exhibit higher expression of ethylene response factor1 and enhanced resistance to *A. brassicicola* by inducing the transcription of pathogen related genes: basic chitinase and β-1,3-glucanase [168]. HDA6 mediates silencing of ribosomal RNA [169], transgenes [170] or transposons [171]. Moreover, HDA6 is required to enhance DNA-methylation [172]. Together with

HDA19, HDA6 regulates repression of embryonic properties after germination [173]. Furthermore, both HDA6 and HDA19 are involved in regulation of ABA and salt stress response [174]. Additionally, HDA6 seems to be required in cold acclimation [175]. HDA18 has been revealed as a key regulator of *Arabidopsis* root epidermis [176]. HDA15 participates in repression of chlorophyll biosynthesis and photosynthetic genes in etiolated *Arabidopsis* seedlings [177]. Through the direct targeting of floral activator agamous-like19, HDA9 prevents early flowering under short day conditions [178].

1.2 Aim of this study

A posttranslational protein modification caused by NO may induce a signaling cascade which results in altered gene expression. A direct interaction of NO with transcription factors or other regulatory regions in the eukaryotic genome leads to extensive transcriptional reprogramming. Moreover, in mammals NO is able to modify chromatin structure and therefore cause the accessibility of DNA for transcriptional machinery by S-nitrosylation of HDA2 [155]. In plants, however, nothing is known about the influence of NO on chromatin remodeling.

Two plant specific histone deacetylases were found to be S-nitrosylated in *Arabidopsis* cell cultures after pathogen treatment suggesting that NO may regulate epigenetic processes in plants [104]. A published study about a reversible NO-dependent inhibition of HDAs activity in nuclear extracts and protoplasts contribute to the hypothesis that NO plays an important role in chromatin modulation and therefore in regulation of gene transcription [179][180].

Based on these facts, the first aim of this study was to investigate the influence of NO on histone acetylation. This was analyzed by using suspension cells and seedlings. A mass spectrometry-based approach as well as an immunoblotting technology were used to identify lysine residues which are regulated by NO-sensitive HDAs. This was done after the treatment of suspension cell cultures or 7-days old *Arabidopsis* seedlings with NO donor, GSNO, or after induced endogenous NO production by a chemically synthesized analog of a plant hormone SA, INA.

The second aim was to find out the mode of action of NO to modulate chromatin structure. A qPCR approach was used to evaluate the influence of NO on the expression of *Arabidopsis* HDAs. Moreover, since it was demonstrated that total HDAs activity is reversibly inhibited upon NO treatment as well as it was supposed that *Arabidopsis* HDA6 and 19 might be NO-

sensitive HDAs [179], the influence of NO on HDA6 activity was also investigated *in-vitro*.

The third aim was to investigate a physiological role of NO in the regulation of chromatin structure. This was done by the omission of pharmacological approach (adding of chemical compounds) and using instead plants grown on soil. Since there is evidence indicating that NO production is light-dependent [38], NO accumulation and histone acetylation level were analyzed in wild type and SNO-accumulating (*hot5-2*) plants under different light conditions. The aim of these experiments is to analyze whether there is a link between light-induced SNO accumulation/S-nitrosylation and chromatin modulation. Additionally, the functions of NO on photosynthetic performance as well as on histone acetylation of photosynthesis-related genes were investigated. This was performed by comparison of H3K9/14ac as well as transcriptional activation of photosynthesis related-genes (found hyperacetylated in response to GSNO treatment in *Arabidopsis* seedlings [180]) in wild type and *hot5-2* plants under dark and high light/temperature conditions. Moreover, H3K9ac was analyzed under dark and moderated light conditions, in order to find photosynthesis-related loci regulated by light-induced NO accumulation.

2 Results

2.1 Effect of NO on chromatin remodeling

HDAs are responsible for maintaining chromatin in deacetylated and inactivated state. It was demonstrated that NO donors, GSNO (S-nitrosoglutathion) and SNAP (S-nitroso-N-acetylpenicillamine), inhibit total HDAs activity in *Arabidopsis* nuclear extracts (*in-vitro*) and protoplasts (*in-vivo*) [179][180]. Therefore, the question arises whether NO-dependent inhibition of HDAs activity influences total protein acetylation and/or impacts chromatin structure?

2.1.1 Tendency towards induced histone acetylation by exogenously applied NO

To investigate the effect of exogenously applied NO on the acetylation state of a plant cell, total protein extracts as well as histone acetylation were analyzed in *Arabidopsis* cell cultures by immunoblotting using an anti-acetyl protein antibody.

First, suspension cells were incubated for 4 h with water, 500 µM GSNO and 500 µM INA (2,6-dichloro-isonicotinic acid) which is known to induce endogenous NO production. Total protein was isolated with DPBS buffer and analyzed for acetylated lysine residues (**Figure 5**). No obvious differences could be observed in the global acetylation level between the control and GSNO and INA treated samples.

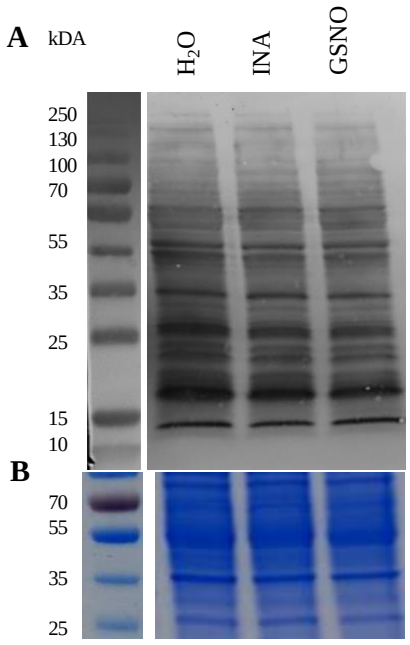

Figure 5: No changes in global protein acetylation level after GSNO and INA treatment in wt suspension cells.
Cell cultures were incubated for 4 h with 500 µM GSNO, 500 µM INA and water (negative control). Total protein was isolated in DPBS buffer. 50 µg of proteins were separated on the 12 % SDS-PAGE gel. A) Proteins were transferred onto nitrocellulose membrane. Acetylated proteins were detected with anti-acetyl protein primary antibody (1:5000) by incubating the membrane over night at 4 °C. A secondary antibody was an anti-rabbit HRP (1:2500). In total three independent experiments were performed (N=3). Shown is one representative experiment. B) A loading control is represented by a Coomassie brilliant blue stained gel.

To analyze histone acetylation, cell cultures were incubated for 4 h with 500 µM GSNO and 1 µM TSA, a well-known HDA inhibitor, and then nuclear proteins were prepared (**Figure 6A**). Immunoblotting demonstrated a 1.7-fold enhanced acetylation level on histone 3 (acetyl-H3) after treatment with GSNO as well as a 2.3-fold increase after TSA compared to the water treated control (**Figure 6B**).

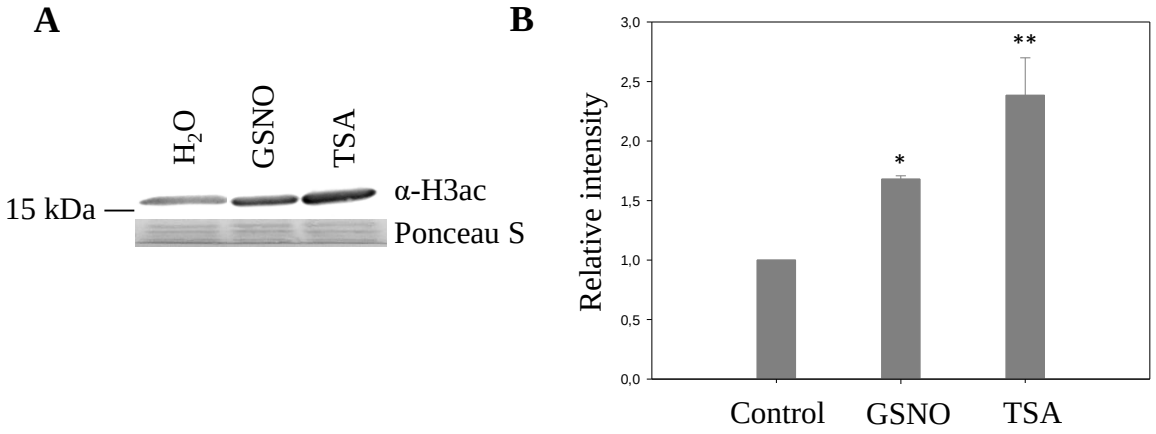

Figure 6: Enhanced H3 acetylation in wt suspension cells after GSNO and TSA treatment.
A) Cell cultures were incubated for 4 h with 500 µM GSNO, 1 µM TSA (positive control) and water (negative control). Nuclear pellet was directly dissolved in 50 µl laemmli buffer and heated for ca. 10 min at 95 °C. The supernatant was transferred into a new tube and concentration measured with RCDC Assay. 15 µg of nuclear protein were separated on the 12 % SDS-PAGE gel and transferred onto nitrocellulose membrane. The membrane was incubated over night with anti-acetyl H3 primary antibody (1:20000) at 4 °C and for 1 h with a secondary antibody coupled to HRP (1:2500). Shown is one representative experiment. B) Quantitative analysis of A. Signal intensity was determined with Image J software. Shown is a ± SE of three independent experiments (N=3). The relative intensity of the control group in all N=3 was set up to 1 [181]. One way ANOVA (DF=2, p=0,005) with Holm-Sidak post-hoc test for each treatment group vs. the control group was performed, *p≤0.05, **p≤0.01.

Next, a more detailed analysis of histone acetylation was examined by mass spectrometry and immunoblotting in *Arabidopsis* seedlings. For more effective application of chemicals, 7-days old seedlings grown in liquid medium were used. 250 µM GSNO was applied to mimic NO production. The decompensation of GSNO results in formation of GSH and NO. Since the latter is able to activate biosynthesis of GSH [182], a 250 µM GSH treatment was used as an additional control to distinguish between a direct effect of GSNO-released NO and those which are induced by an enhanced GSH concentration. A NO scavenger cPTIO (500 µM) was additionally applied to seedlings treated with GSNO to demonstrate the NO-specificity of GSNO. 5 µM TSA was used as a positive control for inhibition of histone deacetylase activity.

The experimental workflow of LC-MS/MS approach is illustrated in **Figure 7A**. Histone bands were cut out from the polyacrylamide gel and derivatized by d6-deuterated acetic

anhydride followed by trypsin digestion. During this process generated peptides of 5 to 10 amino acids in length were further used for LC-MS/MS measurement. N-terminal amino acid sequences of H3 and H4 as well as their different modifications are shown in **Figure 7B**.

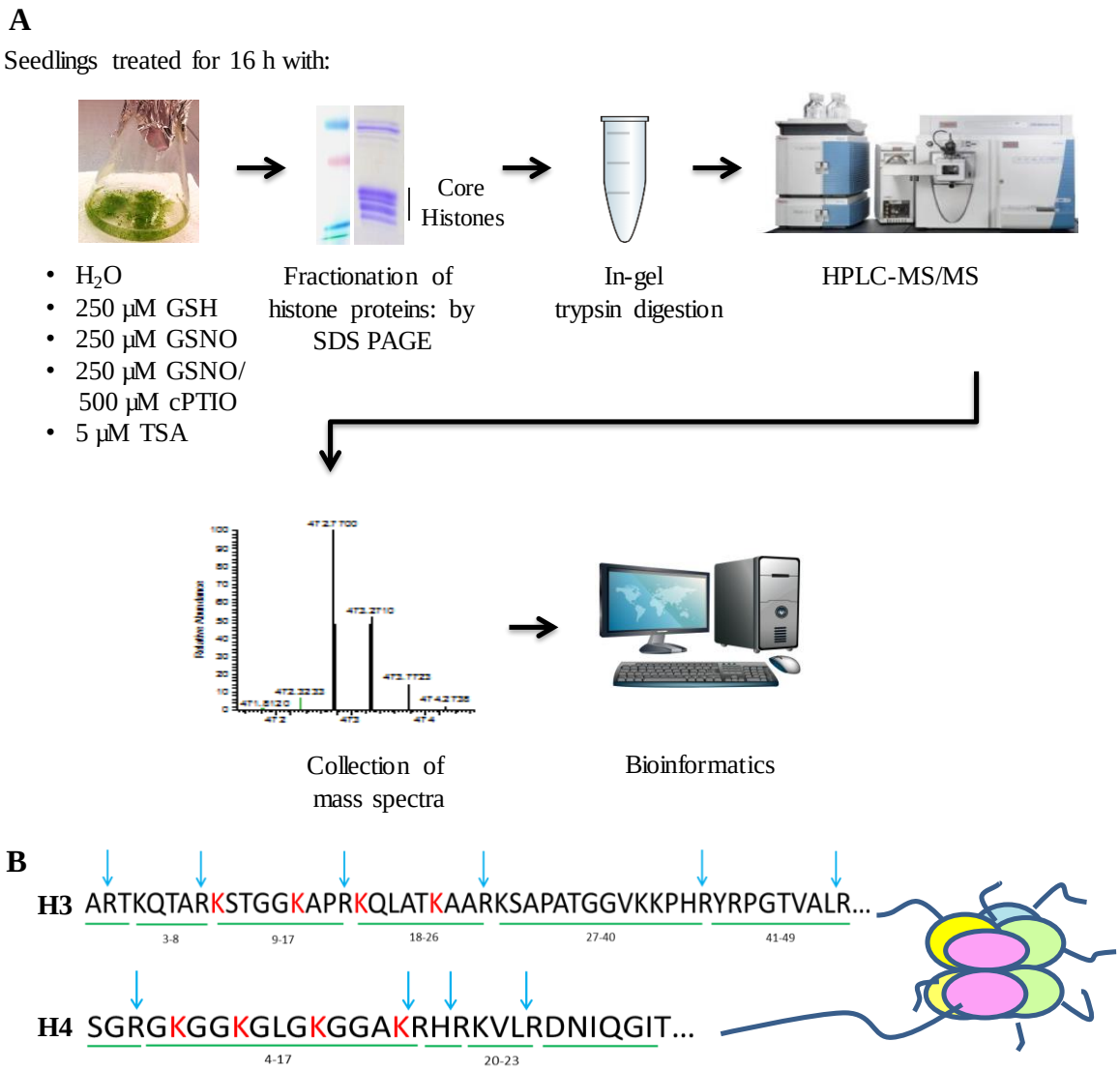

Figure 7: Mass spectrometry workflow.
A) 7-days old seedlings grow in liquid medium were treated for 16 h with H_2O, 250 µM GSNO, 250 µM GSH, 250 µM GSNO/500 µM cPTIO and 5 µM TSA. Histone proteins were extracted using a Histone extraction Kit. Core histones were cut from the gel and digested by trypsin followed LC-MS/MS. Mass spectra were analyzed with Xcalibur™ software (Thermofisher). B) Amino acid sequences of H3 and H4. Trypsin digestion occurs after every arginine (R) which is shown with a blue bolt. Lysines which might be acetylated are marked in red.

Treatment of seedlings with GSNO results in a slight but not significant increase (9 %) in acetylation level on peptide 9-17, that contains lysine 9 (K9) and lysine 14 (K14) on H3, and no changes were observed on peptide 18-26, that contains lysine 18 (K18) and lysine 23 (K23) (**Figure 8A**). Peptide 4-17 on H4 shows an elevated but not significant acetylation level (31.6 %) after GSNO treatment in comparison to the water treated samples. Seedlings treated

with TSA demonstrated a significant rise in acetylation on H3 (between 37 % to 47 %) as well as on H4 (174 %). It should be noted that plants supplied with GSH or NO scavenger cPTIO, showed a decreasing acetylation tendency on H3 and H4, respectively, compared to GSNO treatment alone, indicating that NO might be involved in regulation of histone acetylation.

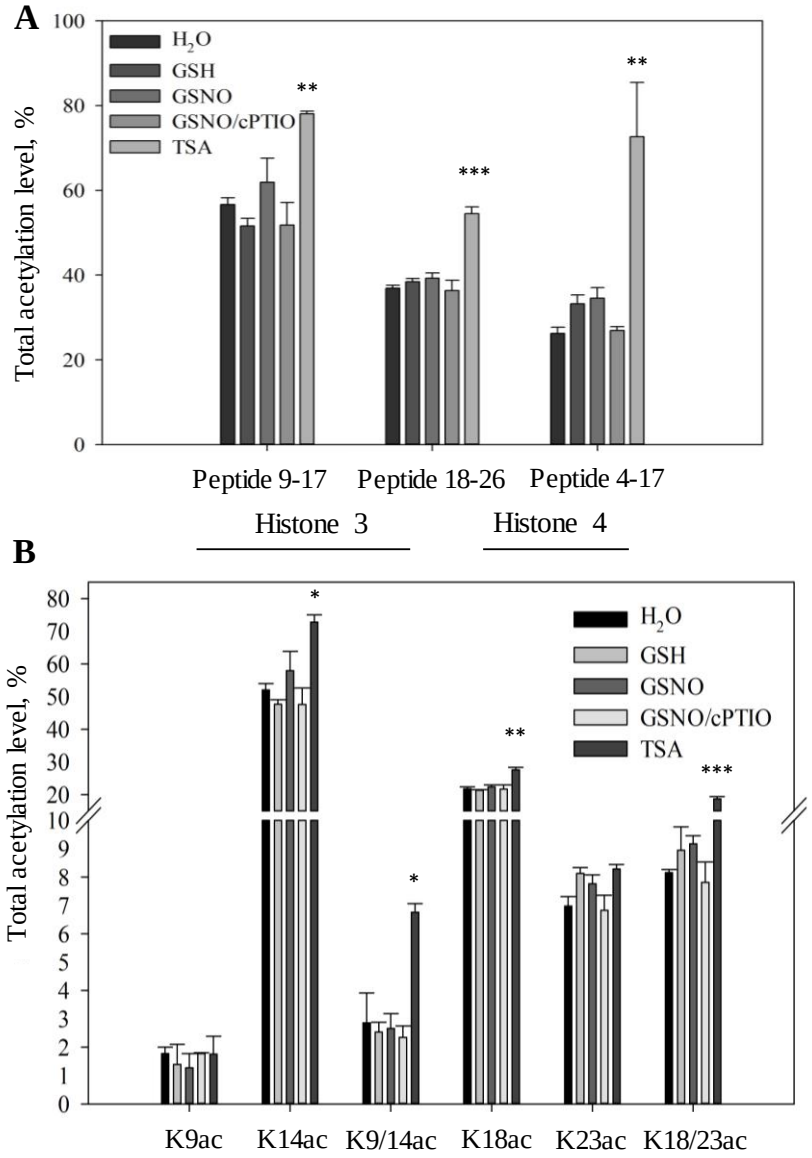

Figure 8: LC-MS/MS analysis revealed a slight but not significant increase of H3 and H4 acetylation level after GSNO treatment in seedlings.
Seedlings growing in liquid culture were treated for 16 h with H_2O, 250 µM GSH, 250 µM GSNO, 250 µM GSNO plus 500 µM cPTIO, and 5 µM TSA. Histones were extracted using a commercial histone purification kit (Active Motif) and loaded on 12 % precast polyacrylamide gel (Bio-RAD). Histone bands were cut out together and distained. Lysines were blocked with deuterated acetic anhydride (Sigma Aldrich) and peptides were digested by trypsin (Promega) followed by release from the gel pieces by acid extraction. Additionally peptides were purified using SPE C18 Carbon (Agilent Technologies) and TOPTIP TT1CAR mini-spin columns (Glysci) before loading to LC-MS/MS. A) Total acetylation abundance was calculated according to [183]. Shown is the ±SE of tree independent experiments (N=3). One way ANOVA (DF=4; peptide 9-17: p=0,002; peptide 18-26: p<0,001; peptide 4-17, p<0,001) with Holm-Sidak post-hoc test for each treatment group vs. the control group (H_2O treatment) was performed. (B) Lysine acetylation on H3. All treatments were compared to H_2O treatment. One way ANOVA (DF=4; K14ac: p=0,015; K9/14ac: p=0,009; K18ac: p=0,004; K18/23ac: p<0,001) with

Holm-Sidak post-hoc test for each treatment group vs. the control group was performed. *p≤0.05, **p≤0.01 and ***p≤0.001.

The lysine acetylation pattern of H3 is quantified and compared to H_2O (control) treatment (**Figure 8B**). A slightly enhanced acetylation level is observed after GSNO treatment at K14 (11.5 %), K23 (11 %) and K18/23 (12 %). Notably, histone acetylation is reduced at these marks when cPTIO was additionally applied. Treatment of seedlings with GSH resulted in increased acetylation at K23 (16 %) and K18/23 (9.7 %). Although the observed results for GSNO and GSH treatment are not statistically significant, there seems to be a trend towards an enhanced histone acetylation at several marks. A significant higher histone acetylation is observed after TSA treatment at K14 (40 %), K9/14 (140 %), K18 (26.7 %) and K18/23 (128 %). All other modifications do not seem to be affected after GSNO or TSA treatment or the differences are too small to be detected by mass spectrometry.

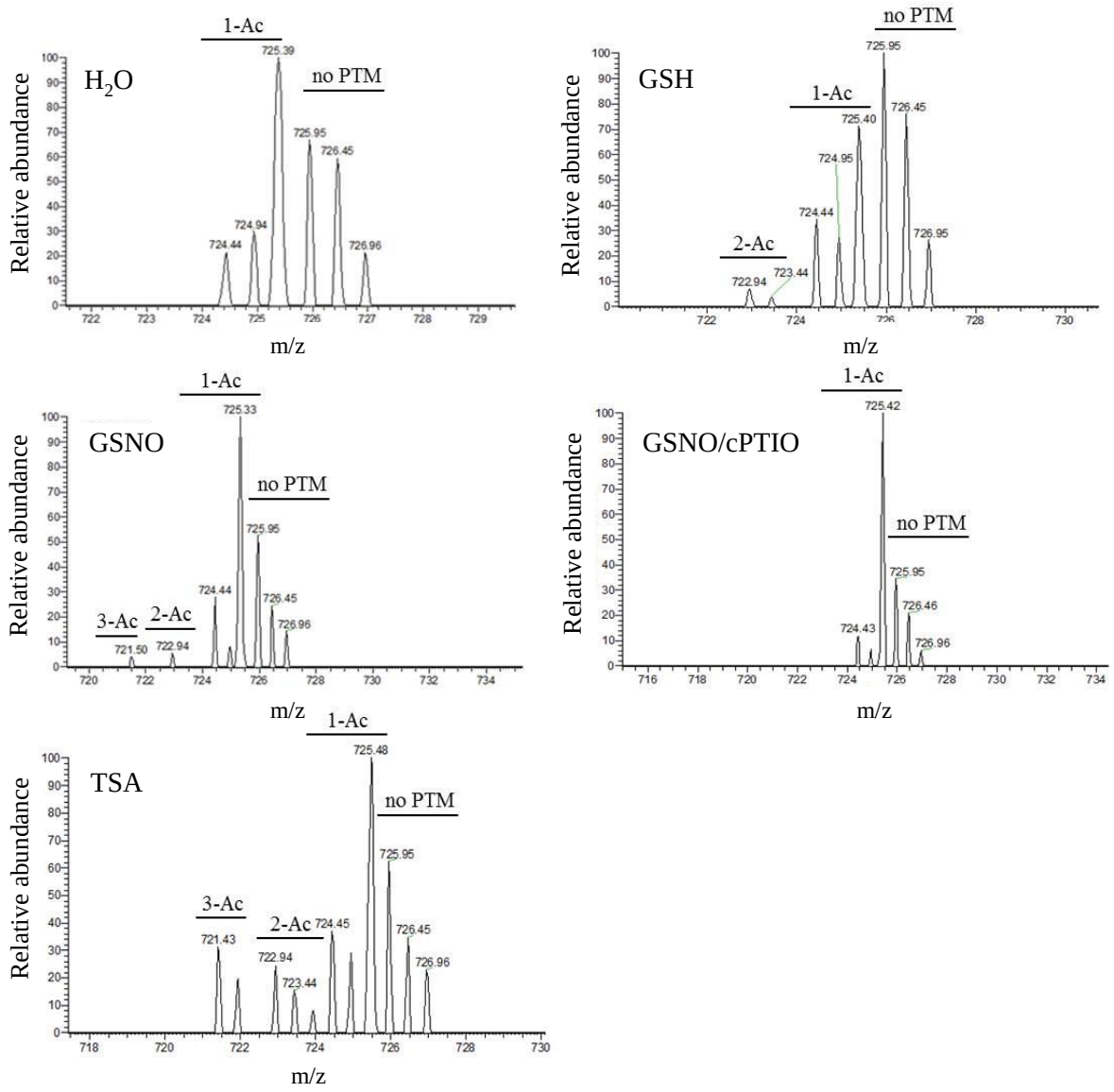

Figure 9: Treatment of seedlings with GSNO and TSA results in a triple acetylation motif on H4.

Seedling in liquid culture were incubated for 16 h with water, 250 µM GSH, 250 µM GSNO, 250 µM GSNO plus 500 µM cPTIO, and 5 µM TSA. Histones were extracted and separated on 12 % precast polyacrylamide gel and stained with Coomassie Brilliant Blue staining solution. H3 and H4 bands were cut together and distained. Lysines were blocked with deuterated acetic anhydride and peptides were digested by trypsin followed by release from the gel pieces through acid extraction. Peptides were purified using SPE C18 Carbon and TOPTIP TT1CAR mini-spin columns before subjecting to LC-MS/MS. MS1 spectra were obtained from Xcalibur 2.2 SP1 software. Theoretical mass to charge (m/z) ratio was calculated using GPMAW 5.0 software. 1-, 2-,3-Ac are acetylated motifs present in the samples. No PTM is a m/z ratio of not posttranslational modified peptide. Shown is one representative experiment of three independent replicates (N=3).

The N-terminal tail of H4 contains four lysine residues that are located at peptide 4-17. All these lysines can be acetylated separately or in combination with each other. In total 15 modifications are possible at this peptide (**Supplemental Figure 1**). Because of this complexity it was not possible to distinguish the differences among those sites in *Arabidopsis* seedlings. But from the MS1 spectra it is clearly seen that after GSNO and GSH treatment a double acetylation motif is present which was not found after H_2O treatment or when seedlings were incubated together with GSNO and cPTIO. A triple acetylation motif could be identified after GSNO and TSA treatment (**Figure 9**).

The same experimental set up was used to analyze a global histone acetylation of *A. thaliana* seedlings by immunoblotting. GSNO enhanced the abundance of all dissected histone marks compared to the water treatment, namely a significant increase was observed on H3ac (2.3-fold) and H3K9ac (2.2-fold). The levels of the histone marks H4ac (2.2-fold) and H4K5ac (4.5- fold) are also more than 2-fold enhanced compared to the control group, however the results are not significant because of the too high relative intensity observed after TSA treatment. If this group would be excluded in the one way ANOVA test, the results for GSNO treatment would become significant. For H3K9/14ac there also seems to be a trend towards a higher histone acetylation level (2.1- fold) in the GSNO treated samples in comparison to the water treated seedlings, however the results did not reach a statistical significance (**Figure 10)**. Enhanced histone acetylation was also observed after application of 5 µM TSA. A significant 2.5-fold increase was detected on H3ac, whereas the increase on H3K9ac (1.4-fold) and H3K9/14ac (1.8-fold) was not significant. Notably, TSA shows a stronger effect on H4. Acetylation of H4 and H4K5 demonstrates a significant 18-fold and 32-fold increase, respectively, compared to the control. Treatment of seedlings with GSH also seems to induce an increase in histone acetylation at the analyzed histone marks, however the results are not significant. Simultaneous application of cPTIO and GSNO to the seedlings seems to explain the decreased acetylation abundance of all analyzed histone marks versus GSNO treatment alone, suggesting again that the tendency of the observed histone acetylation changes might be a result of NO functions on chromatin modulation.

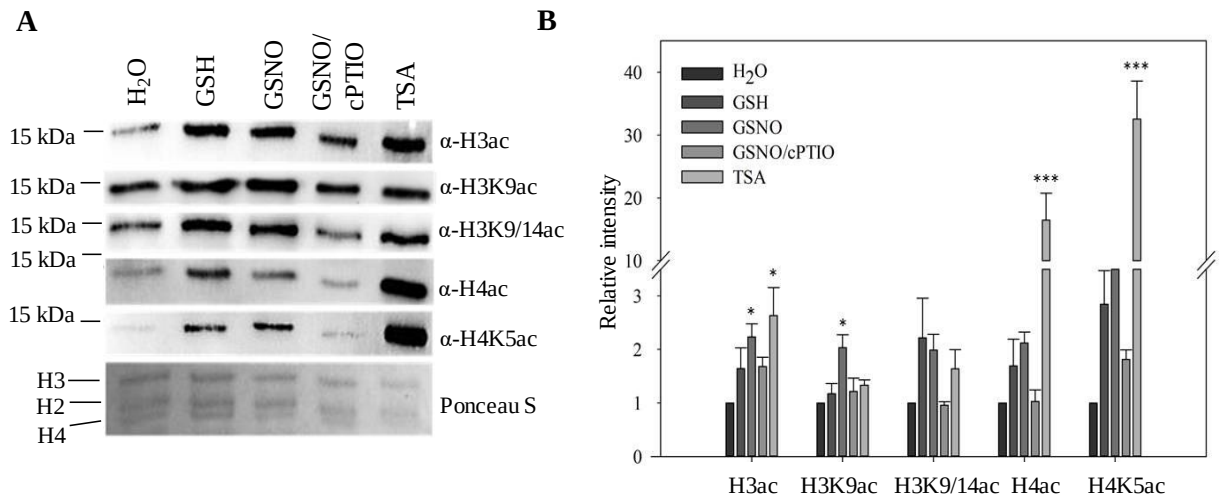

Figure 10: GSNO and TSA treatments of *Arabidopsis* seedlings result in H3 and H4 acetylation.
7-days old seedlings grown in liquid medium were incubated for 16 h with water, 250 µM GSH, 250 µM GSNO, 250 µM GSNO plus 500 µM cPTIO, and 5 µM TSA. Histones were extracted using a commercial histone purification kit and separated on 12 % precast polyacrylamide gel followed by transferring them into nitrocellulose membrane. Antibodies used for analysis: acetylated-H3 (1:20000), acetylated-H3K9 (1:5000), acetylated-H3K9/14 (1:2000), acetylated-H4 (1:20000), and acetylated-H4K5 (1:10000). A second antibody was an anti-rabbit HRP (1:2500). The band detection was performed on a Fusion Fx7. B) Quantitative analysis of A. Signal intensity was determined with Image J software. The relative intensity of the control group in N=3 was set up to 1 [181]. Shown is a ±SE of three independent experiments (N=3). One way ANOVA (DF=4; H3ac: p=0,029; H3K9ac: p=0,020; H3K9/14ac: p=0,153; H4ac: p<0,001; H4K5ac: p<0,001) with Holm-Sidak post-hoc test for each treatment group vs. the control group was performed. *p≤0.05, **p≤0.01 and ***p≤0.001. This result was published in [180].

It appears that an analysis of histone acetylation via immunoblotting seems to be more sensitive than via mass spectrometry for our experimental system. For example, a 18-fold increase in acetylation level was detected on H4 after TSA treatment by immunoblotting (**Figure 10**) whereas only a 2.7-fold increase by mass spectrometry (**Figure 8A**).

All in all, these results provide evidence that there could be an effect of GSNO-released NO on H3ac and H4ac, since the level of the analyzed histone marks in the GSNO treated seedlings is higher than in the corresponding water treated seedlings and in the same time was decreased by cPTIO. However, it has to be emphasized that the differences were not significant for all analyzed histone marks.

2.1.2 Tendency towards enhanced histone acetylation by endogenously produced NO

The use of GSNO as NO donor is prevalent in many studies. However, several indications avoid a widespread view of GSNO as spatially controlled production of NO. First, GSNO itself cannot be directly resorbed by a cell. GSNO can release NO to media, but this process is

strongly dependent on media conditions [184]. Second, it can cause artificial results, since it might not match with the range of physiological NO concentration and moreover it may act in areas other than endogenous produced NO [185]. Therefore, a plant hormone, salicylic acid (SA) and its functional chemical analogue 2,6-dichloro-isonicotinic acid (INA), are used to look for biological NO effects, since both are known to stimulate endogenous NO production [186][180]. The effect of SA and INA on the HDAs activity in protoplasts was analyzed. It was found that HDAs activity is inhibited by both compounds in a concentration dependent manner [179][180].

Subsequently, the impact of INA on global histone acetylation was analyzed by immunoblotting. 7-days old *Arabidopsis* seedlings grown in liquid were treated for 16 h with 500 µM INA, 500 µM INA / 500 µM cPTIO and methanol as a control. It seems that there is a tendency of enhanced histone acetylation induced by INA, however the results were not statistically significant. INA treatment lead to a slight increase of the histone acetylation abundance on the following marks: H3ac (1.4-fold), H3K9/14ac (1.6-fold), H4ac (1.5-fold) and H4K5ac (1.8-fold), whereas acetylation level at H3K9ac seems not to be effected (**Figure 11A and B**). Simultaneous application of INA/cPTIO seems to lead to a tendency towards a deceased histone acetylation (with the exception of H3K9ac and H3K9/14ac) in comparison to INA treatment alone.

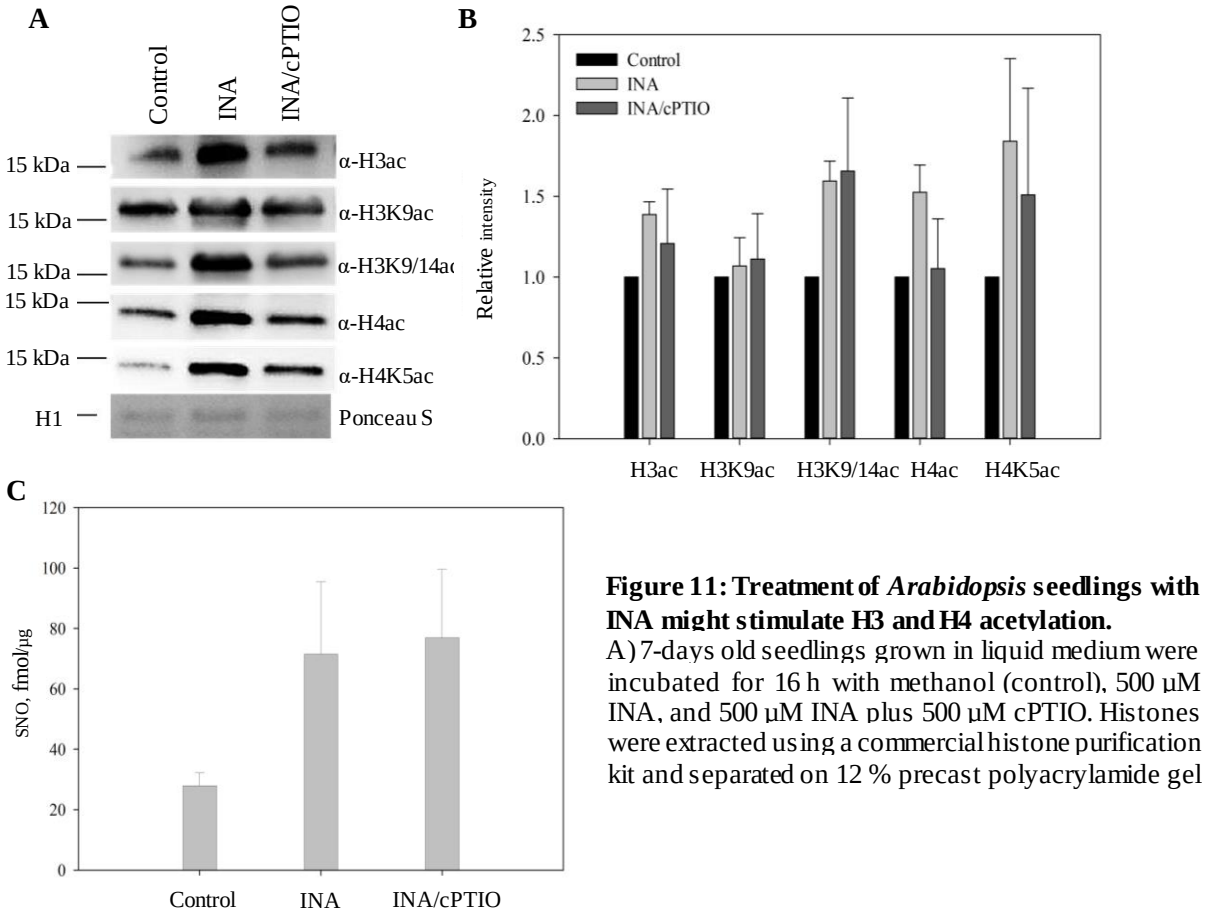

Figure 11: Treatment of *Arabidopsis* seedlings with INA might stimulate H3 and H4 acetylation.
A) 7-days old seedlings grown in liquid medium were incubated for 16 h with methanol (control), 500 µM INA, and 500 µM INA plus 500 µM cPTIO. Histones were extracted using a commercial histone purification kit and separated on 12 % precast polyacrylamide gel

followed by a transfer into nitrocellulose membrane. Antibodies used for analysis: acetylated-H3 (1:20000), acetylated-H3K9 (1:5000), acetylated-H3K9/14 (1:2000), acetylated-H4 (1:20000), and acetylated-H4K5 (1:10000). A second antibody was an anti-rabbit HRP (1:2500). Bands detection was performed at Fusion Fx7. B) Quantitative analysis of A. Signal intensity was determined with Image J software. The relative intensity of the control group in n=3 was set up to 1 [181]. Shown is a ±SE of three independent experiments (N=3). One way ANOVA (DF=2; p=0,439) was performed. C) SNO content was measured using Nitric oxide analyzed NOA 280i. Shown is a ±SE of three independent experiments (N=3). One way ANOVA (DF=2; p=0,328) was performed. No significant changes are observed. These results are published in [180].

Often SNO formation is associated with a ‘’NO reservoir’’ where NO bioactivity is stored [187]. Therefore, SNO content was measured in the same samples. As demonstrated in **Figure 11C** INA treatment leads to more than two times increase (not significant) in formation of SNOs than in control seedlings. However, in INA/cPTIO treated seedlings the SNO amount is unexpectedly as high as in seedlings treated with INA alone.

All in all, although the results are not statistically significant, there seems to be a tendency that the chemical analog of a plant hormone SA, INA, is able to induce SNOs production in *Arabidopsis* seedlings as the observed SNOs amount was higher than in control plants. Furthermore, there is a tendency of INA-induced H3 and H4 acetylation, however a larger sample size would be required to achieve statistically more robust results.

2.1.3 Correlation between histone acetylation and gene expression

Histone acetylation is often associated with active chromatin. Since there is a tendency of NO modulation of histone acetylation, the question arises whether NO is involved in regulation of gene transcription? A link between NO and H3K9/14ac has been demonstrated previously [180] (some parts of this thesis were published in this publication). In this study an anti-H3K9/14ac antibody was used for a ChIP-seq experiment because it has not been used before in profiling genome-wide studies in plants. Moreover, in [180] as well as in this thesis the acetylation level at this position was two times higher than in water treated seedlings, however the increase was statistically not significant in this thesis because one way ANOVA was chosen over t-test in the collaboration work (**Figure 10**). In total 746 NO specific loci were identified after 3 h and 16 h GSNO treatment. Functional classification of these loci demonstrated that most of them are involved in plant defense and cold stress response as well as in chloroplast organization [179][178]. To analyze whether H3K9/14 acetylation of target genes correlates with gene expression, the transcriptional level of several randomly selected genes was dissected by qPCR using the same plant material as for the ChIP-seq. 5 of 14 analyzed genes are upregulated after GSNO treatment, whereas all other genes are transcriptionally inactive despite their high acetylation levels (**Figure 12**), suggesting that histone acetylation does not necessarily correlate with gene expression.

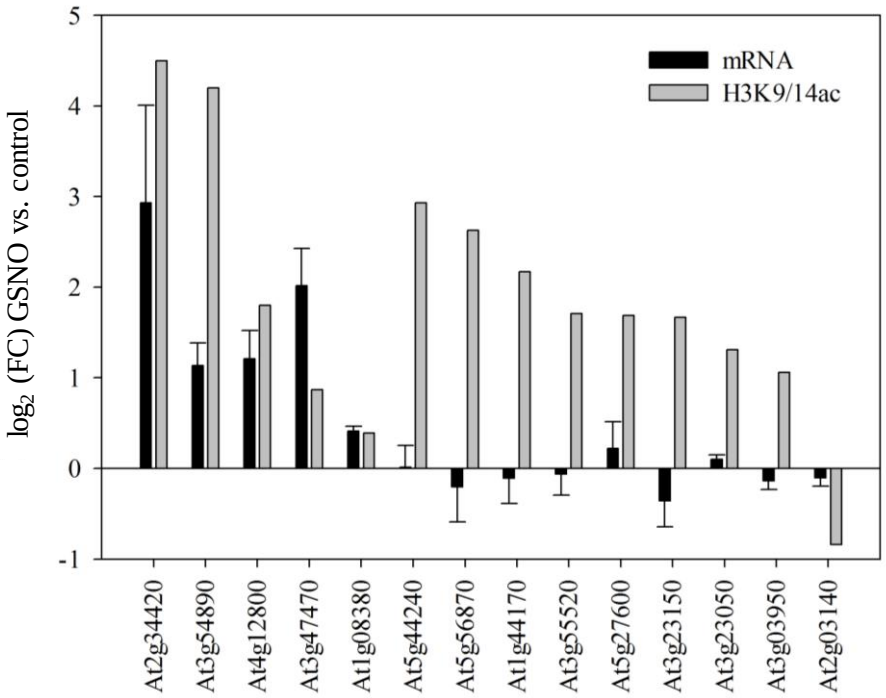

Figure 12: GSNO-altered H3K9/14ac of some genes does not necessarily lead their gene expression. Acetylation of genes after incubation of *Arabidopsis* 7-days old seedlings grown in liquid medium with 250 µM GSNO was found and analyzed [179][180]. qPCR analysis was performed on ABI 7500. mRNA was isolated from the same plant material as for the ChIP-seq and normalized to S16 and UBQ. Shown is a ±SE of two independent experiments. One way ANOVA is performed. No significant changes are observed. These results are published in [180].

2.1.4 NO-dependent modulation of chromatin structure

Several of the previous results point in the direction that there might be a trend in NO-induced modulation of histones. Therefore, the question arises how NO mediates these modifications? Two hypotheses are available to examine this question. The first hypothesis is based on the influence of NO on the expression level of *Arabidopsis* HDAs. The second hypothesis is based on the direct effect of NO on HDAs functions, since it has already been demonstrated that plant total HDAs activity is reduced upon GSNO or SNAP treatment [180][179].

To investigate whether NO effects an expression of HDA genes, transcripts of HDAs were analyzed in 7-days old seedlings of *A. thaliana* after 16 h treatment with 250 µM GSNO or 250 µM GSH. H_2O treated seedlings were used as a control. No significant changes were observed within the treatments (**Figure 13**), suggesting that NO might affect histone acetylation by posttranslational modifications.

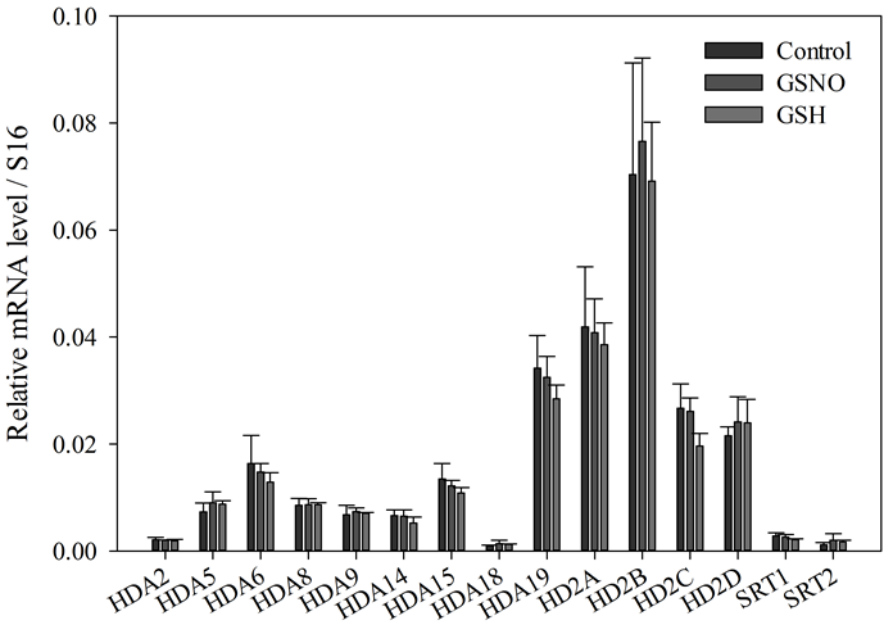

Figure 13: GSNO and GSH treatments do not change transcriptional level of HDAs.
7-days old seedlings grown in liquid medium were incubated for 16 h with water, 250 µM GSH and 250 µM GSNO. 100 mg of seedlings were used for RNA extraction with Rneasy Plant Mini Kit. cDNA was synthetized using QuantiTect Reverse Transcription Kit and diluted for analysis 1:20. qPCR was performed on ABI 7500. mRNA level of HDAs was normalized to S16. Shown is a ±SE of three independent experiments (N=3). One way ANOVA is performed. No significant changes are observed. These results are published in [180].

In the second step the influence of NO on HDAs functions was investigated. Moreover, a search for a putative NO-sensitive HDA was conducted. Since the inhibition of total HDAs activity induced by NO donors has been shown [178][179], it remains to be defined which of the 18 in *Arabidopsis* present HDAs is/are sensitive to NO. Mouse HDA2 was reported to be S-nitrosylated at the cysteine residues Cys-262 and Cys-274 [155]. A BLAST search identified two histone deacetylases, HDA6 and HDA19, as the closest homolog to mouse HDA2 with 61 % and 57 % identity, respectively (**Figure 14**).

```
mHDA2:      ---------TAEEMTKYHSDEYIKFLRSIRPDNMSE--YSKQMQRFNVGEDCPVFDGLFE    49
AtHDA6:     LEISRPSLADASDIGRFHSPEYVDFLASVSPESMGDPSAARNLRRFNVGEDCPVFDGLFD    60
AtHDA19:    --VLKPFPARDRDLCRFHADDYVSFLRSITPETQQD--QIRQLKRFNVGEDCPVFDGLYS    56
                      :: ::*: :*:.** *: *:.  :    ::::**************:.

mHDA2:      FCQLSTGGSVAGAVKLNRQQTDMAVNWAGGLHHAKKSEASGFCYVNDIVLAILELLKYHQ    109
AtHDA6:     FCRASAGGSIGAAVKLNRQDADIAINWGGGLHHAKKSEASGFCYVNDIVLGILELLKMFK    120
AtHDA19:    FCQTYAGGSVGGSVKLNHGLCDIAINWAGGLHHAKKCEASGFCYVNDIVLAILELLKQHE    116
            **:  :***:..:****:   *:*:**.********.*************.****** .:

mHDA2:      RVLYIDIDIHHGDGVEEAFYTTDRVMTVSFHKYGEYFPGTGDLRDIGAGKGKYYAVNFPM    169
AtHDA6:     RVLYIDIDVHHGDGVEEAFYTTDRVMTVSFHKFGDFFPGTGHIRDVGAEKGKYYALNVPL    180
AtHDA19:    RVLYVDIDIHHGDGVEEAFYATDRVMTVSFHKFGDYFPGTGHIQDIGYGSGKYYSLNVPL    176
            ****:***:***********:***********:*::*****.::*:*  .****::*.*:
                                             |          |
mHDA2:      RDGIDDESYGQIFKPIISKVMEMYQPSAVVLQCGADSLSGDRLGCFNLTVKGHAKCVEVA    229
AtHDA6:     NDGMDDESFRSLFRPLIQKVMEVYQPEAVVLQCGADSLSGDRLGCFNLSVKGHADCLRFL    240
AtHDA19:    DDGIDDESYHLLFKPIMGKVMEIFRPGAVVLQCGADSLSGDRLGCFNLSIKGHAECVKFM    236
             **:****:  :*:*:: ****:::* ********************::****.*:..

mHDA2:      KTFNLPLLMLGGGGYTIRNVARCWTYETAVALDCEIPNELPYNDYFEYFGPDFKLHISPS    289
AtHDA6:     RSYNVPLMVLGGGGYTIRNVARCWCYETAVAVGVEPDNKLPYNEYFEYFGPDYTLHVDPS    300
AtHDA19:    RSFNVPLLLLGGGGYTIRNVARCWCYETGVALGVEVEDKMPEHEYYEYFGPDYTLHVAPS    296
            :::*:**::*************** ***.**:. *  :::* ::*:******:.**: **

mHDA2:      NMTNQNTPEYMEKIKQRLFENLRMLPHAPGVQMQAIPEDAVHEDSGDEDG--EDPDKRIS    347
AtHDA6:     PMENLNTPKDMERIRNTLLEQLSGLIHAPSVQFQHTPPVNRVLDEPEDDMETRPKPRIWS    360
AtHDA19:    NMENKNSRQMLEEIRNDLLHNLSKLQHAPSVPFQERPPDTETPEVDE---DQEDGDKRWD    353
             * * *: : :*.*:: *:.:*  * ***.* :*  *      :  :     .   :  .

mHDA2:      IRAS------D--KRI---ACDEEFSDSEDEGEGGRRNVADHKKGAKKARIEEDKKETED    396
AtHDA6:     GTATYESDSDDDDKPLHGYSCRGGATT--------------------DRDSTGEDEMDD    399
AtHDA19:    PDSDMD--VDDDRKPIPSRVKREAVEP-DTKDKDGLKGIMERGKGCEVEVDESGSTKVTG    410
              :       *  * :                                  . .. :  .

mHDA2:      -KKTDVKEEDKSKDNSGEKTDPKGAKSEQLSNP--    428
AtHDA6:     DNPEP----------------------DVNPPSS    411
AtHDA19:    VNPVGVEEASVKMEE--EGTN-KG-GAEQAFPPKT    441
             :                          :   *
```

Figure 14: *Arabidopsis thaliana* HDA6 and HDA19 show a high amino acid sequence homology to mouse HDA2.
Alignment was performed using Clustal Omega. Conserved cysteines are marked in red, cysteines that are S-nitrosylated in mouse HDA2 are indicated with asterisks. Catalytically important residues are shown in blue. Histone deacetylase region is marked in green.

It should be also noted that cysteines, which are nitrosylated in HDA2 are highly conserved in HDA6 and HDA19 and are located at the same positions in the 3D structure of the enzymes (**Figure 15**).

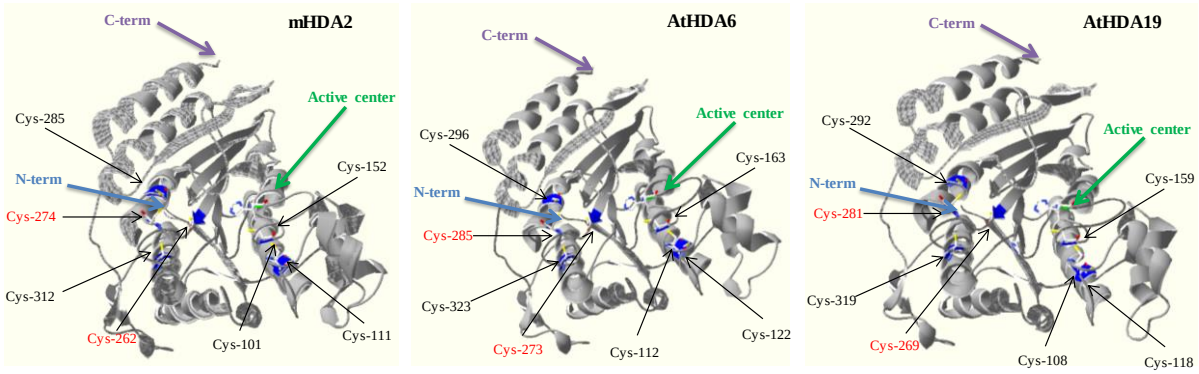

Figure 15: *Arabidopsis thaliana* HDA6 and HDA19 demonstrate a similar protein folding as mouse HDA2.
The HDA domains of HDA6 (amino acids 18 – 386, Uniprot entry Q9FML2) as well as of HDA19 (amino acids 16 – 382, Uniprot entry O22446) were modelled using the SwissProt Modelling server with mammals HDA2 as a template (4lxz.1.A). The models were visualized with Swiss-PdbViewer. Conserved cysteine residues are

shown in blue and marked with an arrow. Cysteines that are S-nitrosylated in mouse HDA2 as well as predicted redox-sensitive cysteines of HDA6 and HDA19 are indicated in red. The active center is depicted in green.

Moreover, it was found that total HDAs activity is not affected neither by TSA nor SNAP in *hda6* suspension cells [179]. Additionally to this finding, H3ac was analyzed in *hda6* cell culture. H3 acetylation remains unchanged after GSNO and TSA treatment (**Figure 16**), although under the same conditions enhanced H3ac was observed in wild type suspension culture (**Figure 6**).

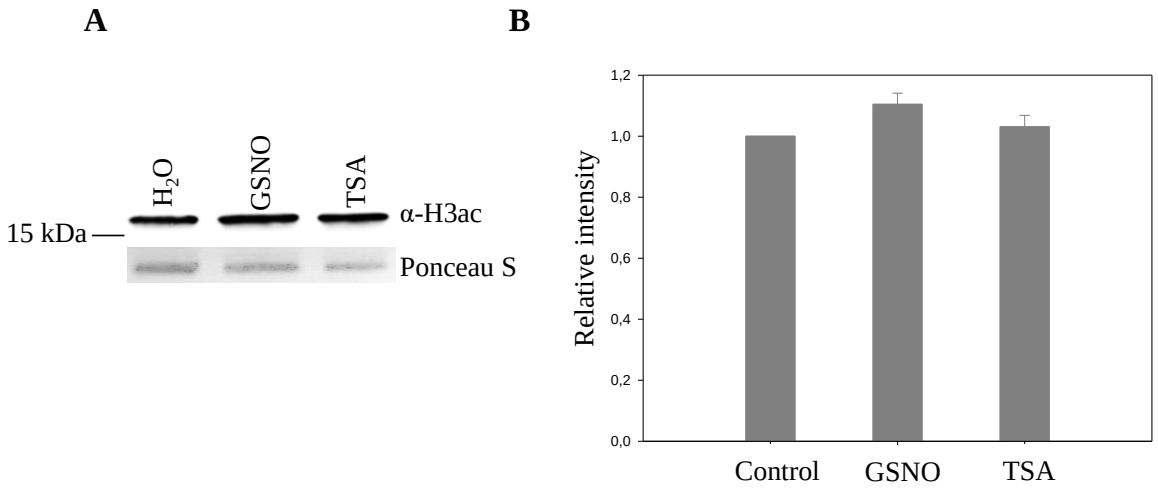

Figure 16: GSNO and TSA treatments do not induce H3 acetylation in *hda6* suspension cells.
A) Cell cultures were incubated for 4 h with 500 µM GSNO, 1 µM TSA (positive control) and water (negative control). Nuclear pellet was directly dissolved in 50 µl laemmli buffer and heated for ca. 10 min at 95 °C. The supernatant was transferred into a new tube and concentration measured with RCDC Assay. 15 µg of nuclear protein was separated on 12 % SDS-PAGE gel and blotted into nitrocellulose membrane. The membrane was incubated over night with anti-acetyl H3 primary antibody (1:20000) at 4 °C and for 1 h with a secondary antibody coupled to HRP (1:2500). A) Shown is one representative experiment. B) Quantitative analysis of A. Signal intensity was determined with Image J software. Shown is a ±SE of three independent experiments (N=3). The relative intensity of the control group in N=3 was set up to 1 [181]. One way ANOVA was performed. No significant changes were observed.

To find out whether HDA6 is NO sensitive, a recombinant Flag-HDA6 was produced in *A. thaliana*. A pEarleyGate202 was used to transform wild type plants by floral dip. Presence of Flag-HDA6 gene in transformed lines was demonstrated by RT-PCR (**Figure 17A**). Lines A18 and A23 were chosen for further selection of homozygous line. Recombinant Flag-HDA6 was purified as described [169]. Immunoblotting analysis using an anti-Flag antibody confirmed the presence of recombinant protein in transgenic lines, with a predicted size around 55 kDa, which was absent in non-transgenic plants (**Figure 17B**). Catalytic activity of Flag-HDA6 was demonstrated by its incubation with 1 µM TSA that reduces the activity of Flag-HDA6 to 36 % (64 % inhibition) in comparison to the control, indicating that the recombinant protein is functional. The influence of NO at the protein activity was measured according to [188] or by using a commercial kit. Both methods proved the hypothesis of NO-

sensitivity of HDA6. Treatment of recombinant protein with 0 – 500 µM GSNO results in a slight reduction of HDA6 activity (**Figure 17C and D**, **Supplemental Figure 2**). Application of 1 mM GSNO leads to 30 % inhibition of HDA activity. However, its activity was not restored by a subsequent treatment with 5 mM DTT how it normally would be expected if the inhibition would be a result of S-nitrosylation; even more DTT leads to a higher reduction of HDA6 activity. Treatment of Flag-HDA6 with GSH does not impair the catalytic activity at all (**Supplemental Figure 2**).

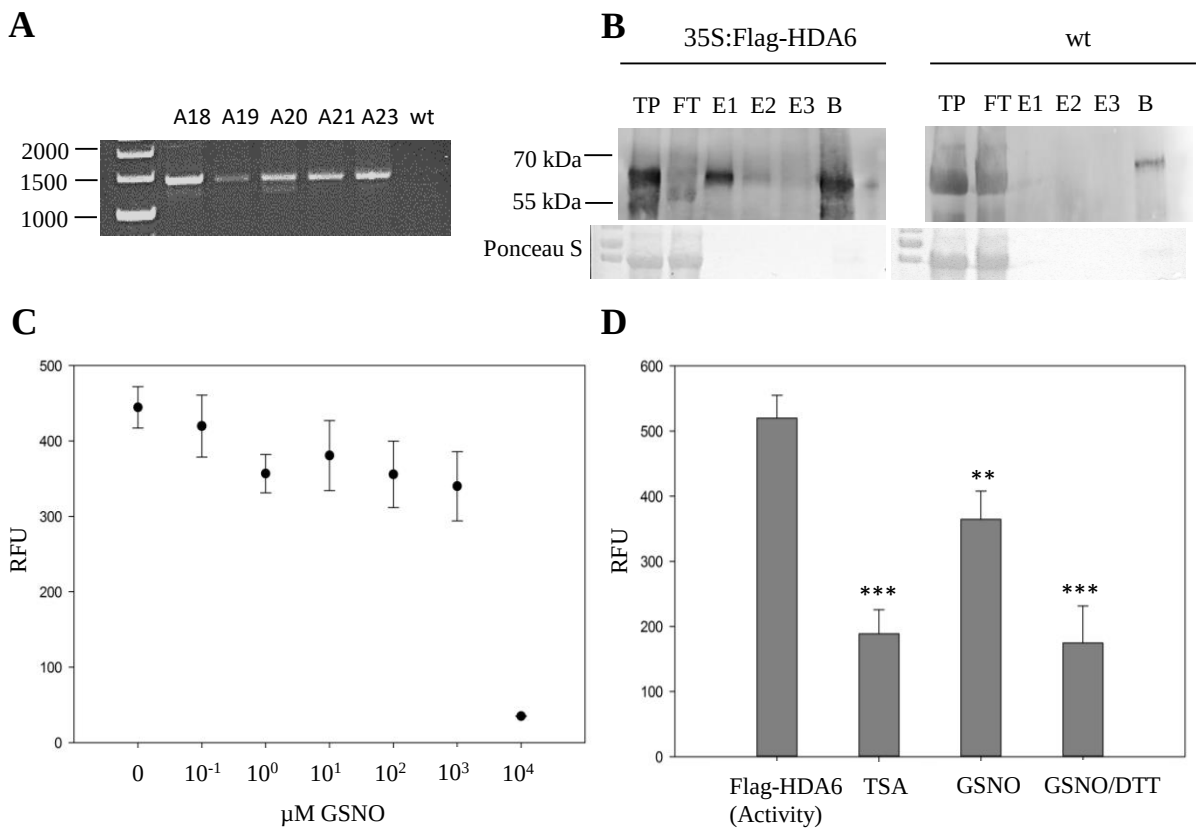

Figure 17: GSNO inhibits an activity of recombinant 35S:Flag-HDA6.
A) RT-PCR of transgenic 35S:Flag-HDA6. Five heterozygous lines A18-A21, and A23 were determined. cDNA of wt was used as a negative control. Predicted size of 35S:Flag-HDA6 is around 1470 bp. B) Immunoblot of overexpressed 35S:Flag-HDA6. Total protein (TP) was extracted from 1g of freshly ground leaves of A18 transgenic and wt line using CelLytic P buffer. Not bounded proteins (FT) to FLAG resin were discarded. Recombinant protein was eluted with 200 ng/ml Flag peptide for three times (E1-E3). Anti-Flag tag antibody (1:1000) was used for detection. Predicted size of 35S:Flag-HDA6 is around 57 kDa. Shown is one representative experiment of at least of three replicates. C) Inhibition of 35S:Flag-HDA6 activity by GSNO. The recombinant plant HDA6 was incubated with 0.1 – 10000 µM GSNO for 20 min. D) Activity of 35S:Flag-HDA6 after its treatment with 1 µM TSA, 1 mM GSNO and 1 mM GSNO/5 mM DTT. HDA activity was measured using Fluorogenic HDA Activity Assay. Shown is a ±SE of at least three independent experiments (N>3). One way ANOVA (DF=3; p<0,001) with Holm-Sidak post-hoc test for each treatment group vs. the control group (Flag-HDA6 activity) was performed, **p≤0.01, ***p≤0.001.

In conclusion, these results let assume that the observed NO-induced trends in histone acetylation are due to NO-dependent inhibition of HDAs activity. Moreover, two putative

Arabidopsis HDAs (HDA6 and HDA19) were identified as candidates for NO-sensitive HDAs.

2.2 Interaction between NO and light/temperature

Five genes, which were coincidently selected in chapter 2.1.3 and whose transcriptions correlate with enhanced H3K9/14ac function in chloroplast organization. Analyzing the functions of these genes in more detail, it was found that they are encoding for different light harvesting complex proteins and for photosystem I subunit L (**Table 1**). Interestingly, the same genes are upregulated after fumigation of 4-weeks old *Arabidopsis* plants with NO as well [77]. This indicates that NO might be involved in the regulation of the photosynthetic apparatus. Since photosynthesis is a light-dependent process, the influence of light on NO production and the impact of NO and light on chromatin structure were investigated. To investigate the physiological functions of SNO/NO in these processes a *hot5-2 Arabidopsis* mutant, which is impaired in GSNO reductase function and therefore results in GSNO accumulation, was used for all further experiments instead of a pharmacological approach with NO donors.

Table 1: NO-induced hyperacetylation and upregulation of photosynthesis-related genes.

TAIR	Name	Hyperacetylated gens (ChIP-Seq) after 3 h GSNO treatment in the dark (Col-0)	Microarray data of fumigated plants with 3 ppm over the vegetation period (Was)
		Log2 fold change wt vs. wt 250 µM GSNO	Fold change wt vs. wt 3 ppm
At3g54890	Lhca1	4.17	2.09
At3g47470	Lhca4	0.86	2.65
AT5g54270	Lhcb3	3.15	2.53
At2g34420	Lhb1B2	4.5	2.61
At4g12800	PsaL	1.79	2.03

ChIP-seq experiment was performed by comparison of 7-days old seedlings treated either with H_2O or 250 µM GSNO [180]. Microarray experiment was performed by comparison 4-weeks old plants grown on soil and fumigated with Mock or 3 ppm NO over the vegetation period [77].

2.2.1 Effect of enhanced endogenous SNO/NO on photosynthetic apparatus

To quantify the effect of enhanced levels of SNO on photochemical and non-photochemical properties of photosystem II, a MINI-PAM fluorometer was used. The electron transport rate (ETR), an important parameter indicating the photosynthetic performance of plants (efficiency of carbon uptake), seems to be reduced in *hot5-2* mutant (20 % at 616 PAR) compared to wild type plants (**Figure 18A**).

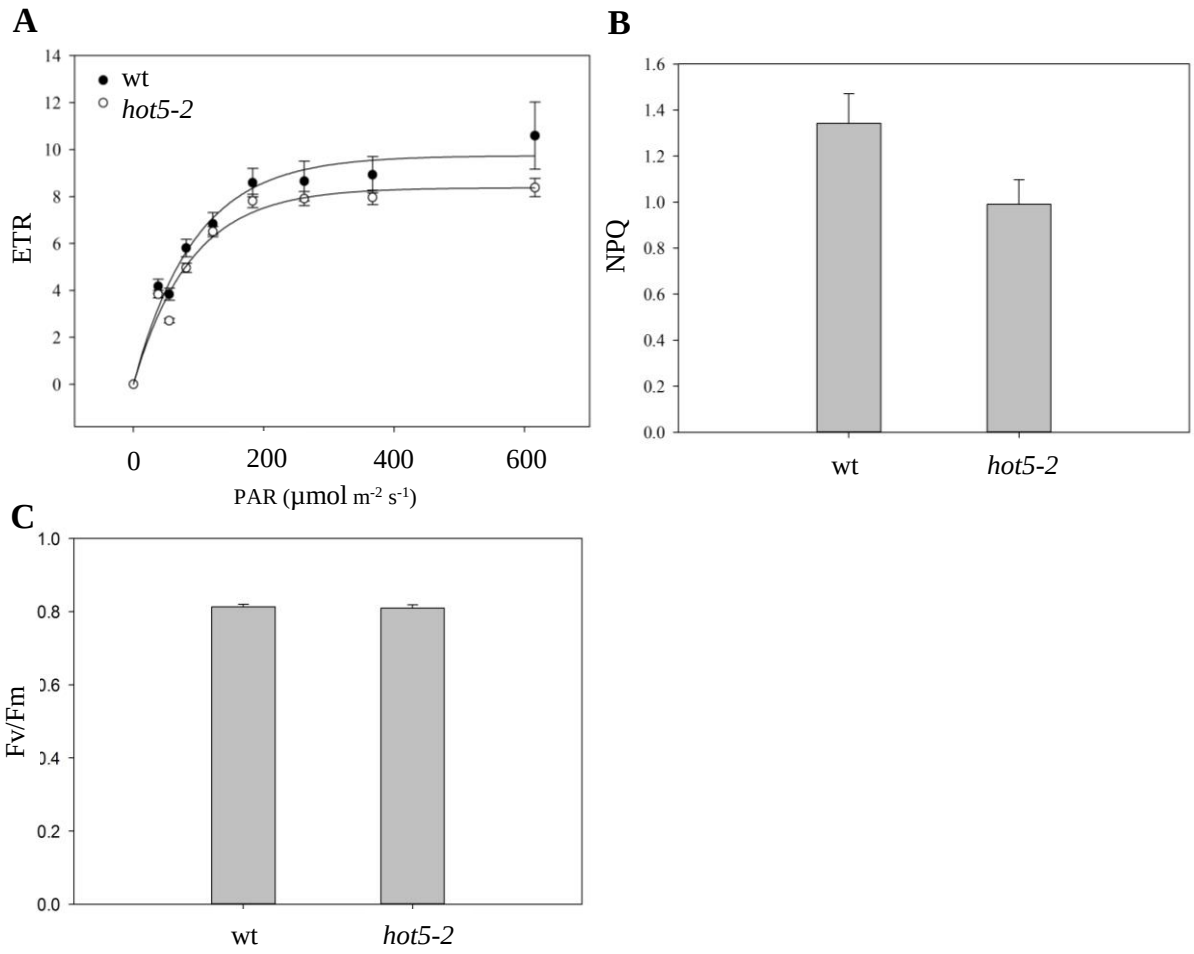

Figure 18: SNOs seems to induce changes in some photosynthetic parameters.
Plants were grown for 4 weeks on soil under short day conditions (10/14 h dark/light, 20/17 °C). A) Photosystem II (PSII) electron transport rate under increasing irradiance (ETR). B) Maximal efficiency of PSII photochemistry (*Fv/Fm*). C) Non-photochemical quenching (*NPQ*). Values are means ±SE (N=16). Student t-test is performed.

There is tendency indicating that accumulation of SNOs leads also to a decrease of non-photochemical quenching (NPQ, 26 %), which is a protective mechanism that plants use to dissipate excess of light energy (**Figure 18B**). Notably, maximum quantum efficiency (Fv/Fm), which also describes how well plants can assimilate light, does not seem to be affected by an elevated SNO level (**Figure 18C**). These results support the idea that NO might selectively attacks photosynthetic parameters and may act in different ways depending on environmental conditions and NO concentration [189].

2.2.2 Light-dependent production of NO

To investigate, whether light is involved in NO production, the NO amount was analyzed by measuring NO emission of a single plant in a closed cuvette using a CLD Supreme NO analyzer. No differences between low light (LL, 200 µmol $m^{-2}s^{-1}$, T 22°C) and dark (D, T

22°C) conditions could be observed (**Figure 19A**), probably because the NO emission of *Arabidopsis* plants under this condition is below the detection limit.

Additionally, endogenous SNO concentration was measured during the short day conditions (10/14 h light/dark, 20/17°C) when 4-weeks old plants were exposed to light for 3 h (at 10:00), 5.5 h (at 11:30) and 7 h (at 14:00) after the light in the growing chamber was switched on and finishing when light was switched off again for 1 h (18:00), 4 h (21:00) and 15 h (at 06:00), respectively. SNO content seems to be light-dependent. A tendency to enhanced SNO concentration was measured under light exposure and lower SNO amounts were observed in the dark. *hot5-2* pointed in the direction of higher levels of SNOs as wild type plants (**Figure 19B**).

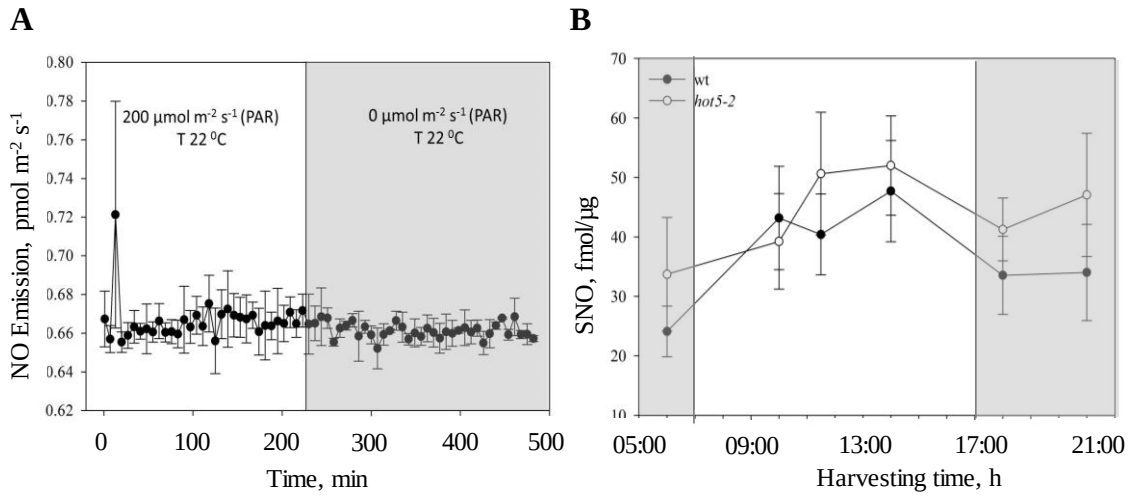

Figure 19: NO emission and SNO content of 4 weeks old plants in light and dark conditions.
Plants were grown on soil for 4-weeks at a short day cycle (10/14 h light/dark, 20/17 °C). A) To obtain the emission only from a plant, the soil was covered with a transparent plastic foil. In a second step it was measured without a plant. The released emission was then subtracted from the plant emission. Light or dark was applied for 4 h using the same temperature (T 22 °C) condition. B) Total S-nitrosothiol level was determined at 06:00, 10:00, 11:30, 14:00, 18:00 and 21:00 o'clock. The light in the chamber was switched on at 07:00 and switched off at 17:00 o'clock. SNOs were reduced with triiodide and the emitted NO was photochemically detected through its reaction with ozone. Shown is a ±SE of at least three independent experiments (N>3). One way ANOVA was performed. No significant changes are observed.

To analyze the role of NO under physiological conditions without application of NO donors, environmental conditions are required which enable a controlled endogenous NO production (production which could be switched on and off). Since under low light exposure only a slight NO production could be observed, a high light condition was applied. Under the natural conditions high light intensity is usually associated with high temperature. Therefore 30°C were adjusted for the high light intensity experiments. The enhanced light intensity (1000 µmol $m^{-2}s^{-1}$) and high temperature (T 30°C) demonstrate a stronger emission of NO in both wild type (ca. 5-fold) and *hot5-2* (ca. 10-fold) than under low light and low temperature conditions (LL, 200 µmol $m^{-2}s^{-1}$, T 22°C) (**Figure 20A**). Under low light and high

temperature conditions (LL, 200 µmol $m^{-2}s^{-1}$, T 30°C) the NO emission was the same as under low light and low temperature (LL, 200 µmol $m^{-2}s^{-1}$, T 22°C) conditions. Moreover, NO emission was analyzed under low and high light intensity without increasing the temperature (**Figure 20B**). Here again NO emission in wild type seems to be increased only under the enhanced light intensity and reaches a similar amount (ca. 5 pmol $m^{-2}s^{-1}$) as under high light and high temperature conditions (**Figure 20A**), concluding that the observed NO emission is probably a response to the light intensity and not a result of higher temperature.

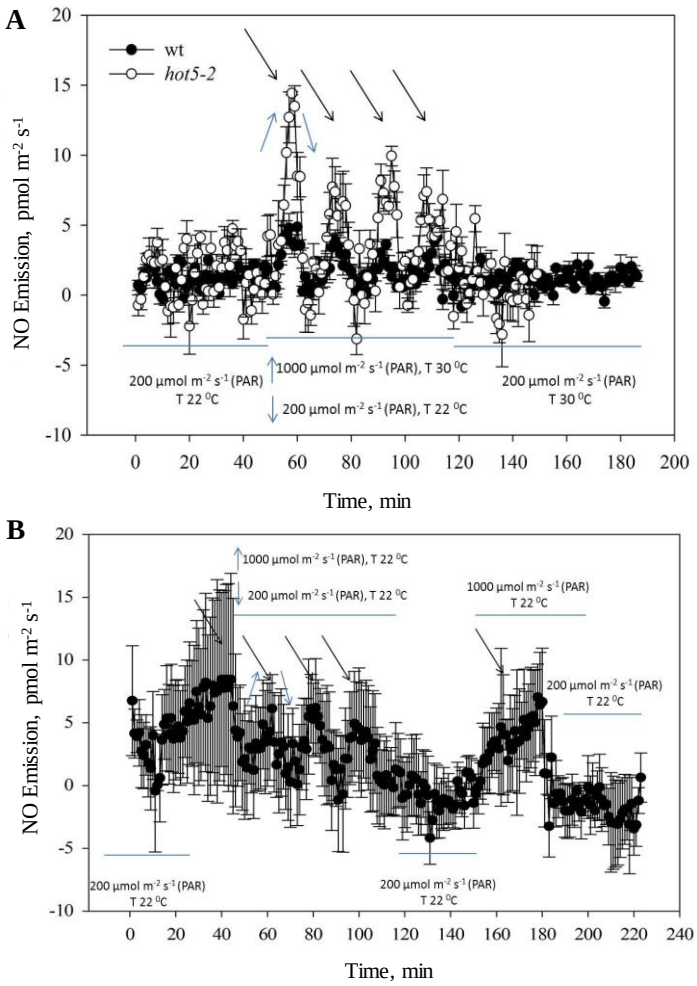

Figure 20: Enhanced light intensity induces NO emission of 4-weeks old plants.
First, plants were kept under similar conditions as those in the climate chambers (T 22 °C, 200 µmol $m^{-2}s^{-1}$). A) Then, temperature (30 °C) and light intensity (1000 µmol $m^{-2}s^{-1}$) were increased for 10 min, and then decreased back to 22 °C and 200 µmol $m^{-2}s^{-1}$, respectively for another 10 min. Such condition was repeated in total for four times followed by measuring of NO emission under high temperature (30 °C) and standard light (200 µmol $m^{-2}s^{-1}$). B) Applying of enhanced and low light intensity was performed without increasing the temperature. PAR, photosynthetically active radiation (µmol $m^{-2}s^{-1}$). Shown is a ±SE of at least three independent experiments (N>3).

Besides the NO emission, the SNO content in *Arabidopsis* leaves was measured. Plants were grown for 4 weeks under short day conditions (14 h dark/10 h light) and transferred at noon (after 4 h exposure to light) for 4 h to low light (LL, 200 µmol $m^{-2}s^{-1}$, T 22°C), dark (D, 0 µmol $m^{-2}s^{-1}$, T 22°C) and intense light (HL, 1000 µmol $m^{-2}s^{-1}$, T 30°C) (**Figure 21A**). The SNO concentration is increased with the light intensity (**Figure 21B**). More than 2-fold higher SNO content was observed under LL (45 and 88 fmol/µg) and HL (55 and 78 fmol/µg)

conditions than under D (19 and 44 fmol/µg) in wild type and *hot5-2*, respectively. However, there is no difference between LL and HL condition in both lines. It should also be noticed that SNO concentration in *hot5-2* is almost 2.5 and 1.5-times higher than in wild type under D, LL and HL conditions, respectively. Nitrite measurement is often used as another possibility to display NO production. Nitrite concentration correlates well with SNO content under different light conditions (**Figure 21C**). Namely 1790 fmol/µg and 2461 fmol/µg nitrite were observed under LL and 2341 fmol/µg and 2165 fmol/µg nitrite under HL conditions, whereas only 834 fmol/µg and 900 fmol/µg nitrite was measured under D in wild type and *hot5-2*, respectively. It should be noted that nitrite levels in *hot5-2* are not significantly different from that in wild type plants.

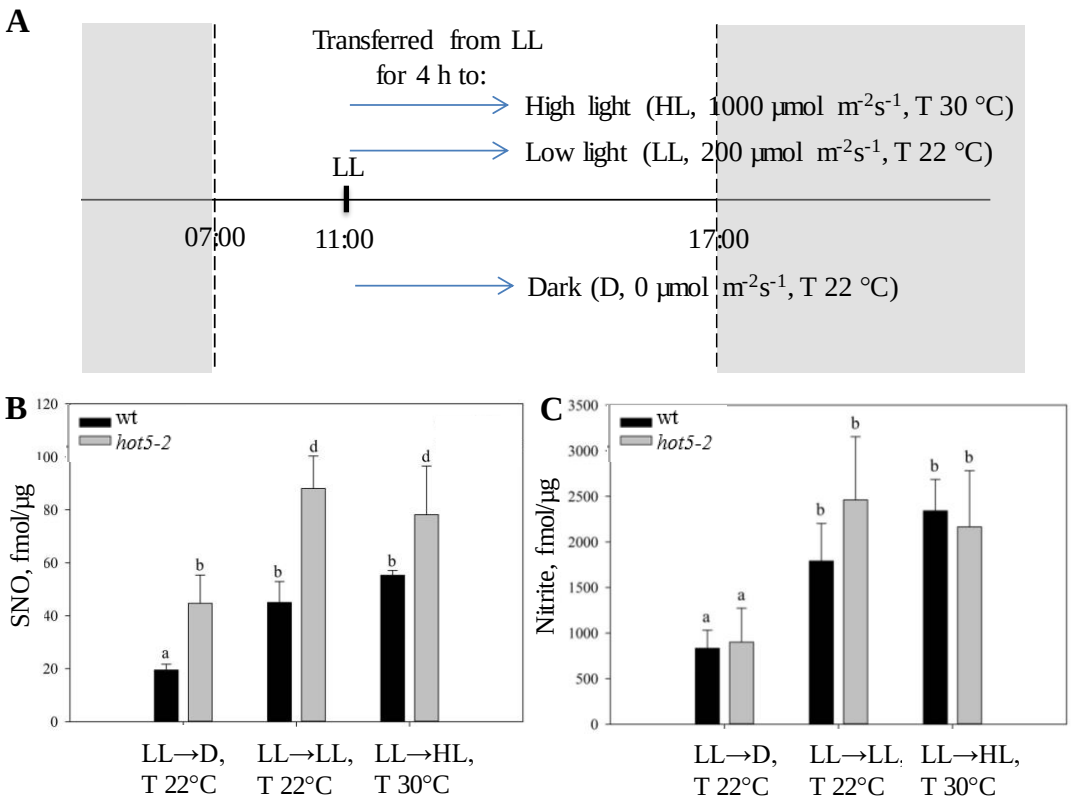

Figure 21: Different light and temperature conditions induce changes in S-nitrosothiol and nitrite concentration of *Arabidopsis* plants.
A) 4-weeks old plants grown on soil at short day cycles (10/14 h light/dark, 20/17 °C) were transferred at noon (11 o'clock) for 4 h to dark (D, T 22 °C), low light (LL, T 22 °C) and high light (HL, T 30 °C). B and C) Total S-nitrosothiol and nitrite levels were determined after 4 h. SNOs were reduced with triiodide and the emitted NO was photochemically detected by its reaction with ozone. Shown is a ±SE of three independent experiments (N=3). Two-way ANOVA was performed. B) Difference among light and temperature conditions – p=0.009, difference among wt and *hot5-2* mutant – p=0.004. Pairwise comparison was performed using Holm-Sidak Test: D, T vs HL, T – p=0.020, D, T vs LL, T - p=0.014. C) Difference among light and temperature conditions – p=0.011. Pairwise comparison was performed using Holm-Sidak Test: D, T vs HL, T – p=0.017, D, T vs LL, T - p=0.029.

2.2.3 Tendency towards light/NO-induced histone acetylation

Previously, an observation was done, pointing in the direction that exogenous applied (by GSNO) and endogenous induced (by INA, not significantly) NO results in histone modifications probably via inhibition of HDAs activity (**Figure 10, Figure 11**). It should be investigated whether NO production under different light/temperature conditions also leads to chromatin remodeling. Hence, global histone acetylation was analyzed. Because the acetylation level of H4 is lower in older plants than in seedlings (**Supplemental Figure 3**), only acetylation of H3 was investigated. 4-weeks old plants were grown on soil under short day cycles (10/14 h light/dark) and transferred at noon (11 o'clock, when plants were already exposed to LL for 4 h) for 4 h to low light (LL, 200 µmol $m^{-2}s^{-1}$, T 22°C), dark (D, 0 µmol $m^{-2}s^{-1}$, T 22°C) and high light/temperature (HL, 1000 µmol $m^{-2}s^{-1}$, T 30°C) (**Figure 21A**). It can be seen that in wild type plants histone acetylation level tends to increase with rising light intensity (**Figure 22**). In detail, when plants were transferred to the dark (D, 0 µmol $m^{-2}s^{-1}$, T 22°C) a minimum 1.5-fold decrease of H3ac (statistically not significant), H3K9ac (statistically significant) and H3K9/14ac (statistically not significant) was observed in wild type plants, whereas *hot5-2* exhibits a tendency of a 1.2-fold and 1.3-fold reduced H3ac and H3K9ac, respectively. No changes between light and dark conditions could be detected at H3K9/14ac of *hot5-2*. It is notable, that *hot5-2* demonstrates a tendency towards a higher histone acetylation than wild type, when plants were transferred to dark. *Hot5-2* shows here ca. 1.5-fold higher H3ac and H3K9ac as well as 1.2-fold higher H3K9/14ac than wild type. When plants were transferred from low light (LL, 200 µmol $m^{-2}s^{-1}$, T 22°C) to high light/temperature (HL, 1000 µmol $m^{-2}s^{-1}$, T 30°C) a tendency towards the enhanced histone acetylation was observed. A 1.6-fold and 1.3-fold increase of histone acetylation was observed for H3 and H3K9/14 in wild type plants. However, no changes in histone acetylation of *hot5-2* mutant were detected under these conditions.

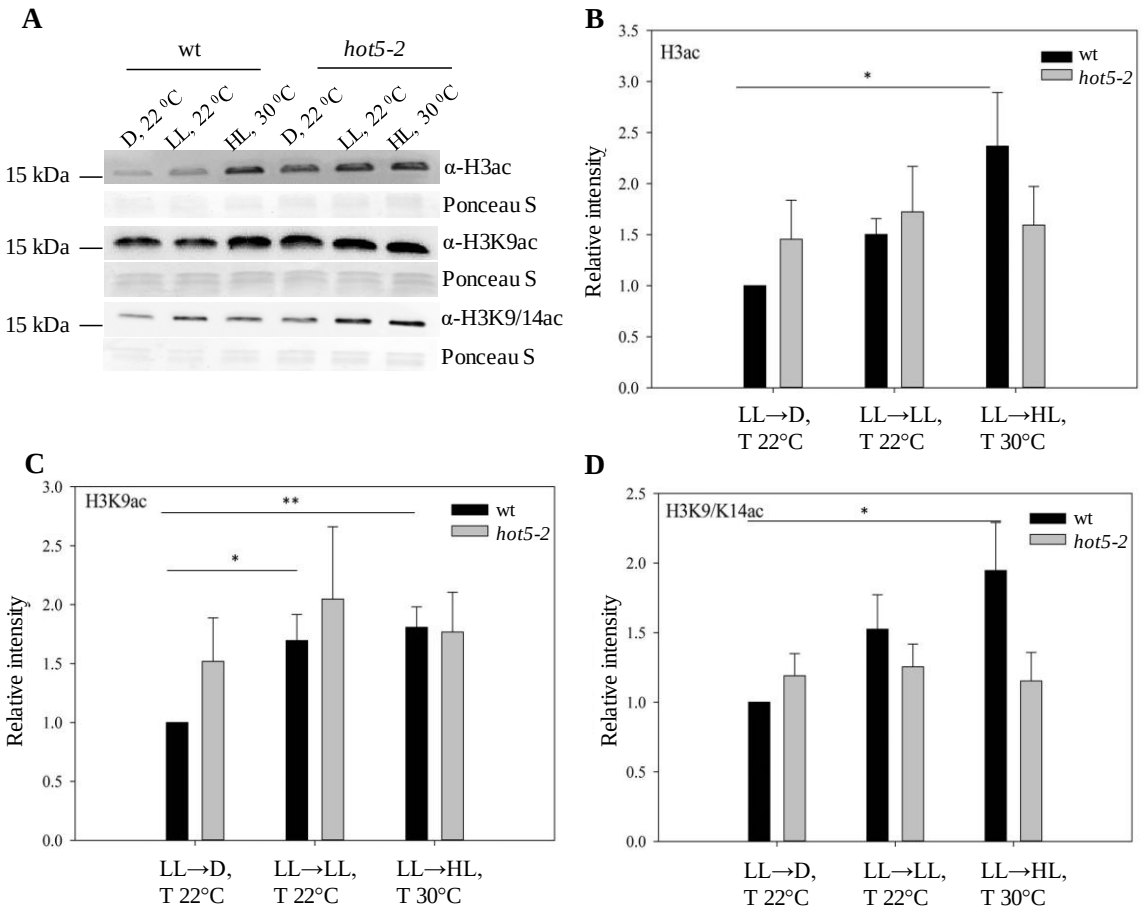

Figure 22: Different light conditions lead to altered H3 acetylation in wild type and *hot5-2* plants.
4-weeks plants grown on soil at short day (10/14 h light/dark, 20/17 °C) were transferred at noon (11 o'clock) for 4 h to dark (D, T 22 °C), low light (LL, T 22 °C) and high light (HL, T 30 °C). Histones were extracted using a commercial histone purification kit and separated on 12 % polyacrylamide gel followed by a transfer into nitrocellulose membrane. Antibodies used for analysis: acetylated-H3 (1:20000), acetylated-H3K9 (1:5000), acetylated-H3K9/14 (1:2000), acetylated-H4 (1:20000), and acetylated-H4K5 (1:10000). A second antibody was an anti-rabbit HRP (1:20000). The bands detection was performed at Fusion Fx7. B) Quantitative analysis of A for H3 acetylation. C) Quantitative analysis of A for H3K9 acetylation. D) Quantitative analysis of A for H3K9/14 acetylation. Signal intensity was determined with Image J software. Shown is a ±SE of at least three independent experiments (N>3). The relative intensity of the histone acetylation in wt under D conditions was set up to 1 [181]. One way ANOVA (DF=2; H3ac: p=0,025; H3K9ac: p=0,005; H3K9/14ac: p=0,043) with Holm-Sidak post-hoc test was performed, *p≤0.05, **p≤0.01.

HDA6 and HDA19 were identified as main candidates, whose enzymatic activity might be regulated by NO (s. Chapter 2.1.4). To analyze whether these two enzymes are involved in regulation of histone acetylation under different light conditions, global histone acetylation level was analyzed in *hda6* and *hda19* knockout mutants under the same light/temperature conditions as described above (**Figure 21A**).

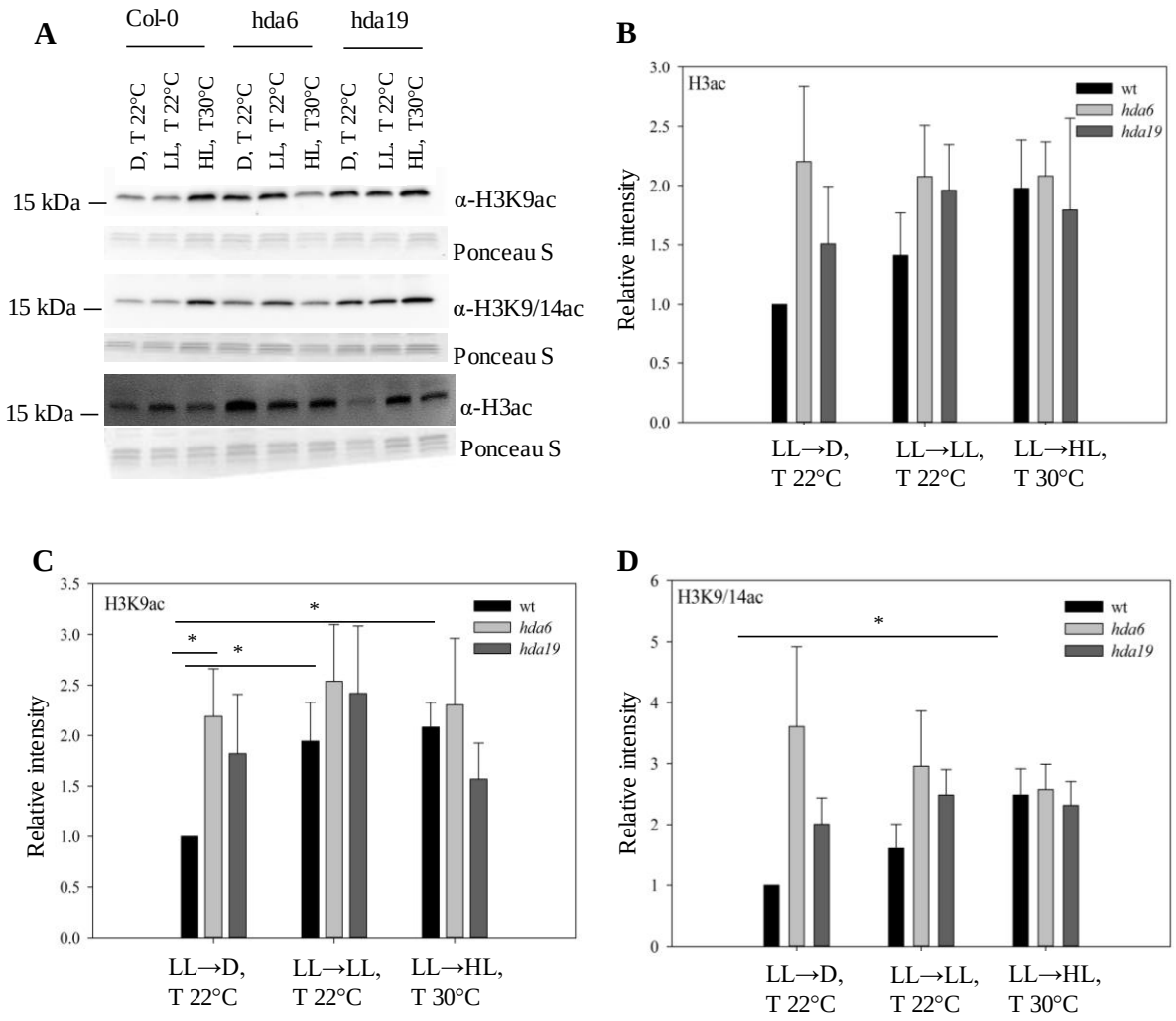

Figure 23: Different light and temperature conditions induce changes in H3 acetylation of *Arabidopsis* wt, *hda6* and *hda19* knockout mutant plants.
4-weeks old plants grown on soil at short day cycles (10/14 h light/dark, 20/17 °C) were transferred at noon (11 o'clock) for 4 h to dark (D, T 22 °C), low light (LL, T 22 °C) and high light (HL, T 30 °C). A) Histones were extracted using a commercial histone purification kit and separated on 12 % polyacrylamide gel followed by transferring them into a nitrocellulose membrane. Antibodies used for analysis: acetylated-H3 (1:20000), acetylated-H3K9 (1:5000), and acetylated-H3K9/14 (1:2000). The second antibody used was an anti-rabbit HRP (1:20000). The bands detection was performed at Fusion Fx7. B) Quantitative analysis of A) for H3 acetylation. C) Quantitative analysis of A for H3K9 acetylation. D) Quantitative analysis of A for H3K9/14 acetylation. Signal intensity was determined with Image J software. Shown is a ±SE of at least three independent experiments (N>3). The relative intensity of the histone acetylation in wt under D conditions was set up to 1 [181]. One way ANOVA (DF=2; H3K9ac: p=0,034; H3K9/14ac: p=0,038) with Holm-Sidak post-hoc test was performed, *p≤0.05.

No significant changes were observed within the mutants under different light/temperature conditions (**Figure 23**). However, there is a tendency towards increased acetylation in these mutants under low light and especially when plants were transferred to the dark acetylation is highly increased compared to wild type plants. When plants were transferred to the dark a 2.2-fold higher acetylation was detected on H3 (statistically not significant) and H3K9 as well as a 3.6-fold increase in H3K9/14 (statistically not significant) in *hda6* in comparison to wild

type. Similar trends were obtained in *hda19* with a 1.5- and 1.8-fold enhanced rate of H3ac and H3K9ac, respectively and a 2-fold higher acetylation on H3K9/14. Under low light condition ca. 1.4-fold, 1.3-fold and 1.8-fold higher H3, H3K9 and H3K9/14 acetylation were observed in *hda6* and *hda19* than in wild type, respectively. However, it has to be emphasized that the observed differences in histone acetylation are not statistically significant and reflect only trends. No differences have been detected between the mutants and wild type plants under intense high light/temperature conditions.

Taken together, this data indicates that NO might be involved in a daily modulation of chromatin structure. Moreover, when plants are transferred to dark HDA6 and HDA19 might be responsible for deacetylation of H3 prominent marks.

2.2.4 Light/NO-dependent histone acetylation and expression of photosynthesis related genes

The previous results demonstrate that NO production is light-dependent. Moreover, there are hints that light-induced NO accumulation might be involved in regulation of histone acetylation. Therefore, a question arises whether the NO-sensitive photosynthesis-related loci found in ChIP-seq change their acetylation level and expression by NO under physiological conditions (without adding NO donors). Since the most pronounced and significant changes in histone acetylation (**Figure 22**) as well as SNO content (**Figure 21B**) were obtained when wild type plants were transferred from low light to dark or high light/temperature conditions, the same experimental setup (see **Figure 21A**) was used to analyze acetylation and transcription of those genes.

Histone acetylation of photosynthesis-related genes was analyzed using the same anti-H3K9/14ac antibody as in the ChIP-seq experiment [180]. After a 4 h exposure of the plants to dark or high light/temperature their leaves were harvested and vacuum infiltrated with 1 % formaldehyde, of which the suitable concentration was determined experimentally (**Supplemental Figure 4**). Isolated chromatin was sheared to the size of 500-1000 bp and incubated overnight either with anti-H3K9/14ac or anti-IgG (as negative control) antibodies. ChIP-qPCR was performed using gene specific primers. The amount of measured chromatin was normalized to Input and peak1pos, a gene which display higher acetylation after 3 h and 16 h GSNO treatment. At5g38430 (RBCS1B) was used as a control, since it was reported that acetylation and transcription of this gene is light-dependent [190]. 4 % to 8 % higher H3K9/14ac was observed at At2g34420 (Lhb1B2, statistically significant), At5g54270 (Lhcb3, statistically not significant) and At5g38430 (RBCS1B, statistically not significant)

when plants were transferred to the intense light/temperature compared to the dark conditions in both *hot5-2* and wild type plants (**Figure 24**). However, there is no difference in the acetylation level of these genes between *hot5-2* and wild type.

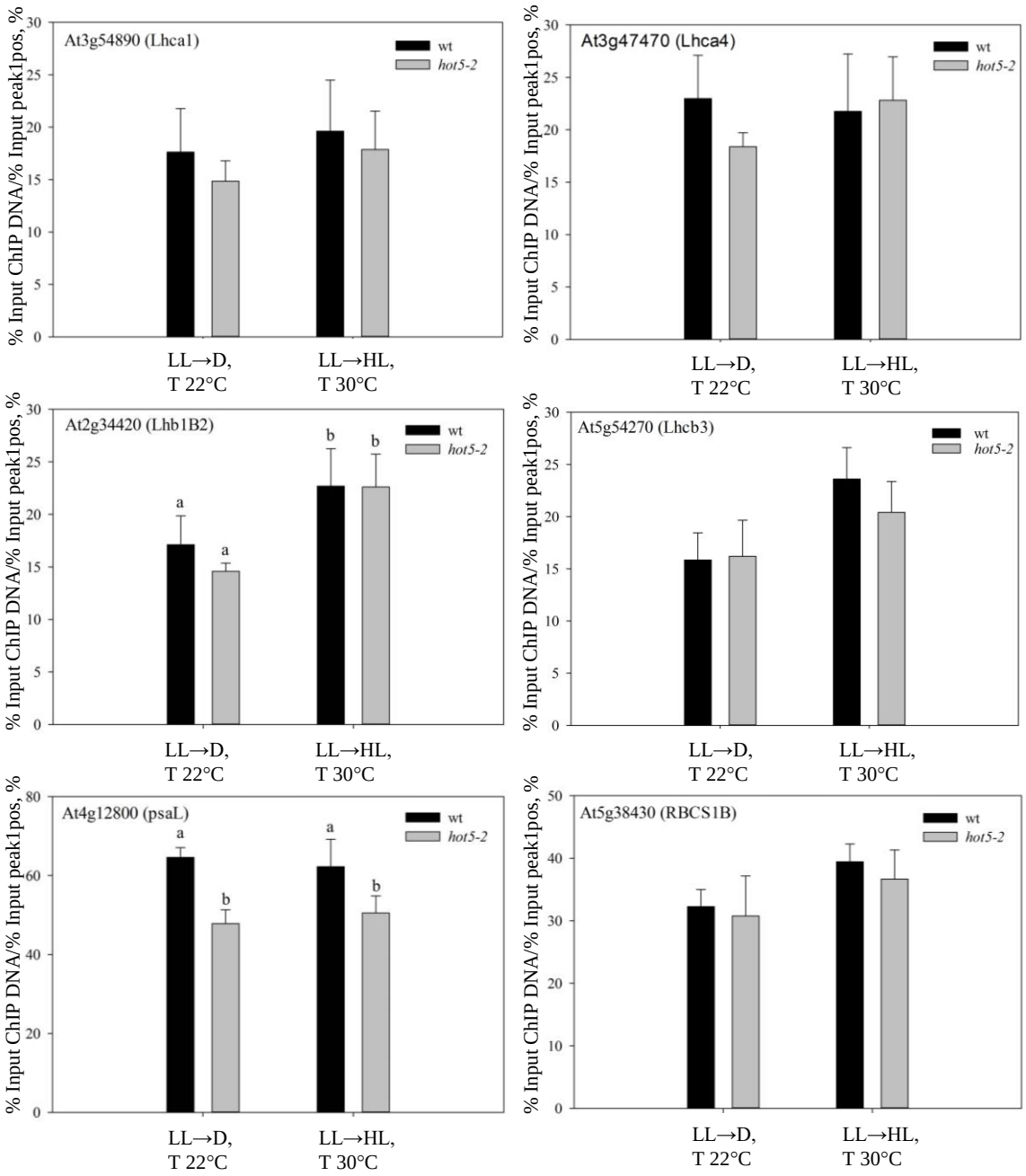

Figure 24: Light leads to a slight increase in H3K9/14 acetylation of some photosynthesis-related genes. 4-weeks old *Arabidopsis* plants grown on soil at short day cycles (10/14 h light/dark, 20/17 °C) were transferred at noon (11 o'clock) to dark (D, T 22 °C) and high light (HL, T 30 °C). After 4 h leaves were pooled and incubated in 1 % formaldehyde. Relative amount of DNA associated with acetylated H3K9/14 for Lhca1, Lhca4, Lhb1B2, Lhcb3, psaL and RBCS1B were determined by ChIP-qPCR in wt and *hot5-2* mutant plants. Chromatin was extracted and immunoprecipitated with acetylated-H3K9/14 (1:2000). qPCR-amplifiered ChIP-DNA was normalized to input DNA and peak1pos. Shown is a ±SE of four independent experiments (N=4). Two way ANOVA is performed. Difference among of light/T conditions – DF=1; p=0.03, difference among of wt and *hot5-2* mutant – DF=1; p=0.009. Pairwise comparison was performed using Holm-Sidak Test: p<0,05.

Using the same experimental setup transcription of photosynthesis-related genes was analyzed via qPCR (**Figure 25**).

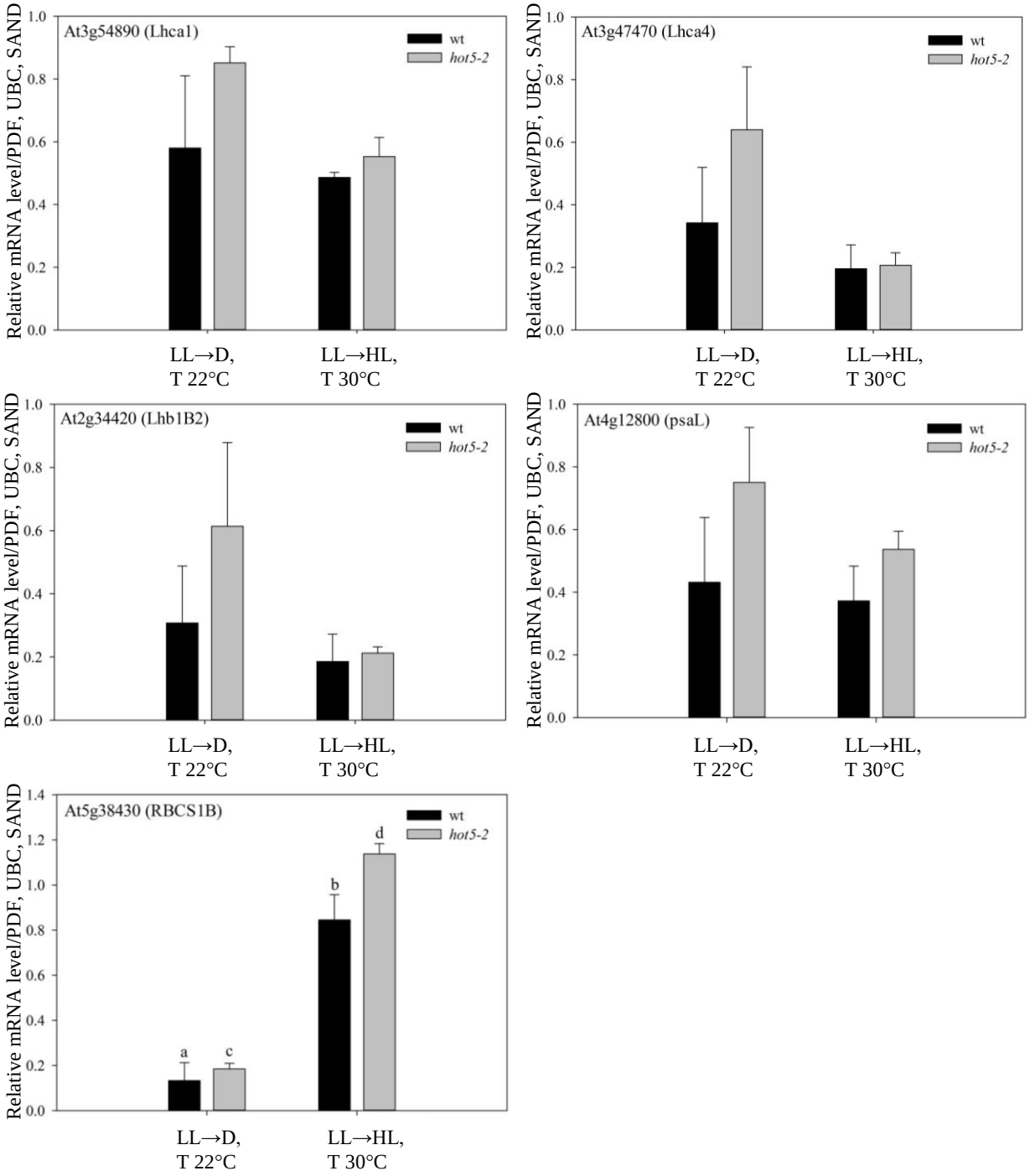

Figure 25: Different light and temperature conditions change transcriptional level of photosynthesis-related genes.
4-weeks old plants grown on soil (10/14 h light/dark, 20/17°C) were transferred at noon to dark (D, T 22°C), low light (LL, T 22°C) and high light (HL, T 30°C). After 4 h leaves (100 mg) were pooled for RNA extraction. cDNA was diluted 1:20. qPCR was performed on ABI 7500. mRNA level was normalized to PDF, UBC and SAND. Shown is a ±SE of three independent experiments (N=3). Two way ANOVA (Holm-Sidak Test) is performed. Difference among of light and T conditions – DF=1; $p \leq 0.001$, difference among of wt and *hot5-2* mutant – p=0.011. Pairwise comparison was performed using Holm-Sidak Test: $p<0,05$.

In wild type plants there seems to be a tendency towards increased transcript levels of At3g54890 (Lhca1, 1.2-fold, statistically not significant), At3g47470 (Lhca4, 1.7-fold, statistically not significant), At2g34420 (Lhb1B2, 1.6-fold, statistically not significant) and At4g12800 (PsaL, 1.2-fold, statistically not significant) when plants were transferred to the dark compared to high light/temperature conditions. The differences in mRNA abundance of the same genes in *hot5-2* were even more pronounced, namely 1.5-fold for Lhca1 and PsaL as well as 3-fold for Lhca4 and Lhb1B2, respectively. However, also the results are statistically not significant. Interestingly, the transcripts of all photosynthesis-related genes in *hot5-2* mutant in the dark seems to be higher (1.5-2 times) than in wild type plants, although no differences in H3K9/14ac were observed in those genes among wild type and mutant plants (**Figure 24**). The mRNA level of At5g38430 (RBCS1B) is at least 6 times higher when wild type and *hot5-2* were transferred to the intense light/temperature than to the dark and correlates with a slight increase in H3K9/14ac of this gene. Moreover, *hot5-2* exhibits a significant higher transcript (1.4-fold) of RBCS1B than wild type under bough conditions.
Taken together, these results demonstrate, first, that genes showing enhanced acetylation at H3K9/14 after GSNO treatment remained unchanged in the mutant with elevated SNOs content. This suggests that exogenous application of SNO (in form of GSNO) is different from the enhanced endogenous SNO levels and cannot be compared with each other. Second, light-induced H3K9/14ac of Lhb1B2 and Lhcb3 does not correlate with their transcriptional level, indicating that except of NO another mechanism might be involved in transcriptional regulation of these genes. However, a positive correlation between H3K9/14ac and mRNA level of RBCS1B as well as a higher transcript abundance of this gene in *hot5-2* suggests that NO might be involved in transcriptional regulation of photosynthesis-related genes, but under physiological conditions other photosynthesis-related genes (not those which were found after GSNO treatment) are regulated by NO.

2.2.5 Light/NO-dependent H3K9 acetylation of photosynthesis-related genes

H3K9ac is usually associated with active promoters and this histone mark is more abundant (however, not significant) in *hot5-2* (**Figure 22C**) and *hda6* (**Figure 23C**) mutants, respectively, in comparison to wild type under both, dark and low light conditions. Therefore, a ChIP-seq experiment was performed using an anti-H3K9ac antibody in order to look for photosynthesis-related genes which might be regulated by light-induced NO. To determine a

genome-wide light/dark-dependent H3K9ac profile, 4-weeks old wild type, *hot-2* and *hda6* plants were either exposed to low light or transferred to the dark condition for 4 h.

Crosslinked chromatin was sheared to small fragments (100 – 400 bp) using Covaris E220 evolution and the size was verified by 1.5 % agarose gel and Agilent 2100 Bioanalyzer (**Supplemental Figure 5**). Immunoprecipitated and Input chromatin were used for library construction and deep sequencing by IGA Technology Services. Sequencing was performed using NextSeq500 and 30 M (75 bp) reads.

2.2.5.1 Genome-wide mapping of H3K9ac

An ultrafast memory-efficient short read aligner, Bowtie [191], was used to align sequenced reads to the reference genome (TAIR10). The alignment results are presented in **Supplemental Table 1**. All ChIP-seq data aligned well with *A. thaliana* genome, resulting in total of 95.31-99.34 % aligned reads. Furthermore, principle compound analysis (PCA) as well as a heatmap of all sequenced peaks were performed to visualize a relatedness between replicates. Plots of two biological replicates are located next to each other and clustered together, suggesting that sequencing data are of high quality (**Supplemental Figure 8**).

Distribution of H3K9ac peaks along the five *Arabidopsis* chromosomes was analyzed by normalizing of H3K9ac reads to the Input read counts and mapping them to genome. The highest peak density was found along chromosome arms, whereas centromeric and pericentromeric regions were considerably less enriched (**Figure 26**).

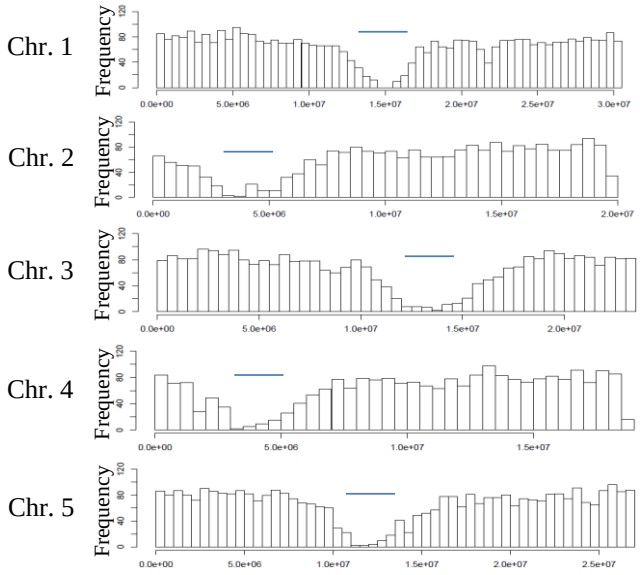

Figure 26: H3K9ac is located along chromosome arms in *Arabidopsis* genome. Each bar represents the number of peaks in the corresponding chromosomal bin. The approximate centromeric and pericentromeric regions are marked by a blue line. Two independent ChiP-seq experiments were performed (N=2).

Further, to determine the abundance of H3K9ac sites along the gene bodies in more detail a coverage analysis around transcription start sites (TSS) was performed as well as the location

of H3K9ac enriched regions was identified. The majority of enriched reads is located in proximity to TSS. And the strong enrichment of H3K9ac was observed within 1000 bp relative to the nearest TSS (**Figure 27A**). It was also found that 44 % of the peaks are located within coding sequence (CDS) followed by 21 % and 20 % within intergenic and intragenic regions, respectively. Only 8.5 % and 3.4 % of the peaks were observed in five prime and three prime untranslated (5´- and 3´-UTR) regions, respectively (**Figure 27B**).

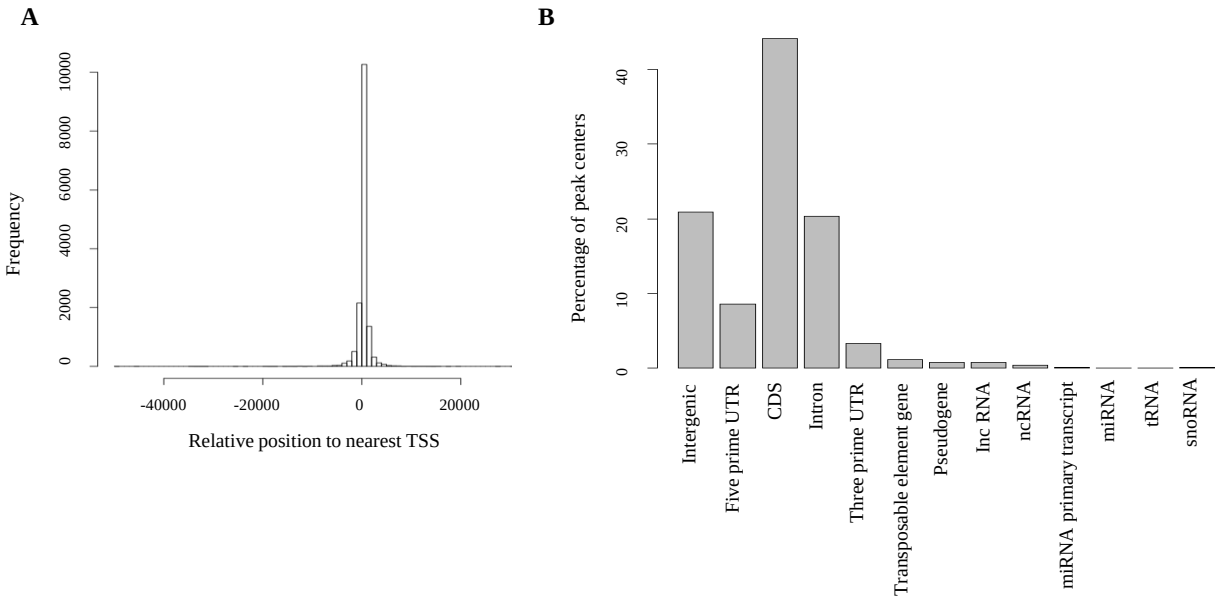

Figure 27: Genomic distribution of H3K9ac among *Arabidopsis* genome.
A) Histogram of peak distribution, where transcription start site (TSS) is centered. The x-axis demonstrates distance from TSS and the y-axis represents frequency. The distance is calculated between the central point of the peak to the nearest TSS. Negative and positive values correspond to sequences upstream and downstream to TSS. B) Distribution of H3K9ac peaks along different regions of *A. thaliana* genome. Two independent ChiP-seq experiments were performed (N=2).

2.2.5.2 H3K9ac level dependent on light/dark condition

To identify differential abundance of H3K9ac loci, the DiffBind software package version 2.8.0 was applied. In total 15290 peaks were found specific for H3K9ac. Analyzing each genotype based on the light/dark condition (e.g. *hda6* light *vs*. *hda6* dark) a high number of peaks was found to be significantly hyperacetylated (FDR≤0.05) in wild type and *hda6*, namely 2774 and 3621, respectively. Whereas 1481 and 1004 peaks were detected as hypoacetylated (peaks which are more acetylated in the dark). In contrast, almost an equal number of peaks in *hot5-2* was identified as hyper- (1305) and hypoacetylated (1782) under low light conditions (**Figure 28A**).

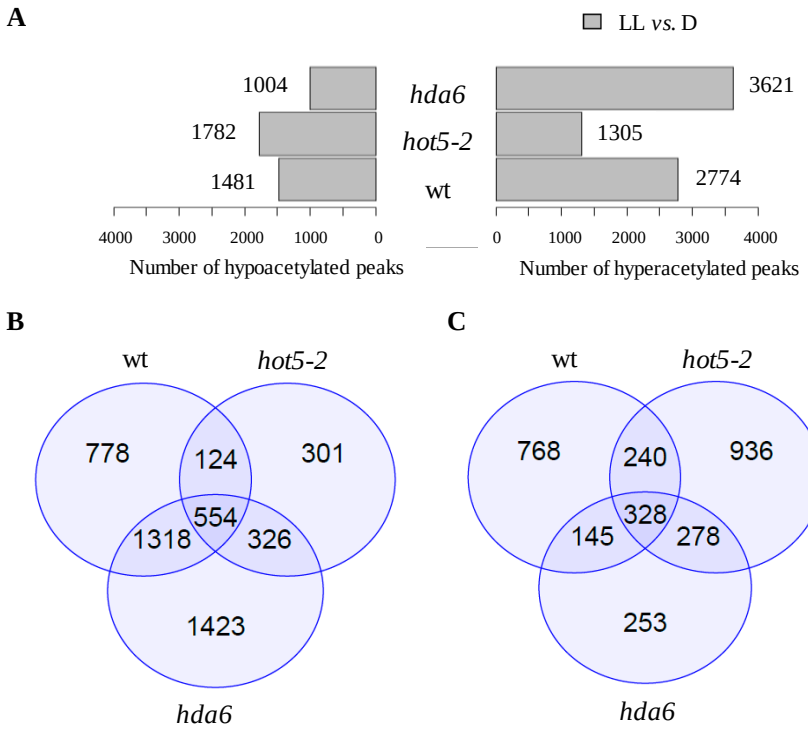

Figure 28: H3K9ac depends on light and dark condition. *Hda6, hot5-2* and wt were either exposed for 4 h to moderate light (LL) or transferred to the dark (D). A) Hyperacetylated and hypoacetylated peaks were found by comparing of each genotype exposed to light with the same genotype transferred to the dark. Hyperacetylated peaks mean the peaks that are more acetylated under the light than under the dark condition. Hypoacetylated peaks mean the peaks that are less acetylated under the light conditions, indicating that these loci are more acetylated in the dark. Depicted only significant peaks with FDR<0.05 (N=2). Venn diagrams of B) hyperacetylated and C) hypoacetylated peaks under the light conditions, respectively.

To examine biological response to light on histone acetylation, first it was looked for all possible relations between the genotypes. Venn diagrams show that all three plant lines share a quite high number of hyper- and hypoacetylated peaks in light relative to dark. In pairwise comparisons, 1872, 678 and 880 identical peaks were found hyperacetylated between wt+*hda6*, wt+*hot5-2* and *hot5-2*+*hda6*, respectively. 554 of those highly acetylated peaks appeared in all three lines (**Figure 28B**). At the same time the plant genotypes showed overlapping peaks that are less acetylated under the light than under the dark conditions. 473 identical peaks were found between wt+*hda6*, 568 - wt+*hot5-2* and 606 - *hot5-2*+*hda6*, whereas 328 of them are shared by all genotypes (**Figure 28C**). It is important to mention, that shared peaks remain still of high interest for further analysis, because it is not clear from the venn diagrams, whether these loci are more or less acetylated in the mutants than in wild type.

Second, a GO enrichment analysis was performed for the hyperacetylated peaks of each genotype and their overlap across all genotypes. H3K9ac seems to play an important role in various biological processes under the dark and light condition. In the response to light, molecular functions of H3K9ac among the genotypes are very diverse and are involved in metabolism, transport and stress responses (**Supplemental Figure 9**). Remarkably,

hyperacetylated peaks of *hot5-2* contain loci related to photosynthesis and light reaction, supporting the hypothesis that NO might be involved in regulation of photosynthetic machinery. Peaks that were hyperacetylated in all three genotypes were enriched for chloroplast-related gene function, consistent with the effect of light expected from prior knowledge. However it is not possible to conclude from this observation whether H3K9ac of these loci is more abundant in the mutants than in wild type plants.

2.2.5.3 H3K9ac level dependent on genotype

Analyzing histone acetylation between the mutants and wild type, it was found that *hot5-2* has a higher H3K9ac than wild type. In detail, 3438 and 829 exclusively hyperacetylated peaks are present in *hot5-2* under light and dark conditions, respectively, whereas only 585 and 133 peaks were hypoacetylated, respectively. Remarkably, four times more *hot5-2*-specific H3K9ac loci were observed in the light than in the dark (**Figure 29**).

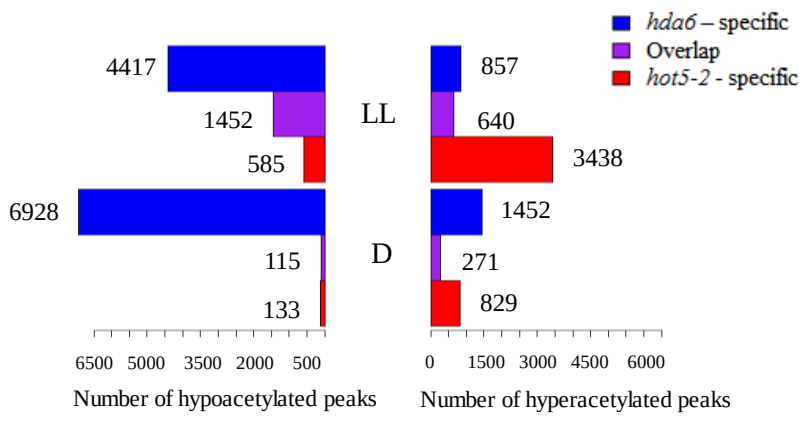

Figure 29: H3K9ac level dependent on genotype. Both mutants were compared to wild type under light and dark conditions. Hyperacetylated peaks are the peaks that are more acetylated in the mutants than in wild type. Hypoacetylated peaks are the peaks that are less acetylated in the mutants than in wild type. Overlapped peaks are the loci which common in both, *hda6* and *hot5-2*. Depicted only significant peaks with FDR<0.05 (N=2).

In contrast, *hda6* consists of more hypoacetylated peaks than hyperacetylated ones in comparison to wild type. In total, 4417 and 6928 specific hypoacetylated peaks were detected under light and dark conditions, respectively. Interestingly, almost double amount of hyperacetylated H3K9 peaks was observed in the dark (1452) than in the light (857).

Comparing the mutation effect between the two mutants, it was found that *hda6* and *hot5-2* share 640 specific loci that are hyperacetylated in the light and 271 loci in the dark. In contrast 1452 and 115 loci were observed less acetylated in both mutants than in wild type under light and dark conditions, respectively.

To examine biological functions affected by the mutations, GO analysis was performed for *hda6* and *hot5-2* shared and specific loci (**Supplemental Figure 10**). Under light condition

hyperacetylated loci shared by both mutants are significantly enriched in genes located in the chloroplast. Interestingly, also in the dark condition *hot5-2*-specific hyperacetylated loci are enriched for functions related to chloroplast, photosynthesis and light reaction.

2.2.5.4 H3K9ac loci affected by both condition and genotype effects

To find out what are the chloroplast-related genes that are possibly regulated by the NO-depended inhibition of HDA6, the intersection between light/dark condition and genotype effects was analyzed. Specifically, we were interested in peaks at chloroplast genes that were hyperacetylated by light and significantly hyperacetylated in mutants compared to the wild type (resulting in a significantly higher acetylation level in mutants under light than in wild type under dark) (**Figure 30**). The first set of candidate peaks was derived as the overlap between peaks hyperacetylated by light in the wild type (wt light *vs.* wt dark) and peaks hyperacetylated in mutants compared to the wild type in light (*hot5-2* light *vs.* wt light, *hda6* light *vs.* wt light). The second set of candidate peaks was derived as the overlap between peaks hyperacetylated in the mutant compared to the wild type in dark (e.g. *hot5-2* dark *vs.* wt dark) and peaks hyperacetylated in light in that mutant (*hot5-2* light vs. *hot5-2* dark).

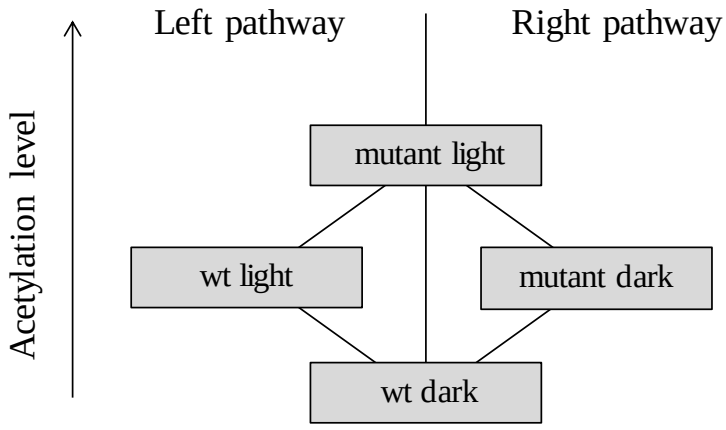

Figure 30: Step-wise induction of peaks at chloroplast genes.
It was looked, first, for the peaks that are hyperacetylated by light in wild type and even higher acetylated in *hot5-2* and *hda6* (left pathway). Second, peaks that are more H3K9 acetylated in the mutants than in wild type, when plants were transferred to the dark and loci that are hyperacetylated in both mutants by light (right pathway).

Both sets of candidate peaks are visualized in a heatmap, where each peak is represented by a column (**Figure 31A**). The majority of found chloroplast-related genes in wild type are more acetylated under light than under dark condition. 74 of these loci showed a significant increase (FDR $\leq$ 0.05, log2FC $\geq$0) in H3K9ac when plants were exposed to low light compared to dark. Both mutants show even higher histone acetylation than wild type under this condition. 80 and 16 significantly higher hyperacetylated sites were found in *hot5-2* and *hda6*, respectively. Among hyperacetylated peaks, 65 (*hot5-2*) and 7 (*hda6*) peaks were light-

induced in wild type as well; however these loci are significantly less acetylated than in the mutants (**Figure 31B**).

Under the dark condition, 37 and 17 chloroplast-related genes were more acetylated in *hot5-2* and *hda6* than in wild type, respectively. When the condition effect was analyzed within each mutant, 59 and 76 H3K9ac loci were found hyperacetylated in *hot5-2* and *hda6* when plants were exposed to light, respectively. It was found that 26 and 15 loci in *hot5-2* and *hda6*, respectively, were more acetylated in the mutants by light than in the dark and in the same time are more acetylated in the mutants than in wild type under the dark conditions (**Figure 31C**).

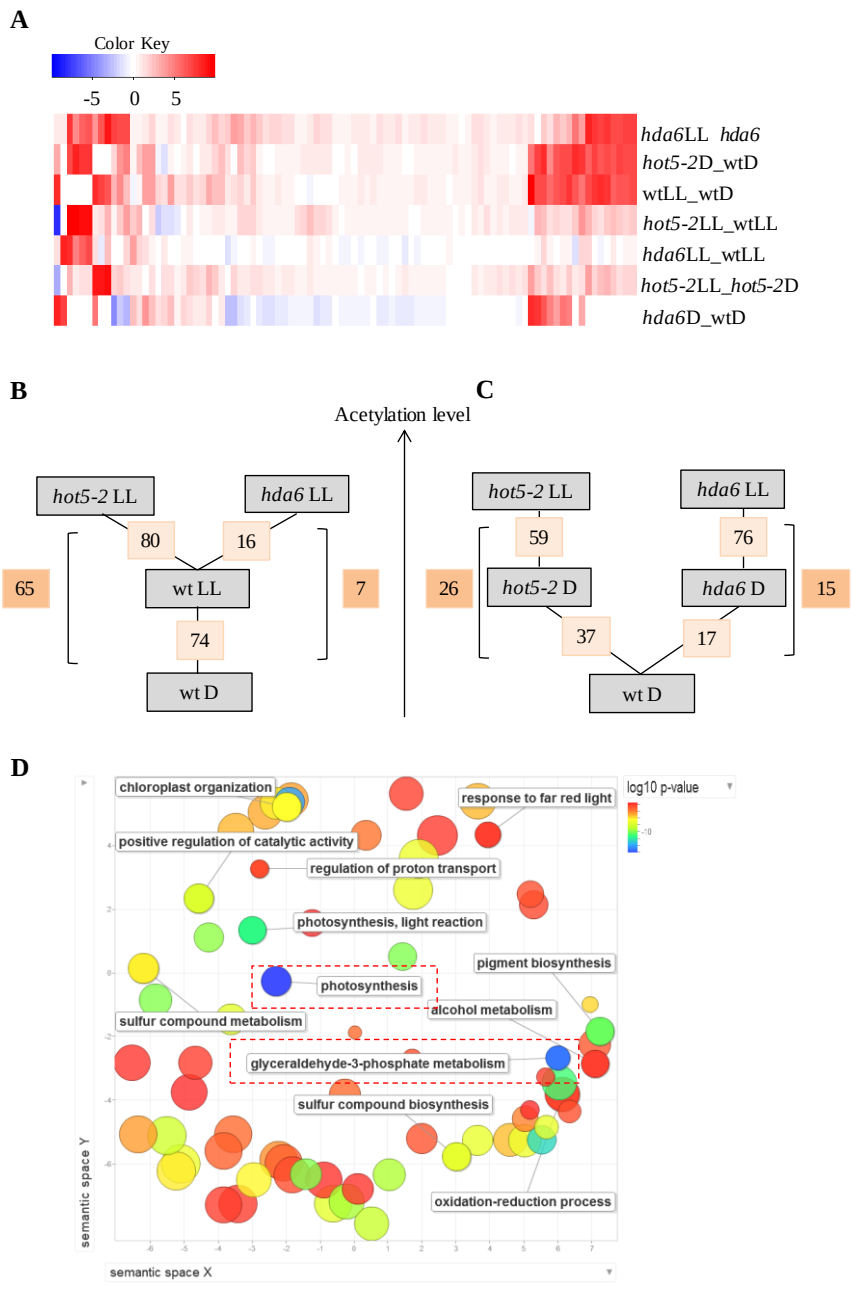

Figure 31: Chloroplast genes are enriched in H3K9ac. A) Heatmap of peaks which changed significantly (FDR ≤ 0.05, N=2) their H3K9 acetylation level depending on phenotype and genotype effect. h*da6*LL_*hda6*D means peaks that are more acetylated under light than under dark conditions in *hda6* mutant, *hot5-2*D_wtD means peaks that are more acetylated in *hot5-2* than in wt in the dark, etc. B) and C) demonstrate a relationship of the significantly regulated H3K9ac loci (FDR ≤ 0.05, log2FC ≥ 0, N=2) at left and right pathways, respectively (Figure 30). Numbers in boxes indicate the amount of peaks. D) ReviGO visualization of significantly enriched terms for the 91 hyperacetylated loci from subfigure A). Blue and green bubbles represent GO terms with more significant FDR values than yellow and red one. Only the most significant and interesting terms are labeled.

In total, 91 (the sum of peaks appeared hyperacetylated in mutants under the light conditions: 65+7+26+15) chloroplast-associated genes were covered by the peaks sets from the left and the right pathways (**Supplemental Table 2**). In order to better understand the underlying biological processes of these genes, a GO enrichment analysis was performed, in which many GO terms were found significantly enriched (FDR ≤ 0.05, log2FC ≥ 0). Among those are terms involved in chloroplast organization, response to far red light, regulation of proton transport, pigment biosynthesis, sulfur compound metabolism and biosynthesis, alcohol metabolism and oxidation-reduction processes. However, the most significantly enriched terms are photosynthesis and glyceraldehyde-3-phosphate metabolism (**Figure 31D**).

Selected light-induced H3K9ac loci are summarized in (**Table 2**, for a complete list see **Supplemental Table 2**). In total, 20 genes (e.g. Lhca6, Lhcb3, PSBY) which are directly involved in photosynthesis were found significantly acetylated under the light in mutants in comparison to wild type. Moreover, several other interesting candidates (e.g. TRX-M4, PGDH3, AOR) involved in redox-processes, which are a crucial part of photosynthesis, were discovered.

All in all, it was found that NO induced specific changes in H3K9ac pattern of photosynthesis-related genes. Loci acetylated by light in wild type were found even more acetylated in *hot5-2* mutant (e.g. HCEF1), supporting the hypothesis that NO might be an important player of photosynthetic machinery by modulating the chromatin structure of photosynthesis-associated genes. An increase of histone acetylation level might be due the inhibition of HDAs activity. This is underpinned by the fact that both mutants, *hda6* and *hot5-2*, share a big number of hyperacetylated genes in comparison to wild type (70 % and 16 % of H3K9ac specific sites of *hda6* were also found acetylated in *hot5-2* under light and dark conditions, respectively). However, only few chloroplast-related candidates were found to be regulated by HDA6. Lhcb3 (gene involved in photosynthesis) was significantly acetylated in both mutants, suggesting that this locus might be directly regulated through the NO-dependent inhibition of HDA6 activity.

Table 2: List of selected significantly changed H3K9ac sites identified in both mutants.

TAIR	Name	Description	Function	Appeared H3K9ac in	
				left pathway	right pathway
AT1G14345	n.a.	NAD(P)-linked oxidoreductase superfamily protein	Photosynthesis, light reaction / GA3P metabolism		hot5-2
AT1G19150	Lhca6	PSI type II chlorophyll a/b-binding protein (Lhca2*1)	Photosynthesis, proton transmembrane transport / GA3P metabolism	hot5-2	
AT1G55480	ZKT	Protein containing PDZ domain a K-box domain and a TPR region	Photosynthesis, response to light stimulus		hot5-2
AT1G65230	n.a.	Transmembrane protein putative (DUF2358)	Photosynthesis / GA3P metabolism	hot5-2	
AT1G67740	PSBY	Photosystem II BY	Photosynthesis, light reaction	hot5-2	
AT1G74880	NdhO	NAD(P)H:plastoquinone dehydrogenase complex subunit O	Photosynthesis, light reaction		hot5-2
AT2G26500	n.a.	Cytochrome b6f complex subunit (petM)	Photosynthesis, light reaction	hot5-2	
AT2G30570	PSBW	Photosystem II reaction center W	Photosynthesis, light reaction	hot5-2	
AT3G13120	n.a.	Ribosomal protein S10p/S20e family protein	Photosynthesis, chlorophyll biosynthetic process / GA3P metabolism	hot5-2	
AT3G21055	PSBTN	Photosystem II subunit T	Photosynthesis, light reaction	hot5-2	
AT3G54050	HCEF1	High cyclic electron flow 1	Photosynthesis, electron transport in photosystem I / GA3P metabolism	hot5-2	hot5-2
AT4G04640	ATPC1	ATPase F1 complex gamma subunit protein	Photosynthesis, ATP synthesis coupled proton transport / GA3P metabolism	hot5-2	
AT4G09650	ATPD	F-type H+-transporting ATPase subunit delta	Photosynthesis, ATP synthesis coupled proton transport	hot5-2	
AT4G22890	n.a.	PGR5-LIKE A	Photosynthesis, electron transport in photosystem I / GA3P metabolism		hot5-2
AT4G27800	TAP38	Thylakoid-associated phosphatase 38	Photosynthesis, electron transport chain	hot5-2	
AT4G28660	PSB28	Photosystem II reaction center PSB28 protein	Photosynthesis, photosystem II / GA3P metabolism	hot5-2	hot5-2
AT5G04140	GLU1	Glutamate synthase 1	Photosynthesis, response to light stimulus	hot5-2	hot5-2
AT5G08050	n.a.	Wiskott-aldrich syndrome family protein putative (DUF1118)	Photosynthesis, nonphotochemical quenching (NPQ) / GA3P metabolism	hot5-2	
AT5G38520	n.a.	Alpha/beta-Hydrolases superfamily protein	Photosynthesis, chlorophyll metabolic process	hot5-2	
AT5G54270	Lhcb3	Light-harvesting chlorophyll B-binding protein 3	Photosynthesis, response to light stimulus	hot5-2, hda6	
AT5G43750	PnsB5	NAD(P)H dehydrogenase 18	Response to oxidative stress	hot5-2	hot5-2
AT1G23740	AOR	Oxidoreductase zinc-binding dehydrogenase family protein	Oxidation-reduction process	hot5-2	
AT3G15360	TRX-M4	Thioredoxin M-type 4	Cell redox homeostasis / GA3P metabolism	hot5-2	
AT3G19480	PGDH3	D-3-phosphoglycerate dehydrogenase	Oxidation-reduction process	hot5-2	hda6
AT5G21430	NdhU	Chaperone DnaJ-domain superfamily protein	Oxidation-reduction process	hot5-2	
AT5G18660	PCB2	NAD(P)-binding Rossmann-fold superfamily protein	Oxidation-reduction process, chlorophyll biosynthetic process	hot5-2	
AT4G15110	CYP97B3	Cytochrome P450 family 97 subfamily B polypeptide 3	Oxidation-reduction process, carotenoid biosynthetic process / GA3P metabolism	hot5-2	
AT3G51820	G4	UbiA prenyltransferase family protein	Chlorophyll biosynthetic process / GA3P metabolism		hot5-2
AT4G18350	NCED2	Nine-cis-epoxycarotenoid dioxygenase 2	Oxidation-reduction process, abscisic acid biosynthetic process		hda6
AT4G33010	GLDP1	Glycine decarboxylase P-protein 1	Oxidation-reduction process / GA3P metabolism		hda6
AT1G24280	G6PD3	Glucose-6-phosphate dehydrogenase 3	Oxidation-reduction process / GA3P metabolism	hot5-2	
AT5G44520	n.a.	NagB/RpiA/CoA transferase-like superfamily protein	Pentose-phosphate shunt / GA3P metabolism	hot5-2	

Depicted are the genes that demonstrate a higher acetylation level in *hot5-2* and *hda6* than in wild type under the light condition (left pathway) and genes that are hyperacetylated in the mutants when they were exposed to light in comparison to the dark condition (right pathway). GA3P – glyceraldehyde-3-phosphate metabolism.

3 Discussion

Before entering into a detailed discussion, it should be emphasized that the research conducted provides evidence to support several of the hypothesis stated in this thesis. Although statistical significance couldn't be shown for all results, tendencies are visible for the remainder which seems to be backing the hypothesized cause-effect relationships. In order to ensure a more robust statistical foundation for further research some of the experiments would ideally need to be repeated with larger sample sizes where possible.

3.1 NO-dependent histone acetylation

The role of NO on histone modification pattern of 7-days old *Arabidopsis* seedlings grown in liquid was analyzed in this study. The seedlings were treated with GSNO to mimic NO production and NO signaling. Two methods were used to quantify histone acetylation: LC-MS/MS and immunoblotting. The first approach provides a powerful tool in monitoring total histone acetylation in a single experiment and is based on a mass shift if lysine modification is present. Moreover, it exhibits a huge advantage over traditional immunoblotting methods because there is no need in using/generation of new antibodies, as it is well known that a success of an immunoblotting experiment depends on quality, specificity and performance of an antibody [192][193]. Treatment of seedlings with TSA resulted in enhanced H3 and H4 acetylation (**Figure 8**), indicating that this approach is suitable to analyze plant histone modifications. Treatment of seedlings with GSNO led to a slight but not significant increase of H3 and H4 acetylation as well. However, the quantification of H4 acetylation turned out to be difficult, because of the high number of lysine residues within the analyzed N-terminal H4 peptide (**Figure 7B**). In order to overcome this problem, a traditional antibody-based method was applied. Immunoblotting confirmed that exogenously applied GSNO might affect histone acetylation in liquid grown seedlings. However, it should be noted that the measured differences in histone acetylation are not statistically significant for all analyzed histone marks and treatments. Nevertheless, a trend of GSNO-induced histone acetylation could be observed (**Figure 10**). NO donor increased histone acetylation abundance in all tested epigenetic marks. A more than 2-fold enhanced histone acetylation level was observed in H3ac (statistically significant), H3K9ac (statistically significant), H3K9/14ac (statistically not significant), H4ac (statistically not significant) and more than a 4-fold increase in H4K5ac (statistically not significant) in comparison with water treated seedlings. Coapplication of cPTIO mostly prevented GSNO-mediated hyperacetylation of chromatin, indicating that

observed histone acetylation changes might be caused by NO. Treatment of seedling with GSH demonstrated unexpectedly a tendency towards induced histone acetylation at several lysine residues, for instance H4K5ac, although the effect was weaker than after GSNO treatment. It was assumed that GSH might also indirectly lead to the formation of NO. This result is in line with a similar observation where GSH-dependent production of nitrite and NOx was found in human umbilical vein endothelial cells (HUVECs) [194]. In agreement with the previous results, GSNO-mediated H3ac was also detected in *Arabidopsis* suspension cells (**Figure 6**). Moreover, a tendency towards an increased H3ac (1.5-fold) and H3K9ac (ca. 1.3-fold) level was observed in SNO-accumulated *hot5-2* plants compared to wild type under dark and low light conditions (**Figure 22**), indicating that endogenous SNO/NO might affect histone acetylation. It should be also mentioned that since global histone acetylation is analyzed in this study only moderate changes/tendencies rather than clear-cut differences can be expected. To obtain statistically significant results the sample size would have to be increased. This assumption is strengthened by other published studies where e.g. a relatively small but significant increase in histone acetylation at almost all lysine sites (ca. 1.5-fold, N>3) with the notable exception at H3K14ac and H3K56ac (ca. 3-fold and 3.5-fold, respectively) was observed in embryonic cells that are double knockout in HDA1/2, enzymes which regulate access to DNA by modulating chromatin structure [195].

Plant hormone SA is known to participate in endogenous NO synthesis [186]. Therefore, the role of its chemical analog, INA, was investigated. SNO formation was analyzed after the treatment of liquid-grown seedlings for 16 h with INA or INA/cPTIO (**Figure 11C**). A trend towards increased SNOs accumulation was observed. The SNO formation in INA treated seedlings increased twice as much as in control plants, however the results were statistically not significant. The obtained results are in line with findings where differences in NO accumulation upon SA treatment were detected in *Arabidopsis* plants with normal or impaired NO homeostasis [186], [196]–[198]. Moreover, an increased NO production was also observed in protoplasts after stimulation for 1 h with 100 µM SA or INA in a time and concentration dependent manner [180][179]. However, the SNO formation could not be prevented by cPTIO in this study (**Figure 11C**). Similar observation was obtained after long-term cPTIO treatment. A 10 min incubation of cell culture with cPTIO was able to scavenge SA-mediated NO, however a pre-treatment for 60 min resulted in a strong decrease of scavenging efficiency, indicating that time might be a limiting factor for cPTIO functions [199]. This evidence is in accord with another study where 3 h incubation of liquid grown

Arabidopsis seedlings with GSNO/cPTIO caused a slight reduction of SNO content, whereas no scavenging effect was observed after 16 h treatment [179].

Since SA as well as INA induce endogenous NO production [179][180], the influence of INA on global changes of histone acetylation was analyzed by western blot (**Figure 11A** and **B**). Incubation of liquid-grown seedlings with INA for 16 h demonstrated a tendency towards an elevated H3ac, H3K9/14ac, H4ac and H4K5ac (however the results were statistically not significant) which cannot be prevented by INA/cPTIO treatment. However, the acetylation level was still lower than after INA treatment alone, indicating that the observed tendency towards hyperacetylation of the histones by INA is probably based on INA-induced NO production. A possible role of INA-dependent chromatin modulation might indicate the functions of NO in a disease resistance. Treatment of tobacco plants or cell suspensions with NO donors resulted in expression of defense related genes, such as phenylalanine ammonia lyase (PAL) and pathogenesis-related protein 1 (PR1) which are marks for phenyl propanoid pathway and salicylic acid (SA)-mediated signaling [64]. The application of NO synthase inhibitors or scavenger attenuated a systemic acquired resistance (SAR) induced by SA. NO was proposed as a positive regulator of transcriptional expression of defense genes, acting upstream of SA-regulated pathway [65]. Other studies demonstrate that dependent on the concentration SA fulfills an important function during abiotic stress responses as well [200].

The data of this study provide hints that NO might be involved in chromatin modulation. In many other studies it was shown that different biotic and abiotic stresses induce NO accumulation and also structural changes of chromatin. Exposing maize seedlings to heat stress resulted in increase of total H3ac, H3K9ac and H4K5ac [201]. An elevated level of H3K9ac and H4K5ac was also measured in maize roots after 200 mM NaCl treatment [202], suggesting that these changes could be associated with enhanced expression and activity of two HATs, HAT-B and GSN5. Moreover, dynamic changes in H3 phosphorylation and acetylation of H4 seem to correlate with the activation of stress-related genes in tobacco and *Arabidopsis* cells in response to high-salinity, cold stress and ABA treatment [203]. According to these observations and our results, it could be assumed that NO might be a part of a signaling cascade which induces a defense mechanism through changes in chromatin structure.

3.1.1 Redox-regulation of HDA6

Histone modifications are highly dynamic. These reactions are catalyzed by two groups of enzymes HATs and HDAs (s. 1.1.5.2). There is some evidence which indicates that NO-induced histone acetylation is mainly based on a negative regulation of HDAs activity. First

of all, it was shown that total HDAs activity is reduced (about 20 %) after the treatment of protoplasts and nuclear extracts with 500 µM GSNO and SNAP. It should be highlighted, when a reduced agent DTT was additionally added, the enzymatic activity was restored, indicating that NO-induced inhibition of HDAs activity is reversible. Moreover, SA- and INA-induced NO synthesis also inhibit catalytic activity of HDAs in protoplasts. This inhibition is NO specific, as the effect of SA and INA could be abolished by NO scavenger cPTIO [179][180]. Aside from that, the influence of NO on a transcriptional regulation of HDAs was analyzed. No effect of GSNO on HDAs expression was observed at the analyzed time point (**Figure 13**). Together these data suggests that NO might modulate histone acetylation through the redox regulation of HDAs activity (**Figure 32**).

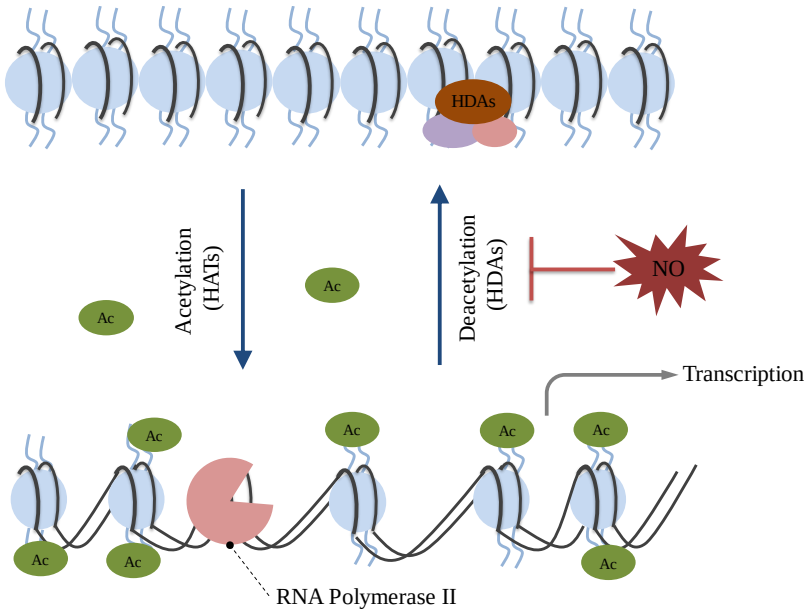

Figure 32: A possible NO mode of action in regulating histone acetylation.
Tightly wrapped around histones DNA form an inactive and closed chromatin structure which is usually associated with gene repression. The dynamic state of chromatin is regulated by HATs and HDAs enzymes. Histone acetylation leads to opened chromatin and allows transcriptional regulators bind to DNA. Histone acetylation is usually associated with gene transcription. NO promotes inhibition of HDAs and leads to the acetylated, active chromatin structure.

There is evidence demonstrating that HDAs might be important enzymes involved in chromatin modifications. Two plant specific nuclear HDTs, HDT2 (HDT2B) and HDT3 (HDT2C), were found S-nitrosylated in *Arabidopsis* suspension cell cultures after pathogen infection [104], however less is known about these modified proteins. It was demonstrated that HDT3 is involved in ribosome biogenesis and plays an important role in rRNA processing [204]. Redox-sensitive Cys residues have been observed in plant HDA19 and

HDA9 in response to SA treatment. It was suggested that the oxidation of HDA19 and HDA9 promotes their deactivation and enhances histone acetylation and expression of associated genes [205]. Redox-regulation of HDAs has been already described in the animal field. It was demonstrated that a brain-derived neurotropic factor (BDNF) causes NO synthesis and S-nitrosylation of HDA2 at Cys-262 and Cys-274 in neurons. Remarkably, S-nitrosylation does not inhibit its deacetylase activity, but causes the release from a CREB-regulated gene promoter. Oxidation of HDA2 results in enhanced H3 and H4 acetylation at neurotrophin-dependent promoter regions and facilitates transcription of many genes [155]. A different study reports about the S-nitrosylation of HDA2 in muscle cells of dystrophin-deficient MDX mice [156]. Although NO-sensitive Cys of this enzyme are not identified yet, it was clearly shown that the enzymatic activity of muscle HDA2 is impaired upon NO donors. The fact that the catalytic activity of neurons HDA2 remains unchanged in response to NO, leads to the hypothesis that S-nitrosylation of HDA2 in muscles occurs at different cysteine residues than in neurons. Moreover, it was assumed that HDA2 in neurons might be a member of another cell-type specific repressive complex than in muscle cells which might influence an association of HDA2 with chromatin as well as its deacatylase activity [206]. Another study partially confirms this hypothesis demonstrating that NO-induced inhibition of HDAs activity depends also on the subcellular location of HDAs. It was shown that GSNO inhibits total HDAs activity in neuronal cytoplasmic fractions, whereas in nuclear fraction the enzymatic activity is not changed in response to GSNO treatment [207]. Recombinant mammals HDA6 and HDA8 have been reported to undergo S-nitrosylation which results in inhibition of their activity [157][208]. Moreover, HDA4 and HDA5, as parts of a large protein complex, migrate into the nucleus upon S-nitrosylation of protein phosphatase 2A [158]. According to the studies above there is a strong hint that animal HDAs are part of redox-signaling pathways.

Mammal HDA2 is the only HDA where NO-sensitive cysteines were identified and demonstrated to be crucial for its biological functions. Therefore, amino acid homology of HDA2 to HDAs of *A. thaliana* was analyzed. Plant HDA6 and HDA19 showed the highest similarity to mammal HDA2, i.e. ca. 60 % identity (**Figure 14**). All three proteins contain seven Cys which are located within the HDAs domain. Moreover, the secondary structure of plant HDAs, according to their 3D modeling (based on crystal structure of HDA2), is almost identical to the folding of HDA2 (**Figure 15**). Additionally, corresponded Cys-273 and Cys-285 of HDA6 and Cys-269 and Cys-281 of HDA19 are located in similar positions as NO-targeted Cys of HDA2, indicating that plant HDA6 and HDA19 are promising candidates for being redox regulated.

HDA6 was suggested as a target for NO since acetylation of H3 in *hda6* was not enhanced (**Figure 16**) in comparison to wild type suspension cells (**Figure 6**). Moreover, the catalytic activity of recombinant purified Flag-HDA6 was partially inhibited by GSNO (**Figure 17, Supplemental Figure 2**).

HDA6 is one of the most studied HDAs in plants. It is involved in various physiological processes, such as silencing of transgenes and rDNA [209][169], postgermination growth [173], plant pathogen interactions [210], leaf development [211] and flowering [212]. The role and diversity of HDA6 functions imply that its catalytic activity might be strictly controlled. However, it remains unclear whether NO-induced inhibition of HDA6 activity is regulated by its posttranslational modification.

3.2 NO regulates gene transcription via modulation of chromatin structure

Histone modifications are essential for the regulation of transcription. In many cases, modification of histone H3 and H4 is associated with the decondensation of chromatin. For instance, the acetylation of H3K9, H3K14 and trimethylation of H3K4 are corresponded to euchromatic regions and associated with the activation of gene transcription while the deacetylation of H3K9, H3K14 and demethylation of H3K9 are the marks of silenced heterochromatin sites [213]. Since it could be demonstrated that NO exhibited enhanced histone acetylation, the link between NO-induced chromatin modifications and gene transcription was investigated. Recently, it was demonstrated that ca. 700 NO-sensitive loci of liquid grown *Arabidopsis* seedlings are associated with H3K9/14ac. In total, 194 NO-targeted H3K9/14ac sites were found after 3 h of GSNO treatment. 148 loci were hyper- and 46 loci were hypoacetylated. After 16 h of GSNO treatment 552 NO-sensitive H3K9/14ac sites were identified whereas 393 genes demonstrated an increased and 159 genes a decreased acetylation [180][179]. qPCR analysis revealed that only 5 of 14 randomly selected loci displaying enhanced H3K9/14ac showed an enhanced expression after GSNO treatment, whereas the rest of the genes remained unchanged despite being hyperacetylated (**Figure 12**). The general view that histone acetylation of specific regions leads to opening of chromosomal domains and therefore is correlated with a transcriptional activation of those genes *per se*, is not necessarily correct. It is more likely that the acetylation of those regions is of transcriptional competence [214]. Similar results were also observed in studies done in maize. The loss of maize HDA101 activity resulted in an increased H4K5ac throughout the entire genome, however more than 90 % of the direct targets of HDA101 did not change their expression in the *hda101* mutant [215]. A weak correlation between histone modifications and

transcriptional response was also observed in *Arabidopsis* seedlings exposed to salt stress [216]. Sometimes only a subsequent stress facilitates gene expression of chromatin regions modified by a pre-stress, indicating a role of histone memory for information storage. Such kind of mechanism is also known under the term of "priming", meaning that primed chromatin allows a faster or stronger response to further challenges [217][218][219]. The role of NO and SNO formation as priming agents was analyzed in several studies. It was observed that the growth of *Pseudomonas syringae pathovar tomato* strain DC3000 (*Pst DC3000*) is significantly reduced after spraying 4-weeks old *Arabidopsis* plants with 1 mM GSNO [182]. These results are in line with studies performed in potato inoculating with necrotrophic pathogen *Phytophtora infestans*. It was assumed that NO together with chromatin modifications are important for the coordination of a potato defense response to a subsequent pathogen attack [220].

Taken together, this data implies that the observed tendency of NO-mediated changes of chromatin landscape might, on the one hand, directly lead to the transcriptional activation of certain genes, but, on the other hand, NO might be responsible for keeping some chromatin regions in a "caution" state for subsequent stress.

3.3 Function of NO in photosynthesis

Photosynthesis is the main source of energy in plants and thus is very important for their viability. The influence of NO on photosynthetic system was analyzed in this study. Electron transport rate (ETR) and non-photochemical quenching (NPQ) seems to be repressed in *hot5-2*, whereas no differences were observed in maximum quantum efficiency (Fv/Fm) of PSII between mutant and wild type plants (**Figure 18**), indicating that NO/SNO might selectively effect PSII photochemistry. The reduction of ETR in SNOs accumulating plants could be explained by the competition of NO with bicarbonate. The last is known to influence the processes related to both the electron acceptor and donor sides of PSII and therefore, regulates the electron flow in order to mitigate the impact of stress conditions [221]. NO was demonstrated to compete with bicarbonate for binding to non-heme iron located between Q_A (a one-electron acceptor plastoquinone) and Q_B (a two-electron acceptor plastoquinone) binding sites [222]. By replacement of bicarbonate, NO is able to reduce photosynthetic ETR that leads to decreasing of thylakoid transmembrane potential and ATP synthesis [74][223]. The significant decline of NPQ values as well as no changes in Fv/Fm were also found when

Arabidopsis leaves were incubated with SNP and SNAP or in spinach thylakoid membranes treated with NO, respectively [224][74].

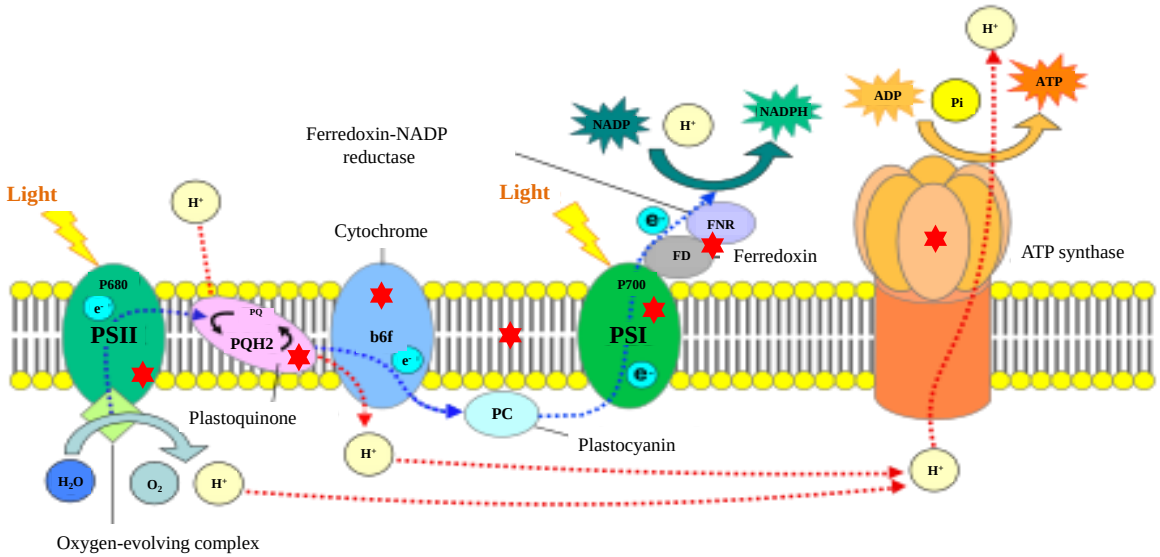

Figure 33: Schematic presentation of NO binding sites in photosynthetic apparatus.
Modified from [225]. Light energy is absorbed by pigment molecules of PSII and PSI and is convereted to chemical energy. In the first stage of photosynthesis NADPH and ATP are produced, which are required later to produce sugars in Calvin cycle (second stage of photosynthesis). NO is known to influence different compounds of photosynthesis, such as PSII and PSI, electron transport flow, and ATP synthase complex. NO may effect on photosynthetic rate and chlorophyll florescence parameters. Possible NO-binding sites are demonstrated by red stars.

Several other studies reported about the involvement of NO on photosynthetic apparatus as well (**Figure 33**). It was demonstrated that the exposure of oats and alfalfa leaves to NO decreases their net photosynthesis rates [226]. Many photosynthesis genes were identified as S-nitrosylated in a site-specific nitrosoproteomic approach [227]. Moreover, it was shown that different NO donors, such as GSNO, SNAP and SNP result in changes of photosynthetic parameters [72]–[74], [228], [229]. However, the results are contradictory, probably because of different chemical properties of NO donors and different experimental conditions.

The fact that photosynthesis-related genes were found hyperacetylated and transcriptionally activated after GSNO treatment [180] as well as upregulated after NO fumigation [77] suggests that NO might be also involved in the regulation of photosynthetic efficiency through the modulating of chromatin structure.

3.3.1 Effect of light on NO production

Experimental results of this study show that light stimulates NO production. First of all, SNO concentration of wild type and *hot5-2* mutant plants demonstrates a tendency towards an inverted U-shape behavior during a typical light-dark cycle (**Figure 19**). A tendency towards the increased SNOs formation was detected during the light conditions, whereas a drop in the SNO amount was observed in the dark. Moreover, when light intensity alone or in combination with temperature were temporarily increased, a NO emission was determined which was not detectable when only the temperature was enhanced (**Figure 20**). Furthermore, SNO and nitrite levels were significantly higher when plants were exposed to light compared to the dark (**Figure 21**). A similar observation was also made by other groups who demonstrated that an endogenous NO production in *Arabidopsis* leaves exhibits a diurnal rhythm. At night the NO concentration was reduced by 30 % in comparison to the NO amount which was measured during the day [38]. This indicates that light seems to be important for the intercellular accumulation of NO. However, this observation does not exclude that light might have only an indirect role in this process by controlling enzymes that synthetize NO in a cell. For instance, it was shown that nitrate-fertilized sunflowers and spinach leaves emitted less NO in the dark than in the light, suggesting that NO emissions in the light are mainly based on light-triggered activation of NR activity [16], since it was shown that NR activity is decreased during darkening [230]. However, NO emission of nitrite reductase (NiR)-deficient tobacco leaves dramatically increased in the light compared with wild type leaves and dropped immediately in the dark phase [231]. This indicates that other factors besides NR activity may regulate NO emission, too. It might be also assumed that NO is produced due to the reduction of nitrite (NO_2^-). It was shown that the reduction of NO_2^- is related to photosynthetic electron flow where ferredoxin is probably a donor in a leaf tissue. However, some studies demonstrated that the amount of the reduced NO_2^- was stoichiometrically associated with the production of α-amino nitrogen [232]. Reduction of NO_2^- to NO is also possible in mitochondria from plants and animals in the presence of NADH. However, this reaction is only feasible under oxygen free condition [233]. NO production in mammals correlated with the expression and activity of NOS which was triggered by light [234][235]. Although NOS enzymes have not been found in plants yet, it was demonstrated that NO can be produced in chloroplast via NADPH-dependent oxidation of L-arginine, which is the NOS substrate. It was shown that L-arginine is one the most common amino acid in chloroplast and is available in nanomolar concentrations [236]. The synthesis of L-arginine is controlled by

photosynthetic light reaction, suggesting that oxidative NO production might also follow a circadian-like pattern [237].

Since there is a positive correlation between photosynthesis and stomatal reactions, the conclusion may be derived that NO emission can be attributed to a stomatal conductance, since stomata is usually opened in the day and closed at night [238]. According to our results from the measurement of NO emission, it cannot be ruled out that the observed NO emission is a result of a stomatal opening at high light intensity. However, the enhanced formation of SNOs and nitrite at moderate and highly irradiance conditions indicates that the process of NO production in light is independent of stomatal conductance (**Figure 21**).

One can also assume that the light-induced NO production is based on the day-night cycle of ROS homeostasis. It was demonstrated that the expression of ROS-responsive genes displays a time-of-day specific pattern and is under circadian control. Moreover, H_2O_2 production and scavenging is also dependent on the time of the day, with more H_2O_2 produced during the light phase and an obvious dip at midnight [239]. It should be highlighted that NO and H_2O_2 contribute to the production of each other [240], indicating that a daily rhythm of H_2O_2 might also lead to an enhanced NO level in light.

3.3.2 Light-induced SNOs formation seems to affect histone acetylation

The results of this study provided hints that light is playing an important role in the regulation of histone acetylation. First, it was found that there seems to be a tendency which indicates that under different light conditions NO accumulation correlates with changes in histone acetylation. A tendency towards histone acetylation changes were observed when light intensity was manipulated: the higher the light intensity, the higher the tendency towards increased H3, HK9 and H3K9/14 acetylation levels (**Figure 22, Figure 23**). However, at this point of time it cannot be ruled out weather an increased histone acetylation under intensive light/temperature conditions is mainly related to the high amount of SNOs generated during this treatment (**Figure 21**) or due to the increased temperature of the experimental assembly, since it is known that heat stress is also able to induce histone modifications [241][201]. However, temperature used to induce the heat stress in these studies was 37°C and 45°C, respectively and is much higher than in our experimental set up. Second, histone acetylation level in *hda6* and *hda19*, the main candidates that might be regulated by NO, seems to be higher under low light and dark conditions than in wild type plants indicating that these two HDAs might be involved in H3 deacetylation under these conditions (**Figure 23**).

Light is known as a major regulator of plant development and plays direct and indirect roles in mediating histone modifications and chromatin remodeling [242] which induces a reprogramming of thousands of plant genes [243]. A direct binding of a repressor of photomorphogenesis (DET1) to a nonacetylated H2B provided evidence about the involvement of light signaling in chromatin reorganization [244]. One of the first examples of light-induced histone acetylation was demonstrated in pea [245], [246]. It was shown that activation of PetE gene, which encodes plastocyanin protein that transfers electrons from cytochrome bf complex into PSI reaction center, is enabled by hyperacetylation of H3 and H4 at its promoter region. Moreover, the requirement of histone acetylation for PetE transcription was confirmed by analyzing of transgenic tobacco GUS plants after treatment with HDA inhibitors (TSA and sodium butyrate). Based on microarray data comparing in dark- and light-grown *Arabidopsis* seedlings [247], it was found that histone acetylation and gene transcription are positively correlated and regulated in response to light changes [190]. Furthermore, it was demonstrated that the enrichment of H3K9ac in analyzed genes is higher in *hda19* mutant plants than in wild type, indicating that HDA19 is required to reduce H3K9ac in a light-dependent manner. Moreover, HDA19 represses transcription of several light-responsive genes [167]. Similarly, HDA15 is involved in a deactivation of transcription of chlorophyll biosynthetic and photosynthesis-related genes in etiolated seedlings by interaction with PIF3 transcription factor by deacetylating and decreasing RNA polymerase II-associated transcription [177]. It should be noted that a HDA15-PIF3 complex was dissociated from target genes by exposure to red light. Taking these studies into account, it is assumed that the transcription of genes which display a day-night rhythm might be partially regulated by HDAs. Moreover, these observations are in accordance with the hypothesis of this thesis, as our results indicate that, on the one hand, NO production demonstrates a tendency towards a typical light-dark cycle and, on the other hand, light-induced SNOs formation seems to mediate histone acetylation which is probably a consequence of SNO/NO-dependent inhibiting of HDAs activity. These observations indicate that light-triggered SNO/NO might have signaling functions in regulation of gene transcription.

3.3.2.1 Light-induced H3K9/14ac is not associated with expression of photosynthesis-related genes

NO-sensitive H3K9/14 loci which were found hyperacetylated in GSNO-treated seedlings include a superfamily of light-harvesting complex proteins (LHC) which are subunits of photosynthesis reaction center (**Table 1**). LHCs are required for the absorption of sunlight and

transferring of excitation energy to the reaction center. Photosystem I (PSI) and photosystem II (PSII) are associated with LHCI and LHCII, respectively, although a part of LHCII can also form a PSI-LHCII complex when there is an imbalance in excitation between PSI and PSII. In higher plants, LHCII is a trimer and is composed of three homolog isoforms, Lhcb1-3, whereas LHCI is made up of four apoproteins: Lhca1-4 [248]. Data of this study demonstrate that only two of five photosynthesis-related genes (Lhb1B2 and Lhcb3) display an enhanced H3K9/14 acetylation in wild type plants under an intensive light condition. The acetylation pattern of *hot5-2* at the same loci follows an identical tendency but is not more noticeable than in wild type as it would be expected if NO/SNOs would affect H3K9/14 acetylation at these loci (**Figure 24**). Reasons for this might be: (i) NO may regulate gene histone acetylation until certain level. When this is reached, it does not matter how much NO is present, histone acetylation would not be higher. (ii) Whereas both systems (GSNO treatment and *hot5-2*) display an elevated SNO/NO level, they can be differed in properties and functions of NO. For instance, genes affected by NO-derived from GSNO might be different from those in the *hot5-2* mutant. This observation is in line with another result where transcription of analyzed genes seems to be accompanied by the daily NO production but the mRNA level of them is significantly lower in *hot5-2* than in wild type (**Supplemental Figure 6**). Although the mRNA abundance of these genes was much higher after GSNO treatment compared to the control plants (**Figure 12**). Moreover, in the H3K9/14ac ChIP-seq study seedling were “flood” with GSNO, whereas *hot5-2* plants may have cell- and tissue-specific differences in SNO/NO level which might lead to conversable results between GSNO-treated and mutant plants. It might be further assumed that other factors were activated upon GSNO treatment which resulted in the hyperacetylation of these loci.

It was also noticed that despite a trend towards the enhanced H3K9/14ac, transcription of photosynthesis related genes (with the exception of *RBCS1B*) seems to be reduced under high light/temperature conditions (**Figure 25**). Similar findings were also observed in the unicellular green alga *Chlamydomonas reinhardtii*, where a decreased expression of genes of light-harvesting components was demonstrated at high irradiance [249]. It was suggested that a drop of PSII antenna size leads to the protection of photosystem against photoinhibition. However, the reason for loss of PSI at the high light intensity is not clear yet. Notably, acetylation of *RBCS1B*, a member of Rubisco small subunit, at H3K9 results in a transcriptional activation of this gene at light [190]. In our experimental setup there is a tendency of a higher acetylation of *RBCS1B* at H3K9/14 in response to light than in the dark conditions and it is positively correlated with its mRNA abundance. Furthermore, the

transcript of *RBCS1B* is significantly higher in *hot5-2* than in wild type plants under both, light and dark conditions, indicating that NO indeed might be involved in a transcriptional activation of photosynthesis-related genes probably via acetylation of H3K9. This idea contributes to the explanation of the results observed from the mRNA level of photosynthesis-related genes in the dark (**Figure 25**): transcript level of these genes seems to be higher in *hot5*-2 than in wild type plants, although no significant differences between both lines in H3K9/14ac at corresponding loci were observed (**Figure 24**). Hence, it might be assumed that other NO-induced histone modifications or histone acetylation marks are involved in light responsive and regulation of gene expression in *hot5-2*. According to the global histone acetylation NO-induced H3ac or H3K9ac might be responsible for this phenomenon (**Figure 22**).

3.3.2.2 Light-induced SNOs formation effects H3K9ac of chloroplast-related genes

ChIP-seq analysis on H3K9ac was performed to examine the functions of SNO and light on chromatin structure. More than 15000 of H3K9ac sites were found in chromatin of the *Arabidopsis* leaf tissue. The large number of peaks was resided within gene rich areas and almost depleted from pericentromeric regions (**Figure 26**). This observation is in line with reports from other plant species or other histone acetylation marks, e.g. H3K9ac and H3K27ac in *Physcomitrella patens* as well as H3K9ac in rice showed a strong enrichment in genic regions [250][251]. A genome-wide profiling of H3K9ac revealed that this histone modification is predominantly located within the regions surrounding the TSSs of genes (**Figure 27**). This findings are in a strong accordance with published data for other histone marks such as H3K14ac, H3K56ac, H3K4me2 and H3K4me3 suggesting that a depletion of nucleosomes might be occurred immediately upstream to TSSs or there are two adjacent nucleosomes flanking the binding sites which might induce a chromatin configuration [252][253][254].

ChIP-seq data provided evidence which supports a model in which H3K9 acetylation of genes is controlled by light-induced NO production/accumulation that might be involved in inhibition of HDA6 activity. First, it was found that transferring plants into dark for 4 h was accompanied by dramatic changes in H3K9ac (**Figure 28**). Second, *hot5-2* and *hda6* share more than 640 and 250 loci that demonstrate a higher level of H3K9ac than wild type under light and dark conditions, respectively (**Figure 29C**). These results are consistent with the findings of many studies where histone acetylation is required to control light-dependent gene expression that is regulated by light-responsive HATs and HDAs [167][255]. For instance,

illumination negatively regulates HDA activity which leads to the H4 hyperacetylation and transcription of C_4-PEPC promotor gene in maize [256]. Since there are hints to a correlation between light-dependent histone acetylation and NO/SNO formation, it was assumed that NO might control gene expression by regulation of HDAs activity during the day. However, further studies, e.g. RNA-seq analysis should be done to proof whether light-dependent acetylation of H3K9 correlates with gene transcription.

The primary aim of the ChIP-seq study was to find out whether histone acetylation is involved in regulation of photosynthetic processes and what are the photosynthesis-related genes whose H3K9ac level is altered in response to SNO/NO and HDA6 activity. To specifically identify NO- and HDA6-related changes, chloroplast associated peaks were filtered by the peaks that demonstrate a higher H3K9ac level in both mutants than in wild type under the light (left pathway, **Figure 31B**) and peaks that are more acetylated in mutants when they were exposed to light than in the dark (right pathway, **Figure 31C**). In total, 20 photosynthesis related genes with wide range of functions were identified. The most of them were involved in light-dependent reactions that are based on an electron flow which is accompanied by redox reactions.

Photosynthesis is known as a self-regulated process which is determined by a molecular redox signaling. It is suggested that redox state of chloroplast molecules involved in photosynthesis couples the expression of nuclear photosynthesis genes with the degree of photosynthetic efficiency. Such mechanism helps plants to adapt changes in light quality and quantity and to carry on photosynthesis in varying environmental conditions. Redox signaling acts not only within the chloroplast but it is also a key regulator in coordinating expression of nuclear-encoded photosynthetic genes [257][258]. Thereby, anterograde (from nucleus to chloroplast) and retrograde (from chloroplast to nucleus) signaling pathways play an important role in communication between both organelles. During the anterograde regulation the nucleus consists of regulators, such as RNA-binding proteins and sigma factors that provide information about the cell state and regulate the expression of genes required for appreciate chloroplast functions. In contrast, during the retrograde signaling expression of nucleus-encoded photosynthetic genes is regulated by signals generated during photosynthetic processes, such as photosynthetic electron flow and oxidation-reduction activity [259][260].

According to the ChIP-seq data, the majority of photosynthesis related loci were found hyperacetylated primarily in the *hot5-2* mutant. Since there is a strong correlation between light-dependent NO production and photosynthetic light reactions it might be assumed that NO is a part of the retrograde signaling pathway, where it might serve as an antioxidant

molecule preventing a cell from oxidative stress and therefore mediating the photosynthetic performance through the regulation of gene expression. This hypothesis is supported by the occurrence of H3K9 acetylated genes involved in antioxidant response which are linked to photosynthetic performance as well.

PnsB5 (AT5G43750) encodes a NADPH dehydrogenase 18, which was identified as a NDH (chloroplast NADH dehydrogenase-like complex) subunit that interacts via Lhca6 with PSI and forms a NDH-PSI super complex. Although an exact molecular mechanism of this complex remains unclear, it was suggested that the complex may facilitate a novel electron transport required for stress tolerance [261]. Interestingly, Lhca6 (AT1G19150) was also found in our study as a target for NO-dependent H3K9ac. NdhU or CRRL (AT5G21430) is also a part of NDH-PSI complex which is required for NDH activity [262]. AOR (AT1G23740) is a NADHP-dependent alkenal/one oxidoreductase residing in chloroplast and catalyzes the reduction of the α,β-carbonyls. The activity of this enzyme is likely to contribute to the maintenance of photosynthetic process via detoxification of reactive carbonyls produced as a result on elevated ROS production [263][264]. Thioredoxins are important antioxidants that facilitate a reduction of disulfides. Isoforms of this protein exist in most organisms and seems to be relevant for intracellular communication in plants [265][266]. TRX-M4 (AT3G15360) is one of the four isoforms which occurs in chloroplast stroma. It was shown that M-type TRXs are involved in plant growth and CO_2 assimilation, suggesting their role in the activation of Calvin cycle enzymes during photosynthesis [267]. Additionally, TRX-M4 controls photosynthetic alternative electron pathways in *Arabidopsis* [268]. The expression of CYP97B3 (AT4G15110), which belongs to cytochrome P450 family, is highly correlated with the expression of carotenoid biosynthetic genes, indicating the role of this enzyme in the carotenoid pathway [269]. Carotenoids itself act as photoprotectants and antioxidants. Additionally, carotenoids may function as oxidative stress sensors during ROS production [270].

In sum, there is evidence that light-induced NO production regulates H3K9ac of hundreds of genes through the inhibition of HDA6 activity. Moreover, it was identified that NO might be a new player in regulation of photosynthetic machinery by controlling of photosynthetic gene acetylation. However, it seems that found in this study photosynthesis-related genes are regulated in NO/HDA6-independent manner, since in our data only a light-harvesting chlorophyll B-binding protein 3 (Lhcb3, AT5G54270) was found significantly hyperacetylated in both mutants, *hot5-2* and *hda6*, suggesting that these genes might be a target for the NO-inhibited HDA6. These results bring us again to the main question of this

study about the NO/SNOs mode of action that mediates H3K9ac of photosynthesis genes. It might be assumed that: (i) other HDAs apart of HDA6-complxe are required for light-dependent H3K9ac of photosynthesis-related genes. (ii) the presence of a third control element, for example HATs, is necessary to control NO-induced histone acetylation.

A model summarizing all data is illustrated in **Figure 34**. Although the results of this thesis are not always statistically significant, the observed trends provided hints to the existence of a light-dependent mechanism for NO production in *Arabidopsis*. During the day SNO/NO is synthesized from L-Arginine and/or NO_2^- in chloroplast or cytoplasm. H_2O_2 which is formed during the reduction of O_2^- by photosynthetic electron transport components may act as a cofactor to promote NO generation as well [271]. NO as a signaling molecule gets to the nucleus and acts negatively on HDAs activity resulting in H3K9 hyperacetylation of photosynthesis-related genes. H3K9ac might further enable transcriptional activation of these genes and therefore might be involved in regulation of photosynthetic machinery. When plants are transferred to the darkness, chromatin might stay still acetylated until SNO/NO production is reduced and HDAs activity is sufficient to remove the hyperacetylation state. In this study *hot5-2* was used as a tool to study the physiological role of NO/SNOs. The observed trends presented above indicate that light-induced SNO formation might be involved in regulation of histone acetylation. Accordingly, it is proposed that SNO/NO might involved in regulation of photosynthetic performance through the transcriptional activation of photosynthesis-related genes.

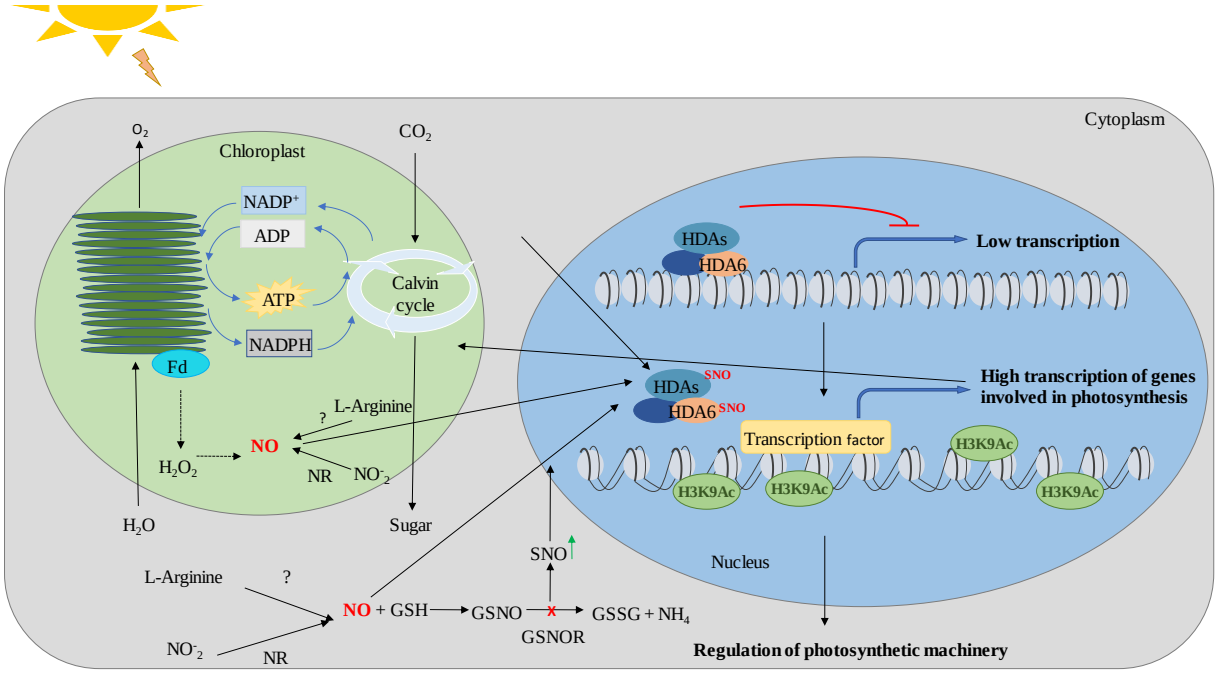

Figure 34: A model of NO regulation of photosynthetic machinery.
Illumination is necessary to promote NO production in a cell. During the day NO may be synthetized by NOS-like activity from L-Arginine or by nitrate reductase (NR) from NO_2^- in chloroplast and cytoplasm. NO may also be promoted by H_2O_2 that is generated by the electron transport chain components during the reduction of O_2^-. NO may react with reduced glutathione (GSH) producing S-nitrosoglutathione (GSNO), the major cellular reservoir of NO. The level of GSNO is controlled by the enzyme GSNO reductase (GSNOR), which catalyses the reduction of GSNO to oxidized glutathione (GSSG) and ammonium (NH_4). As a signaling molecule NO may transport to the nucleus and thereby may regulate the transcription of genes involved in photosynthesis via inhibition of a HDA-complex where HDA6 that was identified as a potential target for NO is a part of it.

4 Outlook

Intense research has been performed in recent years trying to explain the biological functions and mechanism of actions of NO. The results of this thesis in combination with other studies indicate that NO might participate in changes of chromatin structure. Although it was shown that H3K9/14 hyperacetylation does not necessarily lead to the gene transcription, further studies should be performed in order to find out whether a H3K9ac mark, which is usually associated with active chromatin, results in transcriptional activation of H3K9 hyperacetylated loci.

Furthermore, it was observed that some selected genes found H3K9/14 hyperacetylated and upregulated after GSNO treatment in *Arabidopsis* seedlings do not demonstrate the same acetylation pattern in *hot5-2* mutant, hence further questions should be addressed: (i) What are the other factors which might be affected by GSNO treatment that result in H3K9/14ac and their transcriptional activation? (ii) Are there any differences in NO-induced biological

functions between NO arisen from GSNO and NO originated from GSNOR-deficient mutant (*hot5-2*)?

It was shown that there is a tendency demonstrating that NO might be involved in histone acetylation and inhibition of HDAs activity, suggesting that NO might regulate gene expression by S-nitrosylation of HDA-complex. Although HDA6 was found as NO-targeting isoform, it should be still confirmed whether the inhibition of HDA6 activity was induced by S-nitrosylation of this protein. Moreover, measurements of HDA6 activity demonstrate only 30 % inhibition induced by a high GSNO concentration (1 mM), indicating that other members of HDA6-complex might be required for NO-dependent histone acetylation. Therefore, it might be of interest to decode molecular functions of other members of the HDA6-complex.

Besides that, first time evidence was presented indicating a tendency in the light-dependent NO/SNOs production which might be accompanied by changes in histone acetylation. This observation raises a question whether HDAs activity also demonstrates a circadian-like pattern. Therefore, time course investigations of HDAs activity are recommended.

Moreover, findings of this study suggest a new role of NO signaling in regulation of photosynthetic performance. However, it is not clear yet how NO mediates H3K9ac of photosynthesis related genes. Therefore, other HDA isoforms could be used to address this question. Further, the role of NO on regulation of HATs might be studied in this process.

5 Material and Methods

5.1 Materials

5.1.1 Plant Material and Soil

Table 3: Plant Material

Plant lines	Background	Description	Source
Wild type	Col - 0	Wild type line	
Hda6ko (*axe1 – 5*)	Col - 0	Splice site mutant. Base substitution at the third exon-intron junction	[170], [209]
HDA6/Compl	*axe1 – 5*	Complementation of genomic HDA6 (gHDA6) under neutral promoter (2000 bp upstream of ATG). Homozygous line (T3 generation) is obtained	self-made
HDA6/273 C/A	*axe1 – 5*	Point mutation of cysteine 273 to alanine. Homozygous line (T3 generation) is obtained	self-made
HDA6/285 C/A	*axe1 – 5*	Point mutation of cysteine 285 to alanine. Homozygous line (T3 generation) is obtained	self-made
HDA6/273/285 C/A	*axe1 – 5*	Point mutation of cysteines 273 and 285 to alanine. Homozygous line (T3 generation) is obtained	self-made
35S:FLAG-HDA6	Col - 0	Overexpression of cHDA6 under 35S promoter. Homozygous line (T3 generation) is obtained	self-made
Hda19ko	Col - 0	T – DNA insertion line	TAIR
Hot5 - 2	Col - 0	GSNOR knock-out line	[272]
N. benthamiana		Tobacco wild type	

Table 4: Cell lines

Cell lines	Background	Description	Source
Wild type	Col - 0	Generated from root tissue	Lab
Hda6ko (*axe1 – 5*)	Col - 0	Generated from root tissue	Lab

Soil (Floraton 1, Floragard) for cultivation of *A. thaliana* was mixed with silica sand in a 5:1 ratio. For cultivation of *N. benthamiana* "Einheitserde Classic" (Einheitserde- und Humuswerke, Gebr. Patzer GmbH) was mixed with perlite.

5.1.2 Bacterial strains

E. coli strains were used for Gateway® cloning, whereas *Agrobacterium tumefaciens* was used to generate transgenic lines.

Table 5: Bacteria strains

Species	Strain	Application	Source
Escherichia coli	DH5α	Cloning	Lab
Escherichia coli	DB3.1	Maintain Gateway® vectors	Lab
Agrobacterium tumefaciens	*GV3101 (pMP90)*	Plant transformation	Lab

5.1.3 Plasmids and vectors

All plasmids and vectors used in this study are listed below. pDONR222 was used as the entry vector for Gateway® cloning and was transformed into *E.coli DH5α*. pBGW,0 and pAlligator3 were used as destination vectors for transforming of *A.tumefaciens GV3101 (pMP90)*.

Table 6: Plasmids used for Gateway® cloning

Plasmid	Cloning procedure
P_gHDA6_pDONR222	gHDA6 together with endogenous promoter (2000 bp upstream of gHDA6) were amplified from gDNA of A. thaliana using primers # 1 and 3. The product was purified and attB sites were added using primers # 2 and 4. Afterwards the product was transferred into pDONR222 by BP reaction.
P_gHDA6_273C/A_pDONR222	Cysteine 273 was mutated to alanine trough the exchange of TGT to GCT using primers # 5 and 6. P_gHDA6_pDONR222 was used as a template
P_gHDA6_285C/A_pDONR222	Cysteine 285 was mutated to alanine trough the exchange of TGT to GCT using primers # 7 and 8. P_gHDA6_pDONR222 was used as a template
P_gHDA6_273_285C/A_pDONR222	Cysteines 273 and 285 were mutated to alanine trough the exchange of TGT to GCT using primers # 7 and 8. P_gHDA6_273_285C/A_pDONR222 was used as a template
P_gHDA6_pBGW,0	Entry clone P_gHDA6_pDONR222 was transformed into a destination vector pBGW,0 by LR reaction
P_gHDA6_273C/A_pBGW,0	Entry clone P_gHDA6_273C/A_pDONR222 was transformed into a destination vector pBGW,0 by LR reaction
P_gHDA6_285C/A_pBGW,0	Entry clone P_gHDA6_285C/A_pDONR222 was transformed into a destination vector pBGW,0 by LR reaction
P_gHDA6_273_285C/A_pBGW,0	Entry clone P_gHDA6_273_285C/A_pDONR222 was transformed into a destination vector pBGW,0 by LR reaction
P_gHDA6_pAlligator3	Entry clone P_gHDA6_pDONR222 was transformed into a destination vector pAlligator3 by LR reaction

P_gHDA6_273C/A_pAlligator3	Entry clone P_gHDA6_273C/A_pDONR222 was transformed into a destination vector pAlligator3 by LR reaction
P_gHDA6_285C/A_pAlligator3	Entry clone P_gHDA6_285C/A_pDONR222 was transformed into a destination vector pAlligator3 by LR reaction
P_gHDA6_273_285C/A_pAlligator3	Entry clone P_gHDA6_273_285C/A_pDONR222 was transformed into a destination vector pAlligator3 by LR reaction
HDA6_pEarlyGate202	[179]

Table 7: Vectors

Vector	Source
pDONR222	Thermo Fisher Scientific
pBGW,0	Helmholtz Zentrum München, lab ware
pAlliagator3 Δ35S	Zhang, unpublished

5.1.4 Primer

All primers were synthetized by Eurofins MWG Operon (Ebersberg, Germany). 100 µM stock solutions were prepared by dilution with ddH_2O according to descriptive data from manufacturer and stored at – 20 °C.

Table 8: Primer used for cloning and mutagenesis

#	Name	Sequence 5' → 3'
1	P_HDA6_T-fw	AGC CCG ATA ATG ACT GCC AC
2	attB_P_HDA6_T-fw	GGGG ACA AGT TTG TAC AAA AAA GCA GGC TTC AGC CCG ATA ATG ACT GCC AC
3	P_HDA6_T-rv	GGT GAT GAT GAG ACT TCA GTG GT
4	attB_P_HDA6_T-rv	GGGG AC CAC TTT GTA CAA GAA AGC TGG GTC GGT GAT GAT GAG ACT TCA GTG GT
5	gHDA6_273C/A_fw	CTT CAG GCT GGT GCT GAC TCC TTA AGT GGT GAT CGG
6	gHDA6_273C/A_rv	AGC ACC AGC CTG AAG AAC AAC TGC CTC TGG CTG ATA C
7	gHDA6_285C/A_fw	TTG GGT GCC TTC AAC TTA TCA GTC AAG GGT CAC GCT G
8	gHDA6_285C/A_rv	GTT GAA GGC ACC CAA CCG ATC ACC ACT TAA GGA GTC

Table 9: Primer used for sequencing

#	Name	Sequence 5' → 3'
9	M0_fw	GGA GAT AAA CGG TCA AGA TCG ACT
10	M1_fw	GAC TCT GAG TGA GAG AGA GAT TCT GA
11	M2_fw	ATC TAC CTG AAA CCT TGA AGC CTT
12	M3_fw	GGT TGG GTT GCT TCA ACT TAT CAG
13	M4_fw	ACT TTC GGG ACT AAT ACA CGC A

14	M5_fw	ACC TCT TCA TGG TTA CTC ATG TCG
15	M6_fw	GGC TCA TAG CCT AAT CAT TCA CTA TC
16	M6_rv	GAT AGT GAA TGA TTA GGC TAT GAG CC
17	M7_fw	GAT TCT GAG TGA GAG ACG GAG ATG
18	M7_rv	CTG GTT TAA GAC GAT GGA GGA TTC A
19	M8_left border	CTG ACG TAT GTG CTT AGC TC
20	M9_right border	CGC ACT AGT GAT ATC ACC ACT
21	FLAG-HDA6_fw	GAC TAC AAA GAC GAT GAC GAC AA
22	FLAG-HDA6_rv	ACG ATG GAG GAT TCA CGT CTG

Table 10: Primer used for qPCR

#	Name	Sequence 5' → 3'
23	At2g34420.1_fw	TCC TCA ACC ATG GCT TTG TCC TC
24	At2g34420.1_rv	TTG GCG ACA GTC TTC CTC ATG G
25	AT3G54890.1_fw	AGA TGG GCT ATG CTC GCT GTT C
26	AT3G54890.1_rv	TCC TGA GCC TTA ACC CAG TTT CC
27	AT4G12800.1_fw	CCG AGC TGT TAA ATC CGA CAA GAC
28	AT4G12800.1_rv	AAG GTA CCA CGC GAT CAA TGG G
29	AT3G47470.1_fw	TGA TTA TCT CAC CGG CAG TCT TGC
30	AT3G47470.1_rv	TCT GGA TCC TCT GCT AGA CCC AAC
31	AT1G08380.1_fw	AGC GCC AAG AAC CCT TTG AGA C
32	AT1G08380.1_rv	CCA GTT CCT CTC AAA GCA AGT GAC
33	At5g44240_fw	AGA ACT TGT GGG AGC AAT TCA GC
34	At5g44240_rv	ACC ATA GCT GAA GGC AAG CAA TC
35	At5g56870_fw	ACA CAG AGA GTT CCG GTG TGA G
36	At5g56870_rv	GCT GGT GTA GCA AAC GTA GAC TTG
37	At1g44170_fw	CGT GAT TCG TTC TCG ACC TAA GCC
38	At1g44170_rv	TGG CAA TGT GTG AAG TGC AAG ATG
39	At3g55520_fw	TGA AGA GAG AGC CAG GCT AGA AG
40	At3g55520_rv	CTT TCG CAG CTG CAG CAA TCT C
41	At5g27600_fw	CGG CTC AAG ATC ATA GAC AGG AAG
42	At5g27600_rv	CGT GAA TGA AAC ACT GCG AAA CG
43	At3g23150_fw	TGT TAG ATT CTC CGG CGG CTA TG
44	At3g23150_rv	TTC CCA TGA ATC AAC TGC ACC AC
45	At3g23050_fw	AAG CTA CCA GGA TCT TTC TGA TGC
46	At3g23050_rv	ATT CCT TGT GCT CCA TAG TTT CCC
47	At3g03950_fw	TGG CGA ATA ACG AGA ACA AGC C
48	At3g03950_rv	CCC ATG CTC CAG ATT CAC CTC TTG
49	At2g03140_fw	TCC ATA GCT GGT CCT GCT GTT C
50	At2g03140_rv	TGC CAA CAT TGC CAC AAT CCT ATC

5.1.5 Chemicals

All chemicals used in this work were of high purity grade and were purchased either from Sigma Aldrich (Taufkirchen, Germany), Carl Roth GmbH (Karlsruhe, Germany) or Merck (Darmstadt, Germany). Some selected chemicals are listed below:

Table 11: Selected chemicals

Name	Source
S-nitrosoglutathione (GSNO)	No. ALX-420-002, Enzo
S-nitroso-penicillamine (SNAP)	No. BML-CN210-0100, Enzo
2-(4-Carboxyphenyl)-4,4,5,5-tetramethylimidazoline-1-oxyl-3-oxide (cPTIO)	No. ALX-430-001, Enzo
Dichloro-isonicotinic acid (INA)	No. 5398-44-7, Sigma
Trichostatin A (TSA)	No. T8552, Sigma
Boc-Lys(Ac)-MCA	I-1875, Bachem
Trypsin	No. 37289, Serva

5.1.6 Enzymes

Table 12: Enzymes

Name	Application	Source
Phusion® High Fidelity DNA Polymerase	Proof-reading polymerase	No. M0530, New England Biolabs
iProof High-fidelityTM Phusion Polymerase	Proof-reading polymerase	No. 1725300, Biorad
MangoTaq™ DNA Polymerase	High-yield polymerase	No. BIO-21083, Bioline
Gateway® BP Clonase™ Enzyme Mix	Gateway® cloning	Invitrogen
Gateway® LR Clonase™ Enzyme Mix	Gateway® cloning	Invitrogen
SensiMix™ SYBR Low-ROX Kit	Real time PCR analysis	No. BIO-94005, Bioline
Trypsin/Lys-C Mix, Mass Spec Grade	Digestion of chromatin	No. V5072, Promega
Proteinase K Solution	Removal of endogenous nucleases	No. AM2548, Thermo Fisher Scientific
RNase A	Degradation of single-stranded RNA	No. EN0531, Thermo Fisher Scientific
PvuI	Restriction enzyme	No. ER0621, Thermo Fisher Scientific
XbaI	Restriction enzyme	No. ER0681, Thermo Fisher Scientific
NdeI	Restriction enzyme	No. ER0581,

SspI	Restriction enzyme	New England BioLabs No. ER0771,
ApaI	Restriction enzyme	New England BioLabs No. ER1411,
BamHI	Restriction enzyme	New England BioLabs No. ER0051,
EcoRV	Restriction enzyme	Thermo Fisher Scientific No. ER0301,
HpaI	Restriction enzyme	New England BioLabs No. R0105S,
NheI	Restriction enzyme	New England BioLabs No. ER0971,
AvaI	Restriction enzyme	New England BioLabs No. ER0381,
DpnI	Restriction enzyme	New England BioLabs No. ER1701, New England BioLabs

5.1.7 Antibiotics

All Stock solutions were dissolved in ddH_2O and sterilized using 0.22 µm sterile filters (Millipore, No. SLGP033RS). Aliquots were stored at -20 °C.

Table 13: Antibiotic selection of bacteria

Name	Stock concentration, (mg/ml)	Working concentration, (µg/ml)	Source
Ampicillin	100	100	Duchefa Biochemie
Kanamycin	50	50	Duchefa Biochemie
Chloramphenicol	34	25	Serva
Gentamycin	25	25	Roche
Rifampicin	50	50	Duchefa Biochemie

5.1.8 Antibodies

Table 14: Antibodies

Name	Species	Dilution	Source
Anti-acetyl Histone H3	rabbit	1:20000	No. 06-599, Millipore
Anti-acetyl H3K9	rabbit	1:5000	No. ab4441, Abcam
Anti-acetyl H3K9K14	rabbit	1:2000	No. C15410200, Diagenode
Anti-acetyl Histone H4	rabbit	1:20000	No. 06-866, Millipoer

Anti-acetyl H4K5	rabbit	1:10000	No. ab51997, Abcam
Anti-acetylated protein	rabbit	1:5000	No. A5463, Sigma
Anti-rabbit-IgG-HRP	mouse	1:2500	No. W401B, Promega
Goat anti-rabbit IgG-HRP	goat	1:20000	No. As09602, Agrisera
Monoclonal anti-FLAG M2	mouse	1:1000	No. F3165, Sigma-Aldrich
Anti-FLAG tag	rabbit	1:5000	No. ab1162, Abcam
Anti-mouse-IgG-HRP	goat	1:2500	No. W4021, Promega

5.1.9 Solutions and media

All media for plant and bacterial cultivation were autoclaved after adjustment of the pH.

Table 15: Media used for plant cultivation

Name	Composition (per liter)	pH	Source
½ MS agar	2.2 g MS plus Vitamins 10 g Sucrose 10 g Phyto agar	5.7 (KOH)	Duchefa Biochemie Duchefa Biochemie
Plant growth media	4.4 g MS plus Vitamins 10 g Sucrose 0.5 g MES Monohydrate	5.7 (KOH)	Duchefa Biochemie

Table 16: Media used for bacterial cultivation

Name	Composition (per liter)	pH	Source
LB media	25 g LB broth high salt	7.0 (NaOH)	Duchefa Biochemie
LB agar	LB media 12.5 g Agar for microbiology	7.0 (NaOH)	Sigma

Table 17: Buffer for nucleic acid agarose gel

Name	Composition
TAE-buffer	40 mM TRIS 1 mM EDTA pH 8.0 (acetic acid)
DNA size standard	GeneRuler 1kb DNA ladder, No. SM0313, Thermo Fisher scientific

Table 18: Glycin-SDS-Polyacrylamidgelelektrophoresis

Name	Composition
Resolving gel buffer	1.5 M Tris/HCl pH 8.8 4 % (w/v) SDS
Stacking gel buffer	0.5 M Tris/HCl pH 6.8 4 % (w/v) SDS

10% SDS Running buffer	250 mM Tris 2 M Glycin 1 % (w/v) SDS
2 x sample buffer	No. S3401, Sigma Aldeich
4 x sample buffer	No. 1610747, Bio-Rad
Protein ladder	PageRuler prestained protein ladder, No. 26616, Thermo Fisher scientific

For SDS-PAGE applications either Mini-PROTEAN® TGX™ Precast Gels (12%) (No. 4561043, Bio Rad) or self-made gels were used.

Table 19: 2 x Glycin-SDS gel

Compound	Stop gel	Resolving gel	Stacking gel
dH_2O	575 µl	3.7 ml	2.5 ml
Resolving gel buffer	625 µl	2.75 ml	-
Stacking gel buffer	-	-	1.25 ml
Acrylamid (30%)	1.25 ml	4.4 ml	1 ml
SDS (10%)	25 µl	110 µl	50 µl
TEMED	6.26 µl	5.5 µl	20 µl
Ammonium persulfate (10%)	18.75 µl	55 µl	40 µl

Table 20: Buffers for transfer and immunodetection of proteins (Western Blot)

Name	Composition
Transfer buffer	25 mM Tris 192 mM glycine 20 % (v/v) methanol
1 x TBS	10 mM Tris/HCl pH 7.5 0.9 % NaCl 1 mM $MgCl_2$ x 6 H_2O
TBST	1 x TBS 0.05 % Tween 20
Blocking buffer	5 % BSA TBST

Table 21: Buffers for protein staining

Name	Composition
Coomassie R-250 staining solution	0.25 % (w/v) Coomassie brilliant blue R-250 50 % Methanol 10 % Acetic acid
Coomassie R-250 destaining solution	30 % Methanol 10 % Acetic acid
Ponceau S solution	No. 09276-6X1EA-F, Sigma-Aldrich

Table 22: Buffers for plant transformation

Name	Composition
Infiltration buffer	10 mM MES 10 mM $MgSO_4$ pH 5.6 (NaOH)
Floral dip buffer	5 % Sucrose 0.05 % Silwet L77

Table 23: Buffers for protein extraction

Name	Composition
CelLytic P buffer	No. C2360, Sigma Aldrich
PBS buffer	137 mM NaCl 2.7 mM KCl 10 mM Na_2HPO_4 1.8 mM KH_2PO_4 If necessary 0.8 % Triton x-100 was added to solubilize membrane associated proteins
Nuclear lysis buffer (NLB)	20 mM Tris/HCl, pH 7.4 25 % glycrol 20 mM KCl 2 mM EDTA 2.5 mM $MgCl_2$ 250 mM Sucrose 1 mM DTT Protease inhibitor
Nuclear wash buffer 1 (NRBT)	20 mM Tris/HCl, pH 7.4 25 % glycrol 2.5 mM $MgCl_2$ 0.2 % Triton x-100
Nuclear wash buffer 2 (NRB)	20 mM Tris/HCl, pH 7.4 25 % glycrol 2.5 mM $MgCl_2$
Nuclear protein lysis buffer (NPLB)	1 x IP (Life technologies, Cat No. 158266100) 75 mM NaCl 2 mM MgCl2 1 mM DTT
Nuclear storage buffer (NSB)	20 mM Tris/HCl, pH 7.4 25 % glycrol 2.5 mM $MgCl_2$ 250 mM Sucrose
Nuclear protein extraction buffer (NPEB)	1 x IP (life technologies) 100 mM NaCl 2 mM $MgCl_2$ 1 mM DTT

	Protease inhibitor

Table 24: Buffers for HDA activity assay

Name	Composition
HDA Buffer	25 mM Tris/HCl, pH 8.0 137 mM NaCl 2.7 mM KCl 1 mM MgCl2 sterile-filtered
2 x Stopping Buffer	100 mM Tris/HCl, pH 8.0 200 mM NaCl sterile-filtered

Table 25: Buffers for chromatin immunoprecipitation

Name	Composition
Crosslinking buffer	400 mM sucrose 10 mM Tris-HCl pH 8.0 5 mM β-mercaptoethanol 1 % formaldehyde
Extraction buffer # 1	400 mM sucrose 10 mM Tris-HCl pH 8.0 5 mM β-mercaptoethanol Protease inhibitor
Nuclei sonication buffer	50 mM Tris-HCl pH 8.0 10 mM EDTA pH 8.0 1 % SDS Protease inhibitor
RIPA buffer	50 mM Tris-HCl pH 8.0 150 mM NaCl 2 mM EDTA pH 8.0 1 % NP-40 0.5 % Sodium Deoxychlorate 0.1 % SDS Protease inhibitor
Low salt wash buffer	0.1 % SDS 1 % Triton X-100 2 mM EDTA 20 mM Tris-HCl pH 8.0 150 mM NaCl
High salt wash buffer	0.1 % SDS 1 % Triton X-100 2 mM EDTA

	20 mM Tris-HCl pH 8.0 500 mM NaCl
LiCl wash buffer	0.25 M LiCl 1 % NP-40 1 % Sodium Deoxychlorate 1 mM EDTA
	10 mM Tris-HCl pH 8.0
TE buffer	10 mM Tris-HCl pH 8.0 1 mM EDTA
Elution buffer	1 % SDS 100 mM $NaHCO_3$

5.1.10 Kits

Table 26: Applied Kits

Name	Application	Source
RNeasy® Plant Mini Kit	RNA isolation from plant tissue	No. 74904, Qiagen GmbH
innuPREP Plant RNA Kit	RNA isolation from plant tissue	No. 845-KS-2060050, Analytic Jena
QuantiTect® Reverse Transcription Kit	cDNA synthesis for qPCR	No. 205311, Qiagen GmbH
QIAquick® Gel Extraction Kit	DNA extraction from agarose gel	No. 28704, Qiagen GmbH
QIAprep® Spin Miniprep Kit	Plasmid DNA isolation from bacteria	No. 27104, Qiagen GmbH
QIAprep® PCR Purification Kit	Purification of PCR products	No. 28104, Qiagen GmbH
iProof High-Fidelity PCR Kit	DNA amplification	No. 1725331, Bio-Rad
Epigenase™ HDAC Activity/Inhibition Direct Assay Kit (Fluorometric)	Measurement of HDACs activity	No. P-4035, Epigentek
Histone Purification Mini Kit	Histone extraction	No. 40026, Active Motif
Agilent High Sensitivity DNA Kit	Sizing and quantitation of fragmented DNA	No. 5067-4626, Agilent Technologies

5.1.11 Other working materials

Table 27:Working materials

Name	Source
1.5 ml Bioruptor Pico Microtubes	No. C30010016, Diagenode
Nitrocellulose membrane 0.45 µm	No. 10600002, GE Healthcare Life Sciences
Miracloth	No. 475855, Merck Millipore
Anti-FLAG M2 affinity gel	No. A2220, Sigma Aldrich
Flag peptide	No. F3290, Sigma Aldrich

PD 10 desalting columns	No. 17-0851-01, GE Healthcare Life Sciences
Zeba spin desalting columns, 7K MWCO	No. 89882, Thermo Fisher Scientific
Dynabeads protein A	No. 10001D, Thermo Fisher Scientific

Table 28: Devices and accessories

Name	Type	Source
Autoclave	D-150	Systec
Balance	PS600/C/2	Wägetechnik München
	CPA225D	Sartorius
	L2200P	Sartorius
Centrifuge	5415D	Eppendorf
	5417R	Eppendorf
	5810R	Eppendorf
	RC26+	Sorvall
Camera	Powershot G2	Canon
Gel electrophoresis	Power Supply-EPS 601	GE Healthcare
Homogenizer	Silamat S6	Ivoclar vivadent
Magnetic stirrer	IKA-Combimag Ret	IKA
Mastercycler	Nexus Gradient	Eppendorf
Microscope	BX700	Olympus
Microwave	Micromat	AEG
Molecular imaging system	Fusion FX7	IM Biotechnology
NO-Analyzer	Sievers 280i	GE Healthcare
	CLD Supreme	Eco Physics
pH meter	pH 523	WTW
Photosynthesis yield analyzer	Mini-PAM II	Walz
Protein electrophoresis system	Mini-PROTEAN Tetra system	Bio-Rad
Protein blotting system	SemiDry Electroblotter	Sartorius
Rotary evaporator	Univapo 150H	UniEquip
Scanner	Image Scanner II	GE Healthcare
Shaker	Unitherm	UniEquip
Spectrophotometer	Infinite M1000 Pro	Tecan
	NanoDrop ND-1000	NanoDrop Technologies
	Ultrospec 3100 pro	Amersham
Thermo Mixer	Thermomixer comfort	Eppendorf
Transilluminator	UV Transilluminator	UVP
Real time thermal cycler	ABI 7500	Applied biosystem
UltraPure water system	UltraClear	Siemens
Ultrasonic bath	BioRuptor Pico	Diagenode
Ultrasonic device	Sonopuls HD2070	Bandelin
Vortex	Genie 2	Scientific Industries
Water bath	VBW 12	VWR

5.2 Methods

5.2.1 Plant cultivation

5.2.1.1 Cultivation on soil

A.thaliana seeds were sown on moist soil mixed in ratio 1:5 with sand to ensure proper aeration and stratified for 48 hours in dark at 4 °C. Plants were grown under long day (14 h light/10 h dark and 20 °C/18 °C, respectively) or short day (10 h light/14 h dark and 20 °C/16 °C, respectively). The relative humidity during the day and night was 70 and 50 %, respectively. Light intensity in both conditions was ca. 100 to 130 µmol/sm^2. In the first week plants were covered with plastic foil to maintain constant humidity. Plants were watered twice a week.

5.2.1.2 Cultivation in liquid media

Around 50 µl of dry volume of seeds in 1.5 ml reaction vessel were quickly rinsed with 1 ml of 70 % MeOH (ca. 1 min) and sterilized with 1 ml of 50 % bleach solution rotating for 12 min at 4 °C. Seeds were washed at least 5 times with 1 ml of sterile water and stratified for 3 days in dark at 4 °C. Approximately 100 µl of wet seeds (equal to 3 drops of 200 µl pipet) were added to 70 ml of liquid 1 x MS media and let grow for 7 days on shaking platform (120 rpm) under short day condition.

5.2.1.3 Cultivation of suspension cells

Suspension cells were grown shaking (200 rpm) in sterilized AS media in dark at 26 °C and 2.5 g of cells were subculted every week.

5.2.2 Molecular biology techniques

5.2.2.1 Quantitative RT-PCR analysis

Around 100 mg of *Arabidopsis* tissue was ground to a fine powder, followed by RNA extraction using a RNeasy Plant Mini Kit (Qiagen, Cat No. 74904) according to the manufacturer's instruction. RNA concentration and quality were determined by NanoDrop 1000. 1 µg of total RNA was used for the cDNA synthesis employing a QuantiTect Rev. Transcription Kit (Qiagen, Cat No. 205311). A qRT - PCR reaction was composed of 10 µl of Sybr green (Bioline, Cat No. QT625-05), 5 µl of dH_2O, 0.5 µl of 10 µM specific primers and 4 µl of 1:20 diluted cDNA template. Thermocycling conditions were:

Table 29:Cycler program for qPCR

Temperature	Time	Number of cycles
95 °C	10 min	
95 °C	15 s	45
55 °C	15 s	
72 °C	45 s	
Dissociation step		
95 °C	15 s	
60 °C	60 s	
95 °C	15 s	

Each sample was quantified by triplicate analysis and normalized to a house keeping gene as internal control.

5.2.2.2 DNA extraction

1 to 3 young leaves were ground in liquid nitrogen. 250 µl of CTAB buffer were added to the powder. The mixture was incubated for 10 min at 65 °C. The sample was cool down and 200 µl of chloroform/isoamylalcohol (24:1) were added and vortexed. The sample was centrifuged for 5 min at max speed. Then the upper aqueous phase was transferred to a new reaction vessel and 1 µl of 1 % LPA followed by 600 µl of ice cold ethanol were added. The mixture was short vortexed and incubated at – 20 °C for 1 h. The participated DNA was spun down for 10 min at 4 °C and max speed. The supernatant was discarded and the pellet washed with 70 % ethanol and centrifuged for 2 min. The pellet was air dried for approximately 10 min and resolved in 50 µl dH_2O. The concentration of DNA was determined by NanoDrop 1000.

5.2.2.3 Polymerase chain reaction (PCR)

PCR was applied to amplify specific DNA regions. Presence of DNA fragments or colony screening was obtained using Mango*Taq* polymerase. For high fidelity PCRs iProof polymerase (Biorad, Cat No 1725301) was preferred. Usually 500 ng – 1 µg of cDNA or genomic DNA, respectively as well 1 ng of plasmid was used to amplify a gene of interest. Annealing temperature was altered depending on the melting temperature of primer pair while an elongation step was dependent on the size of the product.

5.2.2.4 BP reaction

To create an entry clone 150 ng of donor vector was incubated with 50 fmol attB sites containing PCR product in the presence of 1 µl of BP - clonase buffer and 1 µl BP - clonase mix. Ingest 5 µl of reaction was incubated over night at 25 °C in a thermocycler. The reaction was stopped by adding 0.5 µl of Proteinase K and incubated for 10 min at 37 °C. In the end 2 µl of BP recombination reaction was transformed to DH5α competent cells. After one night several bacterial colonies were picked and search for the presence of insert DNA was performed by PCR.

5.2.2.5 LR reaction

150 ng of destination vector were incubated with 50 – 150 ng of entry clone together with 1 µl of LR clonase and LR clonase buffer. 5 µl of reaction were incubated for 4 h at 25 °C in a thermocycler. 0.5 µl of Proteinase K were added and incubated for 10 min at 37 °C to stop the reaction. 2 µl of reaction were transformed to *DH5α* competent cells. Several bacterial colonies were picked and grown over night in a LB media with appreciate antibiotic. Plasmid was isolated using Plasmid mini kit (Qiagen, Cat No 12123) and sequenced (Eurofins MWG).

5.2.2.6 Site mutation

A single site mutation of genomic HDA6 was based on a double primer mutation protocol described in [273]. Genomic HDA6 driven under endogenous promoter (2000 bp upstream the HDA6 sequence) was introduced into pDONR222 vector and used as a template. The primers for the exchange of a Cys to Ala were designed in the way that the mutation position was located in the 5' end of the primer pair that was complementary to each other. The 3' end of the primer pair was consisted of the non-overlapping segment, which was larger than the overlapping part to make the melting temperature of the non-complementary part higher. The PCR reaction of 20 µl contained 50 ng of the template, 0.5 µM of each primer, 200 µM of dNTP mix and 0.02 U/µl of iProof polymerase (Bio-rad, Cat No 1725301). The PCR program was as follow:

Table 30: Cycler program for site mutation

Temperature	Time	Number of cycles
98 °C	3 min	
98 °C	25 s	20 cycles
62 °C	20 s	
72 °C	3.5 min	
72 °C	5 min	

8 °C	forever

The PCR reaction was treated with 5 units of DpNI under follows conditions:

Temperature	Time
37 ^{0}C	10 h
65 ^{0}C	7 min
8 ^{0}C	forever

5 µl of the PCR reaction was analyzed by the electrophoresis. 2 µl of reaction were transformed in *DH5α* by heat shock and plated on the plate with an appreciate antibiotic. After one night growth the plasmid was extracted using a plasmid extraction kit (Qiagen, Cat No 27104) and sequenced (Eurofins MWG).

5.2.2.7 Heat shock transformation of chemically competent bacteria

50 – 100 ng of plasmid were added to 50 µl of chemically competent bacteria cells DH5α that were thawed on ice and mixed gently. The mixture was incubated on ice for 15 min followed 1 min heat shock in a 42 °C water bath. Subsequently the bacteria mixture was put on ice for 5 min. 800 µl of LB media without antibiotic was added and bacteria were grown for one hour in shaking incubator at 37 °C and 200 rpm. Afterwards ca. 50 µl of bacteria were plated on the LB agar plate containing the appreciate antibiotic and let grow overnight in an incubator at 37 °C.

5.2.2.8 Transformation by electroporation

Ca. 100 ng of plasmid was mixed gently with 50 µl of *Agrobacteria* cell suspension *GV3101 pMP90* by flicking the bottom of the tube and the mixture was added into a precooled cuvette. The cuvette was placed in the holder of electroporation device and shocked one time at 1.25 kV with a 25 µF capacitance and the resistance of 400 Ω. The transfected cells were diluted with 2 ml of LB medium without antibiotic and shacked one hour at 28 °C and 200 rpm. After that the cells were transferred into a new 2 ml tube and centrifuged 3 min at 3800 x g. The bacteria cells were resuspended in 500 µl of LB medium and 10 µl were plated on the LB agar plate containing three antibiotics (gentamicin, rifampicin and a selection antibiotic for a plasmid). Finally the bacteria were grown for 2 days at 28 °C.

5.2.2.9 Plasmid purification

Plasmid DNA was isolated from overnight bacteria culture using QIAprep Spin Miniprep Kit (Qiagen, Cat No 27104) according to manufactory's instruction.

5.2.2.10 Restriction digest

A total reaction volume of 20 µl was composed of 0.5 µg of PCR product that was incubated with 1 µl of restriction enzyme and a recommended buffer. After incubation at the optimal reaction temperature usually at 37 °C for 2 h digestion was visualized by gel electrophoresis.

5.2.2.11 Agarose gel electrophoresis

Depending on the size of DNA fragments 1 to 2 % agarose gel (1 – 2 g agarose ultra-pure solved in 100 ml of TAE buffer) supplemented with ethidium bromide (Roth) was used. Electrophoresis of DNA was conducted under constant voltage condition of 120 V for 30 – 45 min and was visualized on UV transilluminator (MegaCapt).

5.2.2.12 DNA extraction from gel

DNA extraction from gel was performed using QIAquick® Gel Extraction Kit (Qiagen, Cat No 28704) according to manufactory's instruction.

5.2.3 Generation of transgenic lines

5.2.3.1 Agrobacterium-mediated transformation of A. thaliana by floral dip

Arabidopsis plants were grown until flowering stage. To get more floral buds, inflorescences were cut to stimulate the growth of the secondary bolts. Plants were dipped when the secondary inflorescences were 1 to 10 cm high.

One colony of *Agrobacterium tumefaciens* strain carrying a plasmid was grown shaking overnight in LB medium with the appreciate antibiotics at 28 °C. The overnight culture was diluted in a fresh prepared 300 ml LB medium with antibiotics and let grow shaking for one more night. Afterwards the cells were harvested by centrifugation for 25 min at 4000 rpm. The bacteria pellet was resuspended in an infiltration medium to a final OD_{600} of 0.8 - 1. 0.05 % silwet L-77 was added to the infiltration medium just before the floral dipping. For the transformation inflorescences were dipped into the infiltration medium and gentle agitated there for ca. 30 sec. After infiltration the plants were coved with a plastic bag to maintain the humidity and left overnight in a low light. The plants were returned in a growing chamber next day.

5.2.3.2 Selection of homozygous line

Seeds of the transformed plants (T1) were sawn on the soil and after one and a half week of germination small seedling were sprayed with a BASTA. The spraying was repeated a week after once more time. Up to ten survived plants were left to grow to produce the seeds of T2 generation. The seeds of T2 plants were collected separately and approximately 100 seeds of each plant were sawn again. After the germination seedling were sprayed with a BASTA as described above and the number of resistant plants was counted. The T2 generation should have ¾ resistant for a signal insertion. Each line of T2 generation that showed a deviation of this rule was rejected. Up to 10 plants of each T2 line carrying a single insertion was left to produce the seeds of T3 generation. The seeds were collected separately and sawn again. The lines that showed 100 % resistance after the BASTA spraying were named as homozygous.

5.2.4 Protein methodologies

5.2.4.1 Nuclear protein extraction

Nuclear proteins were extracted from *Arabidopsis* cell culture or seedlings according to the protocol of [274] with small modifications. Ca. 0.5 - 0.6 g of grinded *Arabidopsis* tissue or cell culture were homogenized in 3 ml of LB buffer and filtered through two layers of miracloth and 40 µm nylon mesh sequentially. The homogenate was centrifuged for 10 min at 1500 g and 4 °C. The supernatant was discarded and the pellet was resuspended in 3 ml of NRBT buffer and centrifuged as described above. This step was repeated two more times or until the green color is gone (chloroplast contaminations). The triton X - 100 was removed from the nuclei pellet by washing it in 3 ml of NRB buffer. If the nuclei were not used immediately, they were resuspended in 400 µl of NSB buffer, frozen at liquid nitrogen and stored at - 80 °C.

Two methods were used to break a nuclear envelope and solubilize proteins. For quick detection of nuclear proteins by western blot, nuclear pellet was resuspended in 50 µl of laemmli buffer, heated for ca. 10 min at 95 °C and centrifuged for 15 min at maximal speed. Protein concentration was measured using a RC DC protein assay (Biorad, Cat No 5000121). The second method was based on the sonication procedure using micro tip MS 72 (Bandelin, Cat No 492). The nuclei pellet was resuspended in ca. 300 µl of NPLB buffer and sonicated for 30 sec, step 3 and 20 – 40 %. The sonication step was repeated in total 5 times with ca. 1 min break in between. Protein concentration was measured using a Bradford reagent (Biorad, Cat No 5000006).

5.2.4.2 Crude extracts preparation

Cell suspension or plant samples were grounded to fine powder and homogenized in two volumes of extraction buffer rotating for approximately one hour at 4 °C. For the extraction of rec. Flag:HDA6 CelLytic P Puffer (Sigma, Cat No C2360) was used. Extraction of crude extracts for other purposes was performed with DPBS buffer (Thermo Fisher Scientific, Cat No 14190144). The extracts were filtered through two layers of miracloth and centrifuged at max speed for 15 min. The supernatant was transferred in a new tube and protein concentration was measured using a Bradford reagent (Biorad, Cat No 5000006).

5.2.4.3 Histone preparation

Histone proteins were extracted either from in liquid grown seedlings or from leaf tissue with a Histone Purification Kit (Active Motif, Cat No. 40025) using manufacturing instruction with some modifications. 0.5 – 0.6 g start material were ground to a powder and incubated for 2 h with 2.5 ml extraction buffer on a rotating platform at 4 °C. The extracts were centrifuged at 4 °C for 10 min at maximal RCF. Afterwards the supernatants were transferred to PD 10 columns (GE Healthcare, Cat No. 17085101), which prior were equilibrated two times with 3.5 ml pre-cooled extraction buffer. The proteins were eluted with 3.5 ml extraction buffer. The eluates were neutralized with ¼ volumes of 5 x neutralization buffer (0.875 ml) to reach a pH of 8. Purification of core histones was the same as in the instruction following the buffer exchange procedure using Zeba spin desalting columns 7K MWCO (Thermo Fisher, Cat No. 89882). Columns were prepared by adding three times 300 µl dH_2O with a Protease Inhibitor EDTA-free tablet (Roche, Cat No. 04693132001). 100 µl of purified core histones were added to the column and centrifuged for 2 min at 1500 RCF. Histone amount was measured by NanoDrop 1000 at 230 nm.

5.2.4.4 Bradford protein assay

Protein content was determined using a Bradford reagent (Biorad, Cat No 5000006). Initially standard curve was generated using a bovine serum albumin (BSA) as a reference protein. The dilution series from 0 to 10 µg/ml protein were prepared from a stock solution 1mg/ml of BSA and were measured tree times to create a regression curve. The absorption was plotted on the y - axis and BSA concentration on x - axis.

To determine a protein amount of extracts 1 µl of a sample was mixed with 200 µl of Bradford reagent and 200 µl of dH_2O in a cuvette and incubated for 10 min at room

temperature. The absorption was measured at 595 nm against a blank that was composed of 1 µl of extraction puffer instead of crude extract.

5.2.4.5 SDS - PAGE

Protein extracts were equally loaded on a precast 12% polyacrylamide (Biorad, Cat No 4561044) or self-made gel and subjected to a sodium dodecyl sulfate-polyacrylamide gel (SDS-PAGE) using a Mini-PROTEAN® Electrophoresis cell (Biorad, Cat No 1658002EDU). Gels were run at 130 V for ca. 60 min in 1 x running buffer. After separation of proteins a gel was either stained for 30 min with Coomassie brilliant blue solution or further used for western blot.

5.2.4.6 Western blot

Proteins were transferred to a nitrocellulose membrane (Abcam) using a semi - dry western blot system. Pre-wet membrane and gel were sandwiched between whatman papers that were pre-soaked before in a transfer buffer. A transfer was performed for 45 min at room temperature. A flow rate of electric charged was dependent on length (L), width (W) and amount (n) of membranes and was calculated as follows: mA=L x W x 2.5 x n. An efficient transfer of proteins was determined by staining a membrane with Ponceau S solution (Sigma - Aldrich, Cat No 6226-79-5). Afterwards a membrane was incubated for 1 h in a blocking buffer shaking at room temperature followed by binding with primary antibody in 5 % BSA/TBS-T buffer overnight at 4 °C. A membrane was washed three times for 5 min with 1 x TBS-T buffer and incubated for 1 h at room temperature with horseradish peroxidase (HRP) - linked secondary antibody in 5% BSA/TBS-T buffer. A membrane was washed first once with 1 x TBS-T and two times with 1 x TBS buffer. The signal was developed using Western lightning plus-ECL chemiluminescence substrate (PerkinElmer, Cat No NEL105001EA).

5.2.5 Recombinant expression and purification

A vector carrying a N-terminally Flag-targeted HDA6 was obtained from [179] and was transferred to *DH5α* followed by electroporation of *GV3101 pMP90*. Transgenic *A. thaliana* lines overproducing 35S:Flag-HDA6 were generated by floral dip method as described above. Homozygous lines were selected and used for further studies.

Plants expressing recombinant Flag-HDA6 were harvested three weeks after sowing. For analytical studies around 4 g of ground material were used. Protein extracts were prepared in

two volumes (ca.8 ml) of CelLyticP buffer (Sigma-Aldrich, Cat No C2360) with 1 % of a Protease Inhibitor EDTA-free tablet (Roche, Cat No. 04693132001) by rotating for 1 h at 4 °C. Extracts were filtrated trough miracloth (Millipore, Cat No 475855-1R) followed by 15 min centrifugation at 6000 x g and 4 °C. 60 µl of Flag-targeted beads (Sigma-Aldrich, Cat No A2220) were equilibrated with TBS buffer according to the manufacturer's instruction and added to the extracted proteins. A binding of recombinant protein to the beads were performed at 4 °C rotating for 4 h. Afterwards the resin was centrifuged for 30 sec at 8200 x g and supernatant was discarded. The beads were washed tree times with TBS solution and Flag-HDA6 was eluted with 200 ng/µl of Flag-Peptide (Sigma-Aldrich, Cat No F3290) by incubation the resin with synthetic peptide rotating for 30 min at 4 °C.

5.2.6 Measurement of HDA activity

HDA activity was measured using a commercially available Epigenase^{TM} HDAC Activity/Inhibition Direct Assay Kit (Epigentek, Cat No. P-4035-48) according to the manufacturer's instruction. 3-17 µl of purified Flag-HDA6 per well were treated with chemicals such as GSNO, GSH, TSA, DTT and incubated with 50 ng of substrate for 90 min at RT. HDA-deacetylated product was immuno-recognized and the fluorescence at $530_{Ex}/590_{Em}$ nm was measured in a fluorescent microplate reader (Tecan infinite 1000). The RFU values were directly used for relative quantification of HDA activity.

HDA activity was also measured according to [188]. 3-17 µl of purified Flag-HDA6 per well were first treated with GSNO or TSA for 30 min in the dark at RT followed by incubation with DTT (if it was required) for another 30 min. The HDA reaction was started by adding 200 µM of HDA-substrate (Boc-Lys(Ac)-MCA) in 25 µl of HDA buffer followed by 60 min incubation at 37°C. The reaction was stopped by adding 45 µl of 2 x Stopping solution containing 10 mg/ml trypsin and 1 µM TSA. The mixture was incubated for an additional 20 min at 30°C to ensure the tryptic digestion. The release of 7-amino-4-methylcoumarin (AMC) was measured by monitoring of florescence at $380_{Ex}/460_{Em}$ nm.

5.2.7 NO measurements

5.2.7.1 Nitrosothiol and nitrite measurement

S-Nitrosothiols and nitrite were measured using Sievers Nitric Oxide Analyzer NOA 280i (GE Analytical Instruments). The method is based on reduction of SNOs and nitrite to NO, that is further oxidized by ozone to NO_2 (excited state) and O_2. On the way to the ground state NO_2 emits chemiluminescence which can be measured by photomultiplier.

Ca. 300 – 500 mg of plant tissue were homogenized in the same volume of PBS solution and incubated for 20 min rotating at 4 °C. Protein extracts were separated from plant debris by centrifugation for 15 min at maximal speed. 20 – 100 µl of analyte were injected into triiodide solution. For the detection of SNO content sulfanilamide (1:9) was additionally added to protein extracts to scavenge nitrite and 200 µl were injected. Every measurement was performed in duplicates. A standard curve was created with sodium nitrite.

5.2.7.2 Measurement of NO emission

NO emission was measured from 3.5 – 4-week old *Arabidopsis* plants using a CLD Supreme chemiluminescence analyzer (ECO PHYSICS). The purified measuring gas with a constant flow of 600 ml/s was first conducted through a cuvette, containing a plant, subsequently through the chemiluminescence analyzer. The gas was purified from NO by pulling it through charcoal column. GFS-3000 (Walz) was connected with a cuvette and used for simulating and controlling parameters important for plant photosynthesis such as temperature, CO_2 (400 ppm), H_2O (13000 ppm), relative humidity (50 %) and light. Temperature and light were dependent from the experimental setup. For the sunflecks experiment a plant was first adapted to ambient conditions (200 µmol/m^2s PAR and 22 °C) for 1 h afterwards a light stress was applied. A sunflecks pattern was created by increasing a light intensity to 1000 µmol/m^2s PAR and temperature to 30 °C for 10 min followed by returning both parameters back to ambient conditions for other 10 min. This pattern was repeated in total for four times. Additionally the emission of soil without a plant was measured and subtracted from plant emission.

5.2.8 LC-MS/MS

5.2.8.1 Destaining

Ca. 20 µg of core histone proteins were separated on 20 % polyacrylamide gel by SDS Page and stained with Coomassie brilliant blue solution. Bands corresponding to H3 and H4 were cut into small pieces and washed with 200 µl H_2O shaking for 1 min at 37 °C. Supernatant was removed and gel pieces were neutralized with 300 µl of 50 mM NH_4HCO_3 shaking for 1 min at 37 °C. Supernatant was discarded and slices were distained in 300 µl 50% ACN/50 mM NH_4HCO_3 shaking at 37 °C until the color is completely gone. Distained gel pieces were washed twice with H_2O and supernatant was removed.

5.2.8.2 Blocking of free lysines

Unmodified lysines were chemically blocked by adding to the gel pieces a master mix of 15 µl d6-deuterated acetic anhydride (99% D, Sigma) and 150 µl 0.1 M NH_4HCO_3. 5 min after the start of the reaction 585 µl of 1 M NH_4HCO_3 were added and the pH was adjusted to neutral (pH 7-8). Acetylation was performed for 1 h at 37 °C. Afterwards, gel pieces were washed tree times with H_2O for 5 min shaking at 37 °C and dehydrated by adding 150 µl of ACN several times until the slices turned to white.

5.2.8.3 Trypsin digestion

Trypsin digesting was performed on ice by adding to the gel pieces a master mix containing 50 µl of 50 mM NH_4HCO_3 and 5 µl of 200 ng/µl trypsin and incubating for 20 min to let the slices absorb the trypsin and turn transparent again. 150 µl of ice-cold 50 mM NH_4HCO_3 were added and samples were incubated overnight shaking at 37 °C.

5.2.8.4 Acid extraction

Subsequently the tryptic peptides (supernatant) were transferred to a 2 ml low binding tube. Parallel 250 µl of 50 mM NH_4HCO_3 were added to the gel pieces, shacked for 15 min at 37 °C and the supernatant was added to the tube. After 100 µl of 0.25 % TFA/50% ACN were added to slices and incubated shaking for 15 min at 37 °C. The supernatant was also added to the tube. This step was repeated twice. Then 60 µl of ACN were supplied to the gel pieces and the supernatant was also added to the tube. This step was repeated twice. Peptides were vacuum concentrated and resuspended in 50 µl of 0.1 % TFA.

5.2.8.5 Peptide processing

Histone peptides were desalted using C18 OMIX Tips (Agilent Technologies, Cat No. A57003100) which were equilibrated first three times with 20 µl of ACN and three times with 20 µl of 0.1 % TFA. All centrifuge steps were performed at room temperature and 800 rpm. Afterwards peptides were added to the C18 Tips, centrifuged and the flow trough was returned back to the tip. This step was repeated two more times and the flow trough was saved for the further application to Carbon TopTip (glysci). C18 Tips were washed three timed with 20 µl of 0.1 % TFA and eluted three times with 20 µl 80 % ACN/0.25 % TFA. Carbon TopTips were equilibrated by applying first of 100 µl ACN and then 100 µl 0.1 % TFA for three to four times separately. The flow through from C18 Tips was added to the Carbon

TopTip and centrifuged. This step was repeated up to ten times. Afterwards the column was washed three times with 100 µl of 0.1 % TFA and eluted with 60 µl of 80 % ACN/0.25 % TFA. The eluates from both columns were mixed together and vacuum concentrated. The peptides were resuspended in 0.1 % TFA and used for LC-MS/MS measurements.

5.2.9 Chromatin immunoprecipitation followed by qPCR (ChIP-qPCR) or deep sequencing (ChIP-seq)

5.2.9.1 Experimental design

Wild type and mutant plants were grown under chamber-controlled conditions (10/14 h light/dark) for 4 weeks. At this time plants achieved similar development stage.
At midday (11 am: 5 h after turn on the light) plants were transferred either to dark (D, 0 µE, 22 °C), low light (LL, 22 °C) or to high light (HL, 1000 µE, 30 °C) conditions for 4 h. After all, they were harvested and immediately cross-linked.

5.2.9.2 Cross-linking

1-2 g of *Arabidopsis* leaves were put in a 50 ml plastic tube and fill up with 30 ml precooled crosslinking buffer containing 1% formaldehyde. Concentration of suitable formaldehyde amount was obtained experimentally. The tubes were put in desiccator and vacuum was applied for 10 min. Crosslinking was stopped by adding to each tube glycine with the end concentration of 0.125 M followed by vacuum infiltration for another 5 min. After that leaves were washed twice with cooled water and dried on paper towels. Collected material was frozen in liquid nitrogen and stored at -80 °C.

5.2.9.3 Antibody coupling to magnetic beads

For each IP 20 µl of magnetic beads A were used. Beads of one biological replicate were washed together by pipetting up and down for 4 times with 1 ml buffer RIPA plus protease inhibitor. After, beads were suspended in the same volume with RIPA. Following antibodies were used to immunoprecipitate protein-DNA complex: anti-H3K9/14ac antibody (1 µg/IP), anti-H3K9ac antibody (1 µg/IP), IgG antibody (1 µg/IP, negative control) were added. Coupling of the antibodies to the beads was performed at 4°C on a rotation platform for approximately 7 h. In between chromatin isolation steps were performed.
After coupling the AB-coated beads were washed with 500 µl RIPA for 3 times and resuspended with the same buffer. The beads were divided into new clean tubes (20 µl/IP).

5.2.9.4 Chromatin isolation

Leaves were ground to fine powder with mortar and pistil in liquid nitrogen. 2.3 g and 1.3 g of grounded material for ChIP-qPCR and ChIP-seq respectively were transferred in a 50 ml plastic tube and mixed with 20 ml Extraction buffer # 1. The suspension was incubated for 15-20 min at rotation platform at 4°C, followed by centrifugation at 4°C and 2800 g for 20 min. After that, supernatant was removed and pellet was suspended in total with 3 ml NRBT buffer. First 1 ml of buffer was added, pellet was suspended with a pipet tip, and then the rest 2 ml were added. Further, the nuclei were extracted using the same procedure as described before.

5.2.9.5 Sonication

After nuclei were isolated, they were carefully suspended (avoiding foam formation) with nuclei sonication buffer. Bioruptor® Pico ultrasonic bath and Covaris E220 Evolution were used to shear isolated chromatin for ChIP-qPCR and ChIP-seq, respectively. To perform DNA shearing for ChIP-qPCR 320 µl of sonication buffer were added to nuclei and transferred to 1.5 ml Bioruptor Microtubes (Cat No. C30010016). In total, 14 cycles with 30 sec ON/OFF was used. To perform DNA shearing for ChIP-seq nuclei were resuspended in 220 µl of sonication buffer and transferred to micro Tube AFA Fiber Pre-SlitSnap Cap (Cat No. 520245). Following sonication conditions were used: PIP - 175, DF – 10 %, CPB - 200, 600 sec. After this, sonicated samples were spun for 5 min at 16000 g and 4°C and the supernatant was used directly for immunoprecipitation assay or for the detection of shearing efficiency.

5.2.9.6 Shearing efficiency

50 µl and 20 µl of sonicated chromatin for ChIP-qCR and ChIP-seq, respectively, were diluted to 100 µl with sonication buffer. De-crosslinking was performed by adding 6 µl of 5 M NaCl and samples were incubated for 20 min at 95 °C and 1300 rpm. After that, 2 µl of RNaseA were added and samples were incubated for another 40 min at 37 °C and 1300 rpm. DNA was extracted using MinElute PCR purification kit (Qiagen, Cat No. 28004) or by phenol-chloroform followed by ethanol precipitation. DNA was eluted with 11 µl of dH_2O. Concentration was measured using NanoDrop.

5.2.9.7 Immunoprecipitation and reverse crosslinking

For ChIP-qPCR 50 µl of sonicated chromatin were diluted with 200 µl buffer RIPA (1:5). 10 µl of diluted chromatin were saved as ‘’Input’’ (4%). For ChIP-seq sonicated chromatin was diluted 1:10 with RIPA and 10 % were saved as “Input”. The diluted chromatin was added to AB-coated beads and incubated over night at 4 °C on a rotating platform. After, the beads were washed for 2 times with 1 ml of following buffers: low salt buffer, high salt buffer, LiCl buffer and TE buffer. Each wash step was performed on a rotating platform for 5 min at 4 °C. Immunoprecipitated chromatin (IP) was eluted with 125 µl of elution buffer plus proteinase inhibitor incubating at thermoblock for 15 min at 1200 rpm and 65 °C. Elution was performed twice and bough eluates were mixed together.

For de-crosslinking to each ‘’Input’’ sample elution buffer was added to reach the same volume as for IP samples (250 µl). De-crosslinking was performed by mixing each sample with 10 µl of 5 M NaCl (0.2 M NaCl end concentration) and incubating at 65 °C for at least 4-5 h and 1300 rpm. After that, samples were treated for 1 h with 4 µl of RNaseA (10 mg/ml) at 37 °C. Proteinase K treatment was performed for another two more hours by adding 2 µl Proteinase K (19.2 mg/ml), 5 µl of 0.5 M EDTA and 10 µl of 1 M Tris-HCl (pH 6.5). DNA was purified as described above. The DNA was eluted with 21 µl of dH_2O for ChIP-qPCR or 15 µl of EB elution buffer (Qiagen, Cat No. 154035622) for ChIP-seq. DNA concentration was measured using Qubit™ dsDNA HS Assay Kit (Cat No. Q32851).

5.2.9.8 ChIP-seq

Size selection of fragmented DNA was additionally performed before library preparation using AMPure XP beads (Beckman Coulter, Cat No. A63881). 21 µl of magnetic beads (1.4:1, ratio of beads to sample) were added to each sample and incubated for 10 min at RT. After, beads were placed to a magnetic stand and the supernatant was disposed. Beads were washed three times with 20 µl of 80 % ethanol and dried. DNA was eluted with 12 µl of EB elution buffer by incubation the beads for 3 min.

The size of immunoprecipitated and “Input” samples was analyzed using Agilent High Sensitivity DNA Kit (Cat No. 5067-4626) at Agilent 2100 Bioanalyzer according to the manufacturing instructions.

Library preparation and deep sequencing was performed by IGA Technology Services (https://igatechnology.com/) using NextSeq500 and 30 M (75 bp) reads.

5.2.9.9 ChIP-qPCR

To analyze the quality of IP, ''Input'' and immunoprecipitated with anti-H3K9/14ac and IgG antibodies samples were diluted 1:5 with dH_2O. The qPCR reaction was composed as described in (qPCR). Peak1pos and peak1neg were obtained from [179] and used as quality controls. Moreover, Actin2 was amplified as well to investigate whether it can be used as external normalization control.

To investigate acetylation of genes of interest, ''Input'' and immunoprecipitated with anti-H3K9/14ac antibody samples were diluted 1:10 with dH_2O followed by ChIP-qPCR amplification:

Table 31: Cycler program for ChIP-qPCR

Temperature	**Time**	**Number of cycles**
95 °C	15 min	
95 °C	30 sec	45
55 °C	30 sec	
72 °C	0:45 sec	
Dissociation step		
95 °C	15 sec	
60 °C	1 min	
95 °C	0:15 sec	

5.2.10 Programs and databases

All statistical analyses were performed using SigmaPlot 12.0 (Systat Software GmbH, Erkrath, Germany). All data are reported as the sample mean ±SE. Significances were analyzed using one way ANOVA or two way ANOVA with the Holm-Sidak post-hoc method for each treatment group vs. the control group, or t-test for normally distributed datasets. The data were considered significantly different with a p-value <0.05. At least 3 independent experiments (N=3) were used for analyzing the statistical significance.

Quantitative analyzes of western blot were performed using Image J (National Institutes of Health, Bethesda, USA). The relative intensity of the histone acetylation of a control group (a group to which other groups were compared) was set up as 1. Therefore, the ±SE value of this group is 0.

GO enrichment analysis was performed using a function fisher.test in R version 3.5.0.

Multiple testing corrections by FDR was performed using a function p.ajust in R version 3.5.0

The GO annotation was taken from the org.At.tair.db package, version 3.6.0.

Bowtie2-2.3.4.1 was used to align the reads against TAIR10reference sequence.
Samtools-1.8 (-q2) was used to filter out ambiguous matches before peak calling, and to convert alignment format from sam to bam for DiffBind.

MACS-1.4.2 with TAIR10 *Arabidopsis* genome size and otherwise standard parameters (100 as shiftsize, 200 as fragment length, model fold=10,30; p-value cutoff 1e-5) were used for peak calling.

DiffBind 2.8.0 for different binding analysis, using consensus filtering of peaks across biological replicates and the DESEQ2 method were used for a differential analysis.

Information about *A. thaliana* genome was obtained from TAIR database (Phoenix Bioinformatics Corporation, Redwood City, USA).

Vector NTI 9.1.0 2004 Invitrogen Corporation was used for designing vector maps.

Primers for RT-PCR were designed using an OligoAnalyzer 3.1 (https://eu.idtdna.com/calc/analyzer).

Primers for qPCR were obtained from QuantPrime [275] (http://www.quantprime.de).

qPCR results were analyzed using [276] (http://ewindup.info/miner/).

XCalibur 2.2 (Thermo Fisher Scientific) was used to quantify LS-MS data.

6 Literature

[1] L. L. Moroz and A. B. Kohn, "Parallel evolution of Nitric Oxide signaling: Diversity of synthesis & memory pathways," *Front. Biosci. (Landmark Ed.*, vol. 16, pp. 2008–2051, Jun. 2011.

[2] "Nitric oxide signaling." [Online]. Available: https://www.ncbi.nlm.nih.gov/pubmed/?term=nitric+oxide+signaling.

[3] I. L. Gruetter CA, Barry BK, McNamara DB, Gruetter DY, Kadowitz PJ, "Relaxation of bovine coronary artery and activation of coronary arterial guanylate cyclase by nitric oxide, nitroprusside and a carcinogenic nitrosoamine.," *J Cycl. Nucleotide Res.*, vol. 5, no. 3, pp. 211–24, 1979.

[4] L. Popova and T. Anh Tuan, *Nitric oxide in plants: Properties, biosynthesis and physiological functions*, vol. 34. 2010.

[5] M. Feelisch and J. F. Martin, "The early role of nitric oxide in evolution," *Trends Ecol. Evol.*, vol. 10, no. 12, pp. 496–499, Dec. 1995.

[6] M. N. Hughes, "Chapter One - Chemistry of Nitric Oxide and Related Species," in *Methods in Enzymology*, vol. Volume 436, K. P. Robert, Ed. Academic Press, 2008, pp. 3–19.

[7] D. D. Thomas, "Breathing new life into nitric oxide signaling: A brief overview of the interplay between oxygen and nitric oxide," *Redox Biol.*, vol. 5, no. Supplement C, pp. 225–233, 2015.

[8] A. Bloodsworth, V. B. O'Donnell, and B. A. Freeman, "Nitric Oxide Regulation of Free Radical– and Enzyme-Mediated Lipid and Lipoprotein Oxidation," *Arterioscler. Thromb. Vasc. Biol.*, vol. 20, no. 7, p. 1707 LP-1715, Jul. 2000.

[9] M. Arasimowicz and J. Floryszak-Wieczorek, "Nitric oxide as a bioactive signalling molecule in plant stress responses," *Plant Sci.*, vol. 172, no. 5, pp. 876–887, 2007.

[10] P. Á. L. PACHER, J. S. BECKMAN, and L. LIAUDET, "Nitric Oxide and Peroxynitrite in Health and Disease," *Physiol. Rev.*, vol. 87, no. 1, pp. 315–424, Jan. 2007.

[11] N. Paolocci *et al.*, "The Pharmacology of Nitroxyl (HNO) and Its Therapeutic Potential: Not Just the Janus Face of NO()," *Pharmacol. Ther.*, vol. 113, no. 2, pp. 442–458, Feb. 2007.

[12] J. Astier and C. Lindermayr, "Nitric Oxide-Dependent Posttranslational Modification in Plants: An Update," *International Journal of Molecular Sciences* , vol. 13, no. 11. 2012.

[13] J. R. Lancaster, "Nitric oxide: a brief overview of chemical and physical properties relevant to therapeutic applications," *Futur. Sci. OA*, vol. 1, no. 1, p. FSO59, Aug. 2015.

[14] ´ Angelique Besson-Bard, Alain Pugin and and David Wendehenne, "New Insights into Nitric Oxide Signaling in Plants," *Annu. Rev. Plant Biol*, vol. 59, pp. 21–39, 2008.

[15] H. Yamasaki, Y. Sakihama, and S. Takahashi, "An alternative pathway for nitric oxide production in plants: new features of an old enzyme," *Trends Plant Sci.*, vol. 4, no. 4, pp. 128–129, May 1999.

[16] K. W. Rockel P, Strube F, Rockel A, Wildt J, "Regulation of nitric oxide (NO) production by plant nitrate reductase in vivo and in vitro.," *J Exp Bot*, vol. 53, pp. 103–10, 2002.

[17] W. M. Kaiser *et al.*, "Modulation of nitrate reductase: some new insights, an unusual case and a potentially important side reaction," *J. Exp. Bot.*, vol. 53, no. 370, pp. 875–882, Apr. 2002.

[18] I. D. Wilson, S. J. Neill, and J. T. Hancock, "Nitric oxide synthesis and signalling in plants," *Plant. Cell Environ.*, vol. 31, no. 5, pp. 622–631, 2008.
[19] C. Cantrel *et al.*, "Nitric oxide participates in cold-responsive phosphosphingolipid formation and gene expression in Arabidopsis thaliana," *New Phytol.*, vol. 189, no. 2, pp. 415–427, 2011.
[20] M.-G. Zhao, L. Chen, L.-L. Zhang, and W.-H. Zhang, "Nitric Reductase-Dependent Nitric Oxide Production Is Involved in Cold Acclimation and Freezing Tolerance in Arabidopsis," *Plant Physiol.*, vol. 151, no. 2, pp. 755–767, Oct. 2009.
[21] Z. Kolbert, L. Ortega, and L. Erdei, "Involvement of nitrate reductase (NR) in osmotic stress-induced NO generation of Arabidopsis thaliana L. roots," *J. Plant Physiol.*, vol. 167, no. 1, pp. 77–80, Jan. 2010.
[22] I. OLIVEIRA, Halley C; SAVIANI, Elzira E; OLIVEIRA, Jusceley F. P and SALGADO, "Nitrate reductase-dependent nitric oxide synthesis in the defense response of Arabidopsis thaliana against Pseudomonas syringae.," *Trop. Plant Pathol.*, vol. 35, pp. 104–107, 2010.
[23] J. Bright, R. Desikan, J. T. Hancock, I. S. Weir, and S. J. Neill, "ABA-induced NO generation and stomatal closure in Arabidopsis are dependent on H2O2 synthesis," *Plant J.*, vol. 45, no. 1, pp. 113–122, 2006.
[24] D. L. D. J. S. X. Z. Z. Xu, "Nitrate reductase-mediated nitric oxide generation is essential for fungal elicitor-induced camptothecin accumulation of Camptotheca acuminata suspension cell cultures.," *Appl Microbiol Biotechnol*, vol. 90, no. 3, pp. 1073–1081, 2011.
[25] O. S. Lillo C, Meyer C, Lea US, Provan F, "Mechanism and importance of post-translational regulation of nitrate reductase.," *J Exp Bot.*, vol. 55, pp. 1275–82, 2004.
[26] W. M. Kaiser and S. C. Huber, "Post-translational regulation of nitrate reductase: mechanism, physiological relevance and environmental triggers," *J. Exp. Bot.*, vol. 52, no. 363, pp. 1981–1989, 2001.
[27] U. S. Lea, F. ten Hoopen, F. Provan, W. M. Kaiser, C. Meyer, and C. Lillo, "Mutation of the regulatory phosphorylation site of tobacco nitrate reductase results in high nitrite excretion and NO emission from leaf and root tissue," *Planta*, vol. 219, no. 1, pp. 59–65, 2004.
[28] D. H. D. Procházková D. Pavlíková, "Nitric oxide biosynthesis in plants – the short overview," *Plant Soil Environ.*, vol. 60, no. 3, pp. 129–134, 2014.
[29] R. P. Stöhr C, Strube F, Marx G, Ullrich WR, "A plasma membrane-bound enzyme of tobacco roots catalyses the formation of nitric oxide from nitrite.," *Planta*, vol. 212, pp. 835–41, 2001.
[30] S. S. Stöhr C, "Formation and possible roles of nitric oxide in plant roots.," *J Exp Bot.*, vol. 57, pp. 463–70, 2006.
[31] H. R. Godber BL, Doel JJ, Sapkota GP, Blake DR, Stevens CR, Eisenthal R, "Reduction of nitrite to nitric oxide catalyzed by xanthine oxidoreductase.," *J Biol Chem.*, vol. 275, p. 7757–63., 2000.
[32] D. R. L. Corpas FJ, Palma JM, Sandalio LM, Valderrama R, Barroso JB, "Peroxisomal xanthine oxidoreductase: characterization of the enzyme from pea (Pisum sativum L.) leaves.," *J Plant Physiol.*, vol. 165, pp. 1319–30, 2008.
[33] Elisabeth Planchet and Werner M Kaiser, "Nitric Oxide Production in Plants. Facts and Fictions," *Plant Signal Behav.*, vol. 1, pp. 46–51, 2006.
[34] P. C. Bethke, M. R. Badger, and R. L. Jones, "Apoplastic Synthesis of Nitric Oxide by Plant Tissues," *Plant Cell*, vol. 16, no. 2, p. 332 LP-341, Feb. 2004.
[35] R. V Cooney, P. J. Harwood, L. J. Custer, and A. A. Franke, "Light-mediated conversion of nitrogen dioxide to nitric oxide by carotenoids.," *Environ. Health*

Perspect., vol. 102, no. 5, pp. 460–462, May 1994.
[36] U. Förstermann and W. C. Sessa, "Nitric oxide synthases: regulation and function," *Eur. Heart J.*, vol. 33, no. 7, pp. 829–837, Apr. 2012.
[37] N. M. C. Fang-Qing Guo, Mamoru Okamoto, "Identification of a Plant Nitric Oxide Synthase Gene Involved in Hormonal Signalingle.," *Science (80-.).*, vol. 302, no. 5642, pp. 100–103, 2003.
[38] Y. He *et al.*, "Nitric oxide represses the Arabidopsis floral transition," *Science (80-.).*, vol. 305, no. 5692, pp. 1968–1971, Sep. 2004.
[39] D. Zeidler *et al.*, "Innate immunity in Arabidopsis thaliana: Lipopolysaccharides activate nitric oxide synthase (NOS) and induce defense genes," *Proc. Natl. Acad. Sci. U. S. A.*, vol. 101, no. 44, pp. 15811–15816, Nov. 2004.
[40] T. Zemojtel *et al.*, "Plant nitric oxide synthase: a never-ending story?," *Trends Plant Sci.*, vol. 11, no. 11, pp. 524–525, May 2017.
[41] N. M. Crawford, M. Galli, R. Tischner, Y. M. Heimer, M. Okamoto, and A. Mack, "Response to Zemojtel et al: Plant nitric oxide synthase: back to square one," *Trends Plant Sci.*, vol. 11, no. 11, pp. 526–527, May 2017.
[42] M. Moreau, G. I. Lee, Y. Wang, B. R. Crane, and D. F. Klessig, "AtNOS/AtNOA1 Is a Functional Arabidopsis thaliana cGTPase and Not a Nitric-oxide Synthase," *J. Biol. Chem.*, vol. 283, no. 47, pp. 32957–32967, Nov. 2008.
[43] B. J. Corpas FJ, Palma JM, del Río LA, "Evidence supporting the existence of L-arginine-dependent nitric oxide synthase activity in plants. Le," *New Phytol.*, vol. 184, pp. 9–14, 2009.
[44] N. Foresi, N. Correa-Aragunde, G. Parisi, G. Caló, G. Salerno, and L. Lamattina, "Characterization of a Nitric Oxide Synthase from the Plant Kingdom: NO Generation from the Green Alga Ostreococcus tauri Is Light Irradiance and Growth Phase Dependent," *Plant Cell*, vol. 22, no. 11, p. 3816 LP-3830, Dec. 2010.
[45] C. W. Jin, S. T. Du, I. H. Shamsi, B. F. Luo, and X. Y. Lin, "NO synthase-generated NO acts downstream of auxin in regulating Fe-deficiency-induced root branching that enhances Fe-deficiency tolerance in tomato plants," *J. Exp. Bot.*, vol. 62, no. 11, pp. 3875–3884, Jul. 2011.
[46] N. N. Tun *et al.*, "Polyamines Induce Rapid Biosynthesis of Nitric Oxide (NO) in Arabidopsis thaliana Seedlings," *Plant Cell Physiol.*, vol. 47, no. 3, pp. 346–354, Mar. 2006.
[47] F. Groß, E.-E. Rudolf, B. Thiele, J. Durner, and J. Astier, "Copper amine oxidase 8 regulates arginine-dependent nitric oxide production in Arabidopsis thaliana," *J. Exp. Bot.*, vol. 68, no. 9, pp. 2149–2162, Apr. 2017.
[48] S. Rümer, J. G. Kapuganti, and W. M. Kaiser, "Oxidation of hydroxylamines to NO by plant cells," *Plant Signal. Behav.*, vol. 4, no. 9, pp. 853–855, Sep. 2009.
[49] K. J. Gupta, A. R. Fernie, W. M. Kaiser, and J. T. van Dongen, "On the origins of nitric oxide," *Trends Plant Sci.*, vol. 16, no. 3, pp. 160–168, 2011.
[50] D. D. Pedroso MC1, Magalhaes JR, "Nitric oxide induces cell death in Taxus cells.," *Plant Sci.*, vol. 157, pp. 173–180, 2000.
[51] H. Yamasaki, "Nitrite-dependent nitric oxide production pathway: implications for involvement of active nitrogen species in photoinhibition in vivo.," *Philos. Trans. R. Soc. B Biol. Sci.*, vol. 355, no. 1402, pp. 1477–1488, Oct. 2000.
[52] H. E. Leshem Y, "The Characterization and Contrasting Effects of the Nitric Oxide Free Radical in Vegetative Stress and Senescence of Pisum sativum Linn. Foliage," *Plant Physiol.*, vol. 148, pp. 258–263, 1996.
[53] S. Gouvêa, C., Souza, J., Magalhães, A., Martins, "NO·–releasing substances that induce growth elongation in maize root segments," *Plant Growth Regul.*, vol. 21, no. 3, pp. 183–187, 1997.

[54] L. Beligni, M., Lamattina, "Nitric oxide counteracts cytotoxic processes mediated by reactive oxygen species in plant tissues.," *Planta*, vol. 208, no. 3, pp. 337–344, 1998.
[55] B. Sun, Y. Jing, K. Chen, L. Song, F. Chen, and L. Zhang, "Protective effect of nitric oxide on iron deficiency-induced oxidative stress in maize (Zea mays)," *J. Plant Physiol.*, vol. 164, no. 5, pp. 536–543, May 2007.
[56] C. G. Mata and L. Lamattina, "Nitric Oxide Induces Stomatal Closure and Enhances the Adaptive Plant Responses against Drought Stress," *Plant Physiol.*, vol. 126, no. 3, pp. 1196–1204, Jul. 2001.
[57] L. Zhao, F. Zhang, J. Guo, Y. Yang, B. Li, and L. Zhang, "Nitric Oxide Functions as a Signal in Salt Resistance in the Calluses from Two Ecotypes of Reed," *Plant Physiol.*, vol. 134, no. 2, pp. 849–857, Feb. 2004.
[58] M. Zhao, X. Zhao, Y. Wu, and L. Zhang, "Enhanced sensitivity to oxidative stress in an Arabidopsis nitric oxide synthase mutant," *J. Plant Physiol.*, vol. 164, no. 6, pp. 737–745, 2007.
[59] S. A.-H.-Mackerness, C. F. John, B. Jordan, and B. Thomas, "Early signaling components in ultraviolet-B responses: distinct roles for different reactive oxygen species and nitric oxide," *FEBS Lett.*, vol. 489, no. 2–3, pp. 237–242, 2001.
[60] L. An, Y. Liu, M. Zhang, T. Chen, and X. Wang, "Effects of nitric oxide on growth of maize seedling leaves in the presence or absence of ultraviolet-B radiation," *J. Plant Physiol.*, vol. 162, no. 3, pp. 317–326, Mar. 2005.
[61] J. Puyaubert and E. Baudouin, "New clues for a cold case: nitric oxide response to low temperature," *Plant. Cell Environ.*, vol. 37, no. 12, pp. 2623–2630, 2014.
[62] C. H. Hsu, Y.T., Kao, "Cadmium toxicity is reduced by nitric oxide in rice leaves.," *Plant Growth Regul.*, vol. 42, no. 3, pp. 227–238, 2004.
[63] Q.-Y. Tian, D.-H. Sun, M.-G. Zhao, and W.-H. Zhang, "Inhibition of nitric oxide synthase (NOS) underlies aluminum-induced inhibition of root elongation in Hibiscus moscheutos," *New Phytol.*, vol. 174, no. 2, pp. 322–331, 2007.
[64] M. Delledonne, Y. Xia, R. A. Dixon, and C. Lamb, "Nitric oxide functions as a signal in plant disease resistance," *Nature*, vol. 394, no. 6693, pp. 585–588, Aug. 1998.
[65] F. Song, R. M. Goodman, and R. M. G. Fengming Song, "Activity of Nitric Oxide Is Dependent On, But Is Partially Required for Function of, Salicylic Acid in the Signaling Pathway in Tobacco Systemic Acquired Resistance.," *Mol. Plant-Microbe Interact.*, vol. 14, no. 12, pp. 1458–1462, Dec. 2001.
[66] J. K. Hong *et al.*, "Nitric oxide function and signalling in plant disease resistance," *J. Exp. Bot.*, vol. 59, no. 2, pp. 147–154, Feb. 2008.
[67] X. L. Zhang H, Shen WB, Zhang W, "A rapid response of beta-amylase to nitric oxide but not gibberellin in wheat seeds during the early stage of germination.," *Planta*, vol. 220, pp. 708–16, 2005.
[68] M. Simontacchi, S. Jasid, and S. Puntarulo, "Nitric oxide generation during early germination of sorghum seeds," *Plant Sci.*, vol. 167, no. 4, pp. 839–847, Oct. 2004.
[69] X. Hu, S. J. Neill, Z. Tang, and W. Cai, "Nitric Oxide Mediates Gravitropic Bending in Soybean Roots," *Plant Physiol.*, vol. 137, no. 2, p. 663 LP-670, Feb. 2005.
[70] L. L. Correa-Aragunde N, Graziano M, "Nitric oxide plays a central role in determining lateral root development in tomato.," *Planta*, vol. 218, pp. 900–5, 2004.
[71] D. Procházková, D. Haisel, N. Wilhelmová, D. Pavlíková, and J. Száková, "Effects of exogenous nitric oxide on photosynthesis," *Photosynthetica*, vol. 51, no. 4, pp. 483–489, 2013.
[72] B. Wodala, Z. Deák, I. Vass, L. Erdei, I. Altorjay, and F. Horváth, "In Vivo Target Sites of Nitric Oxide in Photosynthetic Electron Transport as Studied by Chlorophyll Fluorescence in Pea Leaves," *Plant Physiol.*, vol. 146, no. 4, pp. 1920–1927, Apr.

2008.
[73] R. Vladkova, A. G. Dobrikova, R. Singh, A. N. Misra, and E. Apostolova, "Photoelectron transport ability of chloroplast thylakoid membranes treated with NO donor SNP: Changes in flash oxygen evolution and chlorophyll fluorescence," *Nitric Oxide*, vol. 24, no. 2, pp. 84–90, 2011.
[74] S. Takahashi and H. Yamasaki, "Reversible inhibition of photophosphorylation in chloroplasts by nitric oxide," *FEBS Lett.*, vol. 512, no. 1–3, pp. 145–148, Feb. 2002.
[75] N. V Laspina, M. D. Groppa, M. L. Tomaro, and M. P. Benavides, "Nitric oxide protects sunflower leaves against Cd-induced oxidative stress," *Plant Sci.*, vol. 169, no. 2, pp. 323–330, 2005.
[76] H.-K. Lum, C.-H. Lee, Y. K.-C. Butt, and S. C.-L. Lo, "Sodium nitroprusside affects the level of photosynthetic enzymes and glucose metabolism in Phaseolus aureus (mung bean)," *Nitric Oxide*, vol. 12, no. 4, pp. 220–230, 2005.
[77] G. T. Kuruthukulangarakoola *et al.*, "Nitric oxide-fixation by non-symbiotic haemoglobin proteins in Arabidopsis thaliana under N-limited conditions," *Plant. Cell Environ.*, vol. 40, no. 1, pp. 36–50, Jan. 2017.
[78] C. Servet, N. Conde e Silva, and D.-X. Zhou, "Histone Acetyltransferase AtGCN5/HAG1 Is a Versatile Regulator of Developmental and Inducible Gene Expression in Arabidopsis," *Mol. Plant*, vol. 3, no. 4, pp. 670–677, Jul. 2010.
[79] R. Radi, "Protein Tyrosine Nitration: Biochemical Mechanisms and Structural Basis of its Functional Effects," *Acc. Chem. Res.*, vol. 46, no. 2, pp. 550–559, Feb. 2013.
[80] G. Peluffo and R. Radi, "Biochemistry of protein tyrosine nitration in cardiovascular pathology," *Cardiovasc. Res.*, vol. 75, no. 2, pp. 291–302, Jul. 2007.
[81] S. Saito, A. Yamamoto-Katou, H. Yoshioka, N. Doke, and K. Kawakita, "Peroxynitrite Generation and Tyrosine Nitration in Defense Responses in Tobacco BY-2 Cells," *Plant Cell Physiol.*, vol. 47, no. 6, pp. 689–697, Jun. 2006.
[82] M. Chaki *et al.*, "Involvement of Reactive Nitrogen and Oxygen Species (RNS and ROS) in Sunflower–Mildew Interaction," *Plant Cell Physiol.*, vol. 50, no. 2, pp. 265–279, Feb. 2009.
[83] R. Valderrama *et al.*, "Nitrosative stress in plants," *FEBS Lett.*, vol. 581, no. 3, pp. 453–461, 2007.
[84] M. CHAKI *et al.*, "High temperature triggers the metabolism of S-nitrosothiols in sunflower mediating a process of nitrosative stress which provokes the inhibition of ferredoxin–NADP reductase by tyrosine nitration," *Plant. Cell Environ.*, vol. 34, no. 11, pp. 1803–1818, 2011.
[85] C. Álvarez, J. Lozano-Juste, L. C. Romero, I. García, C. Gotor, and J. León, "Inhibition of Arabidopsis O-Acetylserine(thiol)lyase A1 by Tyrosine Nitration," *J. Biol. Chem.*, vol. 286, no. 1, pp. 578–586, Jan. 2011.
[86] P. M. Melo, L. S. Silva, I. Ribeiro, A. R. Seabra, and H. G. Carvalho, "Glutamine Synthetase Is a Molecular Target of Nitric Oxide in Root Nodules of Medicago truncatula and Is Regulated by Tyrosine Nitration," *Plant Physiol.*, vol. 157, no. 3, pp. 1505–1517, Nov. 2011.
[87] C. Holzmeister *et al.*, "Differential inhibition of Arabidopsis superoxide dismutases by peroxynitrite-mediated tyrosine nitration," *J. Exp. Bot.*, vol. 66, no. 3, pp. 989–999, Feb. 2015.
[88] C. P. J´eremy Astier, Ang´elique Besson-Bard, Izabela Wawer and D. W. Sumaira Rasul, Sylvain Jeandroz, James F Dat, "Nitric Oxide Signalling in Plants: Cross-Talk With Ca2+, Protein Kinases and Reactive Oxygen Species.," *Annu. plant Rev.*, vol. 42, pp. 147–170, 2010.
[89] S. P. L. Cary, J. A. Winger, E. R. Derbyshire, and M. A. Marletta, "Nitric oxide

signaling: no longer simply on or off," *Trends Biochem. Sci.*, vol. 31, no. 4, pp. 231–239, May 2006.

[90] B. Roy and J. Garthwaite, "Nitric oxide activation of guanylyl cyclase in cells revisited," *Proc. Natl. Acad. Sci. U. S. A.*, vol. 103, no. 32, pp. 12185–12190, Aug. 2006.

[91] J. Durner, D. Wendehenne, and D. F. Klessig, "Defense gene induction in tobacco by nitric oxide, cyclic GMP, and cyclic ADP-ribose," *Proc. Natl. Acad. Sci. U. S. A.*, vol. 95, no. 17, pp. 10328–10333, Aug. 1998.

[92] D. F. Klessig *et al.*, "Nitric oxide and salicylic acid signaling in plant defense," *Proc. Natl. Acad. Sci.* , vol. 97, no. 16, pp. 8849–8855, Aug. 2000.

[93] C. Garcia-Mata and L. Lamattina, "Nitric Oxide and Abscisic Acid Cross Talk in Guard Cells," *Plant Physiol.*, vol. 128, no. 3, pp. 790–792, Mar. 2002.

[94] and D. F. K. Daniel Clark, Jörg Durner, Duroy A. Navarre, "Nitric Oxide Inhibition of Tobacco Catalase and Ascorbate Peroxidase," *Mol. Plant-Microbe Interact.*, vol. 13, pp. 1380–1384, 2000.

[95] D. A. Navarre, D. Wendehenne, J. Durner, R. Noad, and D. F. Klessig, "Nitric Oxide Modulates the Activity of Tobacco Aconitase," *Plant Physiol.* , vol. 122, no. 2, pp. 573–582, Feb. 2000.

[96] M. J. Nelson, "The nitric oxide complex of ferrous soybean lipoxygenase-1. Substrate, pH, and ethanol effects on the active-site iron.," *J. Biol. Chem.* , vol. 262, no. 25, pp. 12137–12142, Sep. 1987.

[97] M. Perazzolli *et al.*, "Arabidopsis Nonsymbiotic Hemoglobin AHb1 Modulates Nitric Oxide Bioactivity," *Plant Cell*, vol. 16, no. 10, pp. 2785–2794, Oct. 2004.

[98] B.-W. Yun *et al.*, "S-nitrosylation of NADPH oxidase regulates cell death in plant immunity," *Nature*, pp. 264–268, Oct. 2011.

[99] M. R. Hara *et al.*, "Neuroprotection by pharmacologic blockade of the GAPDH death cascade," *Proc. Natl. Acad. Sci. U. S. A.*, vol. 103, no. 10, pp. 3887–3889, Mar. 2006.

[100] L. M. López-Sánchez *et al.*, "Alteration of S-nitrosothiol homeostasis and targets for protein S-nitrosation in human hepatocytes," *Proteomics*, vol. 8, no. 22, pp. 4709–4720, 2008.

[101] A. Cañas *et al.*, "Maintenance of S-nitrosothiol homeostasis plays an important role in growth suppression of estrogen receptor-positive breast tumors," *Breast Cancer Res.*, vol. 14, no. 6, pp. R153–R153, Dec. 2012.

[102] C. Lindermayr, G. Saalbach, and J. Durner, "Proteomic Identification of S-Nitrosylated Proteins in Arabidopsis," *Plant Physiol.*, vol. 137, no. 3, pp. 921–930, Mar. 2005.

[103] A. M. Maldonado-Alconada, S. Echevarría-Zomeño, C. Lindermayr, I. Redondo-López, J. Durner, and J. V Jorrín-Novo, "Proteomic analysis of Arabidopsis protein S-nitrosylation in response to inoculation with Pseudomonas syringae ," *Acta Physiol. Plant.*, vol. 33, no. 4, pp. 1493–1514, 2011.

[104] M. Chaki *et al.*, "Identification of nuclear target proteins for S-nitrosylation in pathogen-treated Arabidopsis thaliana cell cultures," *Plant Sci.*, vol. 238, pp. 115–126, Sep. 2015.

[105] D. Camejo *et al.*, "Salinity-induced changes in S-nitrosylation of pea mitochondrial proteins," *J. Proteomics*, vol. 79, pp. 87–99, Feb. 2013.

[106] J. Astier *et al.*, "Protein S-nitrosylation: What's going on in plants?," *Free Radic. Biol. Med.*, vol. 53, no. 5, pp. 1101–1110, Sep. 2012.

[107] M. T. Forrester, M. W. Foster, M. Benhar, and J. S. Stamler, "Detection of Protein S-Nitrosylation with the Biotin Switch Technique," *Free Radic. Biol. Med.*, vol. 46, no. 2, pp. 119–126, Jan. 2009.

[108] Y. Zhang, A. Keszler, K. A. Broniowska, and N. Hogg, "Characterization and

application of the biotin-switch assay for the identification of S-nitrosated proteins," *Free Radic. Biol. Med.*, vol. 38, no. 7, pp. 874–881, Apr. 2005.
[109] B. Huang and C. Chen, "An ascorbate-dependent artifact that interferes with the interpretation of the biotin switch assay," *Free Radic. Biol. Med.*, vol. 41, no. 4, pp. 562–567, Aug. 2006.
[110] M. Yu, L. Lamattina, S. H. Spoel, and G. J. Loake, "Nitric oxide function in plant biology: a redox cue in deconvolution," *New Phytol.*, vol. 202, no. 4, pp. 1142–1156, 2014.
[111] I. Kovacs and C. Lindermayr, "Nitric oxide-based protein modification: formation and site-specificity of protein S-nitrosylation," *Front. Plant Sci.*, vol. 4, p. 137, May 2013.
[112] D. T. Hess, A. Matsumoto, S.-O. Kim, H. E. Marshall, and J. S. Stamler, "Protein S-nitrosylation: purview and parameters," *Nat Rev Mol Cell Biol*, vol. 6, no. 2, pp. 150–166, Feb. 2005.
[113] M. Liu *et al.*, "Site-Specific Proteomics Approach for Study Protein S-Nitrosylation," *Anal. Chem.*, vol. 82, no. 17, pp. 7160–7168, Sep. 2010.
[114] J. S. Stamler, E. J. Toone, S. A. Lipton, and N. J. Sucher, "(S)NO Signals: Translocation, Regulation, and a Consensus Motif," *Neuron*, vol. 18, no. 5, pp. 691–696, May 1997.
[115] A. Fares, M. Rossignol, and J.-B. Peltier, "Proteomics investigation of endogenous S-nitrosylation in Arabidopsis," *Biochem. Biophys. Res. Commun.*, vol. 416, no. 3–4, pp. 331–336, Dec. 2011.
[116] Y. Wang, B.-W. Yun, E. Kwon, J. K. Hong, J. Yoon, and G. J. Loake, "S-Nitrosylation: an emerging redox-based post-translational modification in plants," *J. Exp. Bot.*, vol. 57, no. 8, pp. 1777–1784, May 2006.
[117] S. M. Marino and V. N. Gladyshev, "Structural analysis of cysteine S-nitrosylation: a modified acid-based motif and the emerging role of trans-nitrosylation," *J. Mol. Biol.*, vol. 395, no. 4, pp. 844–859, Jan. 2010.
[118] D. V Badri *et al.*, "Transcriptome analysis of Arabidopsis roots treated with signaling compounds: a focus on signal transduction, metabolic regulation and secretion," *New Phytol.*, vol. 179, no. 1, pp. 209–223, Jul. 2008.
[119] R. Ahlfors, M. Brosché, H. Kollist, and J. Kangasjärvi, "Nitric oxide modulates ozone-induced cell death, hormone biosynthesis and gene expression in Arabidopsis thaliana," *Plant J.*, vol. 58, no. 1, pp. 1–12, Apr. 2009.
[120] A. Ferrarini *et al.*, "Expression of Medicago truncatula Genes Responsive to Nitric Oxide in Pathogenic and Symbiotic Conditions," *Mol. Plant-Microbe Interact.*, vol. 21, no. 6, pp. 781–790, May 2008.
[121] M. C. Palmieri *et al.*, "Nitric oxide-responsive genes and promoters in Arabidopsis thaliana: a bioinformatics approach," *J. Exp. Bot.*, vol. 59, no. 2, pp. 177–186, Feb. 2008.
[122] A. Polverari, B. Molesini, M. Pezzotti, R. Buonaurio, M. Marte, and M. Delledonne, "Nitric Oxide-Mediated Transcriptional Changes in Arabidopsis thaliana," *Mol. Plant-Microbe Interact.*, vol. 16, no. 12, pp. 1094–1105, Dec. 2003.
[123] M. Parani *et al.*, "Microarray analysis of nitric oxide responsive transcripts in Arabidopsis," *Plant Biotechnol. J.*, vol. 2, no. 4, pp. 359–366, Jul. 2004.
[124] J. C. Begara-Morales *et al.*, "Differential Transcriptomic Analysis by RNA-Seq of GSNO-Responsive Genes Between Arabidopsis Roots and Leaves," *Plant Cell Physiol.*, vol. 55, no. 6, pp. 1080–1095, Jun. 2014.
[125] S. Xu, D. Guerra, U. Lee, and E. Vierling, "S-nitrosoglutathione reductases are low-copy number, cysteine-rich proteins in plants that control multiple developmental and defense responses in Arabidopsis ," *Frontiers in Plant Science* , vol. 4. p. 430, 2013.
[126] G. T. Kuruthukulangarakoola, "Effect of nitric oxide on the growth and development of

Arabidopsis thaliana," 2013.
[127] S. Grün, C. Lindermayr, S. Sell, and J. Durner, "Nitric oxide and gene regulation in plants," *J. Exp. Bot.*, vol. 57, no. 3, pp. 507–516, Feb. 2006.
[128] I. Kovacs, A. Ageeva, E.-E. König, and C. Lindermayr, "S-Nitrosylation of Nuclear Proteins: New Pathways in Regulation of Gene Expression," in *Nitric Oxide and Signaling in Plants*, vol. 77, no. Supplement C, D. B. T.-A. in B. R. Wendehenne, Ed. Academic Press, 2016, pp. 15–39.
[129] P. Gaudu and B. Weiss, "SoxR, a [2Fe-2S] transcription factor, is active only in its oxidized form.," *Proc. Natl. Acad. Sci. U. S. A.*, vol. 93, no. 19, pp. 10094–10098, Sep. 1996.
[130] H. Ding and B. Demple, "Direct nitric oxide signal transduction via nitrosylation of iron-sulfur centers in the SoxR transcription activator," *Proc. Natl. Acad. Sci. U. S. A.*, vol. 97, no. 10, pp. 5146–5150, May 2000.
[131] A. Hausladen, C. T. Privalle, T. Keng, J. DeAngelo, and J. S. Stamler, "Nitrosative Stress: Activation of the Transcription Factor OxyR," *Cell*, vol. 86, no. 5, pp. 719–729, Jun. 1996.
[132] Y. Sha and H. E. Marshall, "S-nitrosylation in the regulation of gene transcription()," *Biochim. Biophys. Acta*, vol. 1820, no. 6, pp. 701–711, Jun. 2012.
[133] C. Bogdan, "Nitric oxide and the regulation of gene expression," *Trends Cell Biol.*, vol. 11, no. 2, pp. 66–75, Jun. 2001.
[134] S. Ambawat, P. Sharma, N. R. Yadav, and R. C. Yadav, "MYB transcription factor genes as regulators for plant responses: an overview," *Physiol. Mol. Biol. Plants*, vol. 19, no. 3, pp. 307–321, Jul. 2013.
[135] G. F. Heine, J. M. Hernandez, and E. Grotewold, "Two Cysteines in Plant R2R3 MYB Domains Participate in REDOX-dependent DNA Binding," *J. Biol. Chem.* , vol. 279, no. 36, pp. 37878–37885, Sep. 2004.
[136] V. Serpa, J. Vernal, L. Lamattina, E. Grotewold, R. Cassia, and H. Terenzi, "Inhibition of AtMYB2 DNA-binding by nitric oxide involves cysteine S-nitrosylation," *Biochem. Biophys. Res. Commun.*, vol. 361, no. 4, pp. 1048–1053, Oct. 2007.
[137] C. P. Tavares, J. Vernal, R. A. Delena, L. Lamattina, R. Cassia, and H. Terenzi, "S-nitrosylation influences the structure and DNA binding activity of AtMYB30 transcription factor from Arabidopsis thaliana," *Biochim. Biophys. Acta - Proteins Proteomics*, vol. 1844, no. 4, pp. 810–817, Apr. 2014.
[138] Y. Wu *et al.*, "The Arabidopsis NPR1 Protein Is a Receptor for the Plant Defense Hormone Salicylic Acid," *Cell Rep.*, vol. 1, no. 6, pp. 639–647, Jun. 2012.
[139] M. Kinkema, W. Fan, and X. Dong, "Nuclear Localization of NPR1 Is Required for Activation of PR Gene Expression," *Plant Cell*, vol. 12, no. 12, pp. 2339–2350, Dec. 2000.
[140] Y. Tada *et al.*, "Plant Immunity Requires Conformational Charges of NPR1 via S-Nitrosylation and Thioredoxins," *Science*, vol. 321, no. 5891, p. 10.1126/science.1156970, Aug. 2008.
[141] C. Lindermayr, S. Sell, B. Müller, D. Leister, and J. Durner, "Redox Regulation of the NPR1-TGA1 System of Arabidopsis thaliana by Nitric Oxide," *Plant Cell*, vol. 22, no. 8, pp. 2894–2907, 2010.
[142] J. Meiser, S. Lingam, and P. Bauer, "Posttranslational Regulation of the Iron Deficiency Basic Helix-Loop-Helix Transcription Factor FIT Is Affected by Iron and Nitric Oxide," *Plant Physiol.*, vol. 157, no. 4, pp. 2154–2166, Dec. 2011.
[143] F. Maurer, S. Müller, and P. Bauer, "Suppression of Fe deficiency gene expression by jasmonate," *Plant Physiol. Biochem.*, vol. 49, no. 5, pp. 530–536, 2011.
[144] K. Luger, M. L. Dechassa, and D. J. Tremethick, "New insights into nucleosome and

chromatin structure: an ordered state or a disordered affair?," *Nat Rev Mol Cell Biol*, vol. 13, no. 7, pp. 436–447, 2012.
[145] A. J. Bannister and T. Kouzarides, "Regulation of chromatin by histone modifications," *Cell Res.*, vol. 21, no. 3, pp. 381–395, 2011.
[146] M. E. Minard, A. K. Jain, and M. C. Barton, "Analysis of epigenetic alterations to chromatin during development," *Genesis*, vol. 47, no. 8, pp. 559–572, 2009.
[147] R. Jaenisch and A. Bird, "Epigenetic regulation of gene expression: how the genome integrates intrinsic and environmental signals," *Nat. Genet.*, vol. 33, pp. 245–254, 2003.
[148] W. C. E. Thomas D. Pollard, "Cell Biology: Das Original mit Übersetzungshilfen," *Spektrum Akad. Verlag; Auflage 2. Aufl.*, 2007.
[149] © 2019 Promega Corporation, "Epigenetic chromatin changes."
[150] J. R. Hickok, D. Vasudevan, W. E. Antholine, and D. D. Thomas, "Nitric Oxide Modifies Global Histone Methylation by Inhibiting Jumonji C Domain-containing Demethylases," *J. Biol. Chem.*, vol. 288, no. 22, pp. 16004–16015, May 2013.
[151] D. Vasudevan *et al.*, "Nitric oxide regulates gene expression in cancers by controlling histone posttranslational modifications," *Cancer Res.*, vol. 75, no. 24, pp. 5299–5308, Dec. 2015.
[152] J. Hu *et al.*, "Nitric Oxide Regulates Protein Methylation during Stress Responses in Plants," *Mol. Cell*, vol. 67, no. 4, p. 702–710.e4, Aug. 2017.
[153] A. Akhtar and P. B. Becker, "Activation of Transcription through Histone H4 Acetylation by MOF, an Acetyltransferase Essential for Dosage Compensation in Drosophila," *Mol. Cell*, vol. 5, no. 2, pp. 367–375, 2000.
[154] C. A. Hassig and S. L. Schreiber, "Nuclear histone acetylases and deacetylases and transcriptional regulation: HATs off to HDACs," *Curr. Opin. Chem. Biol.*, vol. 1, no. 3, pp. 300–308, 1997.
[155] A. Nott, P. M. Watson, J. D. Robinson, L. Crepaldi, and A. Riccio, "S-nitrosylation of histone deacetylase 2 induces chromatin remodelling in neurons," *Nature*, vol. 455, no. 7211, pp. 411–415, 2008.
[156] C. Colussi *et al.*, "HDAC2 blockade by nitric oxide and histone deacetylase inhibitors reveals a common target in Duchenne muscular dystrophy treatment.," *Proc. Natl. Acad. Sci. U. S. A.*, vol. 105, no. 49, pp. 19183–19187, 2008.
[157] X. W. Feng JH, Jing FB, Fang H, Gu LC, "Expression, purification, and S-nitrosylation of recombinant histone deacetylase 8 in Escherichia coli.," *Biosci. Trends.*, vol. 5, pp. 17–22, 2011.
[158] B. Illi *et al.*, "Nitric Oxide Modulates Chromatin Folding in Human Endothelial Cells via Protein Phosphatase 2A Activation and Class II Histone Deacetylases Nuclear Shuttling," *Circ. Res.*, vol. 102, no. 1, p. 51 LP-58, Jan. 2008.
[159] M. Hartl *et al.*, "Lysine acetylome profiling uncovers novel histone deacetylase substrate proteins in Arabidopsis ," *Mol. Syst. Biol.*, vol. 13, no. 10, p. 949, Oct. 2017.
[160] L. Aravind and E. V Koonin, "Second Family of Histone Deacetylases," *Science (80-.).*, vol. 280, no. 5367, p. 1167 LP-1167, May 1998.
[161] M. Dangl, G. Brosch, H. Haas, P. Loidl, and A. Lusser, "Comparative analysis of HD2 type histone deacetylases in higher plants," *Planta*, vol. 213, no. 2, pp. 280–285, 2001.
[162] P. Bheda, H. Jing, C. Wolberger, and H. Lin, "The Substrate Specificity of Sirtuins," *Annu. Rev. Biochem.*, vol. 85, no. 1, pp. 405–429, Jun. 2016.
[163] C. Hollender and Z. Liu, "Histone Deacetylase Genes in Arabidopsis Development," *J. Integr. Plant Biol.*, vol. 50, no. 7, pp. 875–885, Jul. 2008.
[164] A.-C. Koenig *et al.*, "The Arabidopsis class II sirtuin is a lysine deacetylase and interacts with mitochondrial energy metabolism.," *Plant Physiol.*, vol. 164, no. 3, pp. 1401–1414, Jan. 2014.

[165] M. Soccio, M. N. Laus, M. Alfarano, and D. Pastore, "Measuring Activity of Native Plant Sirtuins - The Wheat Mitochondrial Model ," *Frontiers in Plant Science* , vol. 9. p. 961, 2018.
[166] L. Tian *et al.*, "Reversible Histone Acetylation and Deacetylation Mediate Genome-Wide, Promoter-Dependent and Locus-Specific Changes in Gene Expression During Plant Development," *Genetics*, vol. 169, no. 1, pp. 337–345, Jan. 2005.
[167] M. Benhamed, C. Bertrand, C. Servet, and D.-X. Zhou, "Arabidopsis GCN5, HD1, and TAF1/HAF2 Interact to Regulate Histone Acetylation Required for Light-Responsive Gene Expression," *Plant Cell*, vol. 18, no. 11, pp. 2893–2903, Nov. 2006.
[168] C. Zhou, L. Zhang, J. Duan, B. Miki, and K. Wu, "HISTONE DEACETYLASE19 Is Involved in Jasmonic Acid and Ethylene Signaling of Pathogen Response in Arabidopsis," *Plant Cell*, vol. 17, no. 4, pp. 1196–1204, Apr. 2005.
[169] K. Earley *et al.*, "Erasure of histone acetylation by Arabidopsis HDA6 mediates large-scale gene silencing in nucleolar dominance," *Genes Dev.*, vol. 20, no. 10, pp. 1283–1293, 2006.
[170] J. Murfett, X. J. Wang, G. Hagen, and T. J. Guilfoyle, "Identification of Arabidopsis Histone Deacetylase HDA6 Mutants That Affect Transgene Expression," *Plant Cell*, vol. 13, no. 5, pp. 1047–1062, 2001.
[171] Z. Lippman, B. May, C. Yordan, T. Singer, and R. Martienssen, "Distinct Mechanisms Determine Transposon Inheritance and Methylation via Small Interfering RNA and Histone Modification," *PLoS Biol.*, vol. 1, no. 3, p. e67, Dec. 2003.
[172] W. Aufsatz, Mf. Mette, J. van der Winden, M. Matzke, and A. J. M. Matzke, "HDA6, a putative histone deacetylase needed to enhance DNA methylation induced by double-stranded RNA," *EMBO J.*, vol. 21, no. 24, pp. 6832–6841, Dec. 2002.
[173] M. Tanaka, A. Kikuchi, and H. Kamada, "The Arabidopsis Histone Deacetylases HDA6 and HDA19 Contribute to the Repression of Embryonic Properties after Germination," *Plant Physiol.*, vol. 146, no. 1, pp. 149–161, Jan. 2008.
[174] L.-T. Chen and K. Wu, "Role of histone deacetylases HDA6 and HDA19 in ABA and abiotic stress response," *Plant Signal. Behav.*, vol. 5, no. 10, pp. 1318–1320, Oct. 2010.
[175] T. K. To *et al.*, "Arabidopsis HDA6 is required for freezing tolerance," *Biochem. Biophys. Res. Commun.*, vol. 406, no. 3, pp. 414–419, Mar. 2011.
[176] C.-R. Xu *et al.*, "Histone acetylation affects expression of cellular patterning genes in the Arabidopsis root epidermis," *Proc. Natl. Acad. Sci. U. S. A.*, vol. 102, no. 40, pp. 14469–14474, Oct. 2005.
[177] X. Liu *et al.*, "PHYTOCHROME INTERACTING FACTOR3 Associates with the Histone Deacetylase HDA15 in Repression of Chlorophyll Biosynthesis and Photosynthesis in Etiolated Arabidopsis Seedlings," *Plant Cell*, vol. 25, no. 4, pp. 1258–1273, Apr. 2013.
[178] M.-J. Kang, H.-S. Jin, Y.-S. Noh, and B. Noh, "Repression of flowering under a noninductive photoperiod by the HDA9-AGL19-FT module in Arabidopsis," *New Phytol.*, vol. 206, no. 1, pp. 281–294, 2015.
[179] Mengel, "Nitric oxide affects histone acetylation by inhibiting histone deacetylase activity in Arabidopsis. ," *PhD Thesis*, 2016.
[180] A. Mengel *et al.*, "Nitric oxide modulates histone acetylation at stress genes by inhibition of histone deacetylases," *Plant Physiol.*, 2016.
[181] L. Miller, "Method for using ImageJ to analyze western blots." 2010.
[182] I. Kovacs, J. Durner, and C. Lindermayr, "Crosstalk between nitric oxide and glutathione is required for NONEXPRESSOR OF PATHOGENESIS-RELATED GENES 1 (NPR1)-dependent defense signaling in Arabidopsis thaliana," *New Phytol.*, vol. 208, no. 3, pp. 860–872, Jun. 2015.

[183] C. Feller, I. Forné, A. Imhof, and P. B. Becker, "Global and Specific Responses of the Histone Acetylome to Systematic Perturbation," *Mol. Cell*, vol. 57, no. 3, pp. 559–571, 2015.
[184] K. A. Broniowska, A. R. Diers, and N. Hogg, "S-NITROSOGLUTATHIONE," *Biochim. Biophys. Acta*, vol. 1830, no. 5, pp. 3173–3181, May 2013.
[185] B. Lies, D. Groneberg, S. Gambaryan, and A. Friebe, "Lack of effect of ODQ does not exclude cGMP signalling via NO-sensitive guanylyl cyclase," *Br. J. Pharmacol.*, vol. 170, no. 2, pp. 317–327, Sep. 2013.
[186] M. Zottini, A. Costa, R. De Michele, M. Ruzzene, F. Carimi, and F. Lo Schiavo, "Salicylic acid activates nitric oxide synthesis in Arabidopsis," *J. Exp. Bot.*, vol. 58, no. 6, pp. 1397–1405, Apr. 2007.
[187] J. Marschall, Harvey; Que, Loretta; Stamler, *S-Nitrosothiols in lung inflammation*. 2003.
[188] D. Wegener, F. Wirsching, D. Riester, and A. Schwienhorst, "A Fluorogenic Histone Deacetylase Assay Well Suited for High-Throughput Activity Screening," *Chem. Biol.*, vol. 10, no. 1, pp. 61–68, 2003.
[189] A. N. Misra, R. Vladkova, R. Singh, M. Misra, A. G. Dobrikova, and E. L. Apostolova, "Action and target sites of nitric oxide in chloroplasts," *Nitric Oxide*, vol. 39, no. Supplement C, pp. 35–45, 2014.
[190] L. Guo, J. Zhou, A. A. Elling, J.-B. F. Charron, and X. W. Deng, "Histone Modifications and Expression of Light-Regulated Genes in Arabidopsis Are Cooperatively Influenced by Changing Light Conditions," *Plant Physiol.*, vol. 147, no. 4, pp. 2070–2083, 2008.
[191] B. Langmead, C. Trapnell, M. Pop, and S. L. Salzberg, "Ultrafast and memory-efficient alignment of short DNA sequences to the human genome," *Genome Biol*, vol. 10, 2009.
[192] Y. Zhao and O. N. Jensen, "Modification-specific proteomics: Strategies for characterization of post-translational modifications using enrichment techniques," *Proteomics*, vol. 9, no. 20, pp. 4632–4641, Oct. 2009.
[193] Ö. Önder, S. Sidoli, M. Carroll, and B. A. Garcia, "Progress in epigenetic histone modification analysis by mass spectrometry for clinical investigations," *Expert Rev. Proteomics*, vol. 12, no. 5, pp. 499–517, 2015.
[194] S. McKinley-Barnard, T. Andre, M. Morita, and D. S. Willoughby, "Combined L-citrulline and glutathione supplementation increases the concentration of markers indicative of nitric oxide synthesis," *J. Int. Soc. Sports Nutr.*, vol. 12, p. 27, Jun. 2015.
[195] S. Jamaladdin *et al.*, "Histone deacetylase (HDAC) 1 and 2 are essential for accurate cell division and the pluripotency of embryonic stem cells," *Proc. Natl. Acad. Sci.*, vol. 111, no. 27, p. 9840 LP-9845, Jul. 2014.
[196] L. R. Sun, F. S. Hao, B. S. Lu, and L. Y. Ma, "AtNOA1 modulates nitric oxide accumulation and stomatal closure induced by salicylic acid in Arabidopsis," *Plant Signal. Behav.*, vol. 5, no. 8, pp. 1022–1024, Aug. 2010.
[197] F. Hao, S. Zhao, H. Dong, H. Zhang, L. Sun, and C. Miao, "Nia1 and Nia2 are Involved in Exogenous Salicylic Acid-induced Nitric Oxide Generation and Stomatal Closure in Arabidopsis," *J. Integr. Plant Biol.*, vol. 52, no. 3, pp. 298–307, 2010.
[198] K. Gémes *et al.*, "Cross-talk between salicylic acid and NaCl-generated reactive oxygen species and nitric oxide in tomato during acclimation to high salinity," *Physiol. Plant.*, vol. 142, no. 2, pp. 179–192, 2011.
[199] S. D'Alessandro *et al.*, "Limits in the use of cPTIO as nitric oxide scavenger and EPR probe in plant cells and seedlings ," *Frontiers in Plant Science* , vol. 4. p. 340, 2013.
[200] K. Miura and Y. Tada, "Regulation of water, salinity, and cold stress responses by salicylic acid ," *Frontiers in Plant Science* , vol. 5. p. 4, 2014.

[201] P. Wang *et al.*, "Epigenetic Changes are Associated with Programmed Cell Death Induced by Heat Stress in Seedling Leaves of Zea mays," *Plant Cell Physiol.*, vol. 56, no. 5, pp. 965–976, May 2015.
[202] H. Li *et al.*, "Histone acetylation associated up-regulation of the cell wall related genes is involved in salt stress induced maize root swelling," *BMC Plant Biol.*, vol. 14, no. 1, p. 105, 2014.
[203] A. Sokol, A. Kwiatkowska, A. Jerzmanowski, and M. Prymakowska-Bosak, "Up-regulation of stress-inducible genes in tobacco and Arabidopsis cells in response to abiotic stresses and ABA treatment correlates with dynamic changes in histone H3 and H4 modifications," *Planta*, vol. 227, 2007.
[204] X. Chen, L. Lu, S. Qian, M. Scalf, L. M. Smith, and X. Zhong, "Canonical and Noncanonical Actions of Arabidopsis Histone Deacetylases in Ribosomal RNA Processing," *Plant Cell*, vol. 30, no. 1, p. 134 LP-152, Jan. 2018.
[205] P. Liu, H. Zhang, B. Yu, L. Xiong, and Y. Xia, "Proteomic identification of early salicylate- and flg22-responsive redox-sensitive proteins in Arabidopsis," *Sci. Rep.*, vol. 5, p. 8625, Feb. 2015.
[206] A. Nott and A. Riccio, "Nitric Oxide-mediated epigenetic mechanisms in developing neurons," *Cell Cycle*, vol. 8, no. 5, pp. 725–730, Mar. 2009.
[207] P. M. D. Watson and A. Riccio, "Nitric oxide and histone deacetylases: A new relationship between old molecules," *Commun. Integr. Biol.*, vol. 2, no. 1, pp. 11–13, Oct. 2009.
[208] K. Okuda, A. Ito, and T. Uehara, "Regulation of Histone Deacetylase 6 Activity *via S*-Nitrosylation," *Biol. Pharm. Bull.*, vol. 38, no. 9, pp. 1434–1437, 2015.
[209] A. V Probst *et al.*, "Arabidopsis Histone Deacetylase HDA6 Is Required for Maintenance of Transcriptional Gene Silencing and Determines Nuclear Organization of rDNA Repeats," *Plant Cell*, vol. 16, no. 4, pp. 1021–1034, 2004.
[210] A. Devoto *et al.*, "COI1 links jasmonate signalling and fertility to the SCF ubiquitin–ligase complex in Arabidopsis," *Plant J.*, vol. 32, no. 4, pp. 457–466, Nov. 2002.
[211] M. Luo *et al.*, "Histone Deacetylase HDA6 Is Functionally Associated with AS1 in Repression of KNOX Genes in Arabidopsis," *PLOS Genet.*, vol. 8, no. 12, p. e1003114, Dec. 2012.
[212] M. Luo *et al.*, "Regulation of flowering time by the histone deacetylase HDA5 in Arabidopsis," *Plant J.*, vol. 82, no. 6, pp. 925–936, Jun. 2015.
[213] Z. J. Chen and L. Tian, "Roles of dynamic and reversible histone acetylation in plant development and polyploidy," *Biochim. Biophys. Acta*, vol. 1769, no. 5–6, pp. 295–307, May 2007.
[214] A. Eberharter and P. B. Becker, "Histone acetylation: a switch between repressive and permissive chromatin: Second in review series on chromatin dynamics," *EMBO Rep.*, vol. 3, no. 3, pp. 224–229, Mar. 2002.
[215] H. Yang *et al.*, "Genome-Wide Mapping of Targets of Maize Histone Deacetylase HDA101 Reveals Its Function and Regulatory Mechanism during Seed Development," *Plant Cell*, vol. 28, no. 3, p. 629 LP-645, Apr. 2016.
[216] E. Sani, P. Herzyk, G. Perrella, V. Colot, and A. Amtmann, "Hyperosmotic priming of Arabidopsis seedlings establishes a long-term somatic memory accompanied by specific changes of the epigenome," *Genome Biol.*, vol. 14, no. 6, p. R59, Jun. 2013.
[217] S.-K. Han, D. Wagner, W. D. Han S-K, S.-K. Han, and D. Wagner, "Role of chromatin in water stress responses in plants," *J. Exp. Bot.*, vol. 65, no. 10, pp. 2785–2799, Jun. 2014.
[218] N. Liu and Z. Avramova, "Molecular mechanism of the priming by jasmonic acid of specific dehydration stress response genes in Arabidopsis," *Epigenetics Chromatin*,

vol. 9, no. 1, p. 8, 2016.
[219] M. Jaskiewicz, U. Conrath, C. Peterhansel, and C. Peterhänsel, "Chromatin modification acts as a memory for systemic acquired resistance in the plant stress response," *EMBO Rep.*, vol. 12, no. 1, p. 50 LP-55, Dec. 2011.
[220] J. Floryszak-Wieczorek *et al.*, "Nitric Oxide–Mediated Stress Imprint in Potato as an Effect of Exposure to a Priming Agent," *Mol. Plant-Microbe Interact.*, vol. 25, no. 11, pp. 1469–1477, Jul. 2012.
[221] I. L. McConnell, J. J. Eaton-Rye, and J. J. S. van Rensen, "Regulation of Photosystem II Electron Transport by Bicarbonate BT - Photosynthesis: Plastid Biology, Energy Conversion and Carbon Assimilation," J. J. Eaton-Rye, B. C. Tripathy, and T. D. Sharkey, Eds. Dordrecht: Springer Netherlands, 2012, pp. 475–500.
[222] B. A. Diner and V. Petrouleas, "Formation by NO of nitrosyl adducts of redox components of the Photosystem II reaction center. II. Evidence that HCO−3/CO2 binds to the acceptor-side non-heme iron," *Biochim. Biophys. Acta - Bioenerg.*, vol. 1015, no. 1, pp. 141–149, 1990.
[223] B. Wodala, "The effect of nitric oxide on the photosynthetic electron transport of pea leaves," *PhD Thesis, Univ. Szeged*, 2009.
[224] K. K. Hossain, T. Nakamura, and H. Yamasaki, "Effect of nitric oxide on leaf non-photochemical quenching of fluorescence under heat-stress conditions," *Russ. J. Plant Physiol.*, vol. 58, no. 4, pp. 629–633, 2011.
[225] A. N. Misra, R. Singh, M. Misra, R. Vladkova, A. Dobrikova, and E. Apostolova, *Nitric Oxide Mediated Effects on Chloroplasts, In e-book: Photosynthesis: Structures, Mechanisms, and Applications, Chapter 14*. 2016.
[226] A. Clyde Hill and J. H. Bennett, "Inhibition of apparent photosynthesis by nitrogen oxides," *Atmos. Environ.*, vol. 4, no. 4, pp. 341–348, 1970.
[227] J. Hu *et al.*, "Site-Specific Nitrosoproteomic Identification of Endogenously S-Nitrosylated Proteins in Arabidopsis," *Plant Physiol.*, vol. 167, no. 4, pp. 1731–1746, Apr. 2015.
[228] A. Ördög, B. Wodala, T. Rózsavölgyi, I. Tari, and F. Horváth, "Regulation of guard cell photosynthetic electron transport by nitric oxide," *J. Exp. Bot.*, vol. 64, no. 5, pp. 1357–1366, Mar. 2013.
[229] B. Wodala, A. Ördög, and F. Horváth, "The cost and risk of using sodium nitroprusside as a NO donor in chlorophyll fluorescence experiments," *J. Plant Physiol.*, vol. 167, no. 13, pp. 1109–1111, 2010.
[230] B. Riens and H. W. Heldt, "Decrease of Nitrate Reductase Activity in Spinach Leaves during a Light-Dark Transition ," *Plant Physiol.*, vol. 98, no. 2, pp. 573–577, Feb. 1992.
[231] E. Planchet, K. Jagadis Gupta, M. Sonoda, and W. M. Kaiser, "Nitric oxide emission from tobacco leaves and cell suspensions: rate limiting factors and evidence for the involvement of mitochondrial electron transport," *Plant J.*, vol. 41, no. 5, pp. 732–743, Mar. 2005.
[232] C. A. Neyra and R. H. Hageman, "Dependence of Nitrite Reduction on Electron Transport in Chloroplasts," *Plant Physiol.*, vol. 54, no. 4, pp. 480–483, 1974.
[233] K. J. Gupta, A. U. Igamberdiev, and W. M. Kaiser, "New insights into the mitochondrial nitric oxide production pathways," *Plant Signal. Behav.*, vol. 5, no. 8, pp. 999–1001, Aug. 2010.
[234] M. L. Ko, L. Shi, C. C.-Y. Huang, K. Grushin, S.-Y. Park, and G. Y.-P. Ko, "Circadian phase-dependent effect of nitric oxide on L-type voltage-gated calcium channels in avian cone photoreceptors," *J. Neurochem.*, vol. 127, no. 3, pp. 314–328, Nov. 2013.
[235] E. A. M. F. Aline V Machado-Nils , Larissa O M de Faria, André S Vieira, Simone A Teixeira, Marcelo N Muscará, "Daily cycling of nitric oxide synthase (NOS) in the

hippocampus of pigeons (C. livia).," *J. Circadian Rhythms*, vol. 11, 2013.
[236] S. Jasid, M. Simontacchi, C. G. Bartoli, and S. Puntarulo, "Chloroplasts as a Nitric Oxide Cellular Source. Effect of Reactive Nitrogen Species on Chloroplastic Lipids and Proteins," *Plant Physiol.*, vol. 142, no. 3, pp. 1246–1255, Nov. 2006.
[237] T. Roszer, *The Biology of Subcellular Nitric Oxide*. Springer Netherlands, 2012.
[238] W. L. Araújo, A. R. Fernie, and A. Nunes-Nesi, "Control of stomatal aperture: A renaissance of the old guard," *Plant Signal. Behav.*, vol. 6, no. 9, pp. 1305–1311, Sep. 2011.
[239] A. G. Lai, C. J. Doherty, B. Mueller-Roeber, S. A. Kay, J. H. M. Schippers, and P. P. Dijkwel, "CIRCADIAN CLOCK-ASSOCIATED 1 regulates ROS homeostasis and oxidative stress responses," *Proc. Natl. Acad. Sci. U. S. A.*, vol. 109, no. 42, pp. 17129–17134, Oct. 2012.
[240] J. Zhao, "Interplay Among Nitric Oxide and Reactive Oxygen Species: A Complex Network Determining Cell Survival or Death," *Plant Signal. Behav.*, vol. 2, no. 6, pp. 544–547, Jul. 2007.
[241] M. J. Miller, M. Scalf, T. C. Rytz, S. L. Hubler, L. M. Smith, and R. D. Vierstra, "Quantitative Proteomics Reveals Factors Regulating RNA Biology as Dynamic Targets of Stress-induced SUMOylation in Arabidopsis ," *Mol. Cell. Proteomics*, vol. 12, no. 2, pp. 449–463, Feb. 2013.
[242] G. Perrella and E. Kaiserli, *Light behind the curtain: photoregulation of nuclear architecture and chromatin dynamics in plants*, vol. 212. 2016.
[243] Y. Jiao, O. S. Lau, and X. Wang Deng, *Light-regulated transcriptional networks in higher plants*, vol. 8. 2007.
[244] G. Benvenuto, F. Formiggini, P. Laflamme, M. Malakhov, and C. Bowler, "The Photomorphogenesis Regulator DET1 Binds the Amino-Terminal Tail of Histone H2B in a Nucleosome Context," *Curr. Biol.*, vol. 12, no. 17, pp. 1529–1534, 2002.
[245] Y. L. Chua, A. P. C. Brown, and J. C. Gray, "Targeted Histone Acetylation and Altered Nuclease Accessibility over Short Regions of the Pea Plastocyanin Gene," *Plant Cell*, vol. 13, no. 3, p. 599 LP-612, Mar. 2001.
[246] Y. L. Chua, L. A. Watson, and J. C. Gray, "The Transcriptional Enhancer of the Pea Plastocyanin Gene Associates with the Nuclear Matrix and Regulates Gene Expression through Histone Acetylation," *Plant Cell*, vol. 15, no. 6, pp. 1468–1479, Jun. 2003.
[247] L. Ma *et al.*, "Light Control of Arabidopsis Development Entails Coordinated Regulation of Genome Expression and Cellular Pathways," *Plant Cell*, vol. 13, no. 12, pp. 2589–2608, 2001.
[248] V. H. R. Schmid, "Light-harvesting complexes of vascular plants," *Cell. Mol. Life Sci.*, vol. 65, no. 22, pp. 3619–3639, 2008.
[249] H. Teramoto, A. Nakamori, J. Minagawa, and T. Ono, "Light-Intensity-Dependent Expression of Lhc Gene Family Encoding Light-Harvesting Chlorophyll-a/b Proteins of Photosystem II in Chlamydomonas reinhardtii," *Plant Physiol.*, vol. 130, no. 1, pp. 325–333, Sep. 2002.
[250] W. Thomas, S. Aikaterini, L. Chongyuan, L. Eric, L. Michael, and R. S. A., "The chromatin landscape of the moss Physcomitrella patens and its dynamics during development and drought stress," *Plant J.*, vol. 79, no. 1, pp. 67–81, Apr. 2014.
[251] G. He *et al.*, "Global Epigenetic and Transcriptional Trends among Two Rice Subspecies and Their Reciprocal Hybrids," *Plant Cell*, vol. 22, no. 1, p. 17 LP-33, Jan. 2010.
[252] K. Karmodiya, A. Krebs, M. Oulad-Abdelghani, H. Kimura, and L. Tora, *H3K9 and H3K14 acetylation co-occur at many gene regulatory elements, while H3K14ac marks a subset of inactive inducible promoters in mouse embryonic stem cells*, vol. 13. 2012.

[253] K. A. Lo *et al.*, "Genome-Wide Profiling of H3K56 Acetylation and Transcription Factor Binding Sites in Human Adipocytes," *PLoS One*, vol. 6, no. 6, p. e19778, Jun. 2011.
[254] Y. Nie, H. Liu, and X. Sun, "The Patterns of Histone Modifications in the Vicinity of Transcription Factor Binding Sites in Human Lymphoblastoid Cell Lines," *PLoS One*, vol. 8, no. 3, p. e60002, Mar. 2013.
[255] C. Bertrand *et al.*, "Arabidopsis HAF2 Gene Encoding TATA-binding Protein (TBP)-associated Factor TAF1, Is Required to Integrate Light Signals to Regulate Gene Expression and Growth," *J. Biol. Chem.*, vol. 280, no. 2, pp. 1465–73, 2005.
[256] S. Offermann *et al.*, "Illumination Is Necessary and Sufficient to Induce Histone Acetylation Independent of Transcriptional Activity at the C(4)-Specific Phosphoenolpyruvate Carboxylase Promoter in Maize," *Plant Physiol.*, vol. 141, no. 3, pp. 1078–1088, Jul. 2006.
[257] J. F. Allen, K. Alexciev, and G. Håkansson, "Photosynthesis: Regulation by redox signalling," *Curr. Biol.*, vol. 5, no. 8, pp. 869–872, 1995.
[258] T. Pfannschmidt, K. Schütze, M. Brost, and R. Oelmüller, "A Novel Mechanism of Nuclear Photosynthesis Gene Regulation by Redox Signals from the Chloroplast during Photosystem Stoichiometry Adjustment," *J. Biol. Chem.* , vol. 276, no. 39, pp. 36125–36130, Sep. 2001.
[259] J. O. Berry, P. Yerramsetty, A. M. Zielinski, and C. M. Mure, "Photosynthetic gene expression in higher plants," *Photosynth. Res.*, vol. 117, no. 1, pp. 91–120, 2013.
[260] H.-S. Jung and J. Chory, "Signaling between Chloroplasts and the Nucleus: Can a Systems Biology Approach Bring Clarity to a Complex and Highly Regulated Pathway?," *Plant Physiol.*, vol. 152, no. 2, p. 453, Feb. 2010.
[261] L. Peng, Y. Fukao, M. Fujiwara, T. Takami, and T. Shikanai, "Efficient Operation of NAD(P)H Dehydrogenase Requires Supercomplex Formation with Photosystem I via Minor LHCI in Arabidopsis," *Plant Cell*, vol. 21, no. 11, pp. 3623–3640, Nov. 2009.
[262] H. Yamamoto, L. Peng, Y. Fukao, and T. Shikanai, "An Src Homology 3 Domain-Like Fold Protein Forms a Ferredoxin Binding Site for the Chloroplast NADH Dehydrogenase-Like Complex in Arabidopsis," *Plant Cell*, vol. 23, no. 4, pp. 1480–1493, Apr. 2011.
[263] Y. Yamauchi, A. Hasegawa, M. Mizutani, and Y. Sugimoto, "Chloroplastic NADPH-dependent alkenal/one oxidoreductase contributes to the detoxification of reactive carbonyls produced under oxidative stress," *FEBS Lett.*, vol. 586, no. 8, pp. 1208–1213, 2012.
[264] D. Takagi *et al.*, "Suppression of Chloroplastic Alkenal/One Oxidoreductase Represses the Carbon Catabolic Pathway in Arabidopsis Leaves during Night," *Plant Physiol.*, vol. 170, no. 4, pp. 2024–2039, Apr. 2016.
[265] E. S. J. Arnér and A. Holmgren, "Physiological functions of thioredoxin and thioredoxin reductase," *Eur. J. Biochem.*, vol. 267, no. 20, pp. 6102–6109, Dec. 2001.
[266] L. Meng, J. H. Wong, L. J. Feldman, P. G. Lemaux, and B. B. Buchanan, "A membrane-associated thioredoxin required for plant growth moves from cell to cell, suggestive of a role in intercellular communication," *Proc. Natl. Acad. Sci. U. S. A.*, vol. 107, no. 8, pp. 3900–3905, Feb. 2010.
[267] Y. Okegawa and K. Motohashi, "Chloroplastic thioredoxin m functions as a major regulator of Calvin cycle enzymes during photosynthesis in vivo," *Plant J.*, vol. 84, no. 5, pp. 900–913, Oct. 2015.
[268] A. Courteille *et al.*, "Thioredoxin m4 Controls Photosynthetic Alternative Electron Pathways in Arabidopsis," *Plant Physiol.*, vol. 161, no. 1, pp. 508–520, Jan. 2013.
[269] M. Á. Ruiz-Sola and M. Rodríguez-Concepción, "Carotenoid Biosynthesis in Arabidopsis: A Colorful Pathway," *Arabidopsis Book*, vol. 10, p. e0158, Jan. 2012.

[270] N. Nisar, L. Li, S. Lu, N. C. Khin, and B. J. Pogson, "Carotenoid Metabolism in Plants," *Mol. Plant*, vol. 8, no. 1, pp. 68–82, 2015.
[271] L. Niu and W. Liao, "Hydrogen Peroxide Signaling in Plant Development and Abiotic Responses: Crosstalk with Nitric Oxide and Calcium ," *Frontiers in Plant Science* , vol. 7. p. 230, 2016.
[272] U. Lee, C. Wie, B. O. Fernandez, M. Feelisch, and E. Vierling, "Modulation of Nitrosative Stress by S-Nitrosoglutathione Reductase Is Critical for Thermotolerance and Plant Growth in Arabidopsis," *Plant Cell*, vol. 20, no. 3, pp. 786–802, 2008.
[273] H. Liu and J. H. Naismith, "An efficient one-step site-directed deletion, insertion, single and multiple-site plasmid mutagenesis protocol," *BMC Biotechnol.*, vol. 8, no. 1, pp. 1–10, 2008.
[274] F. X. and C. Copeland, "Nuclear Extraction from Arabidopsis thaliana," *Bio Protoc. 306*, vol. 2 (24), no. http://www.bio-protocol.org/e306, 2012.
[275] S. Arvidsson, M. Kwasniewski, D. M. Riaño-Pachón, and B. Mueller-Roeber, "QuantPrime – a flexible tool for reliable high-throughput primer design for quantitative PCR," *BMC Bioinformatics*, vol. 9, no. 1, p. 465, 2008.
[276] S. Zhao and R. D. Fernald, "Comprehensive Algorithm for Quantitative Real-Time Polymerase Chain Reaction," *J Comput Biol*, vol. 12, no. 8, pp. 1047–1064, 2005.

7 Supplement

A

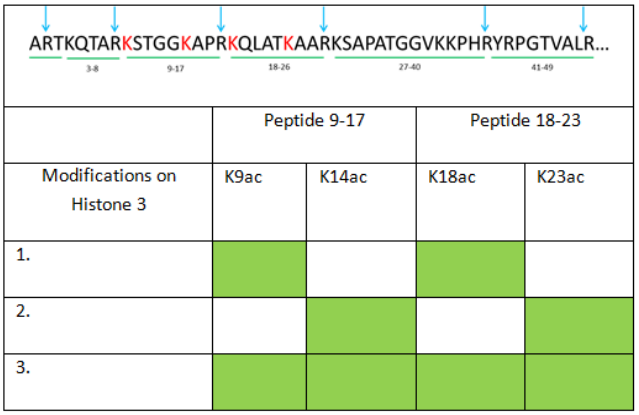

	Peptide 9-17		Peptide 18-23	
Modifications on Histone 3	K9ac	K14ac	K18ac	K23ac
1.				
2.				
3.				

B

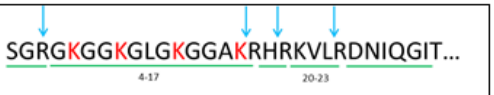

Modifications on Histone 4	K5ac	K8ac	K12ac	K16ac
1.				
2.				
3.				
4.				
5.				
6.				
7.				
8.				
9.				
10.				
11.				
12.				
13.				
14.				
15.				

Supplemental Figure 1: Possible acetylation motifs at H3 and H4.
Acetylation pattern is indicated with a green box. After trypsin digesting there are two peptides at H3 that contain lysines, peptide 9-17 with lysine 9 (K9) and lysine 14 (K14), as well peptide 18-26 with lysine 18 (K18) and lysine 23 (K23). H4 consists of one peptide 4-17 with four lysine residues, lysine 5 (K5), lysine 8 (K8), lysine 12 (K12) and lysine 16 (K16). Each of these lysines might be modified alone or in combinations with other lysines.

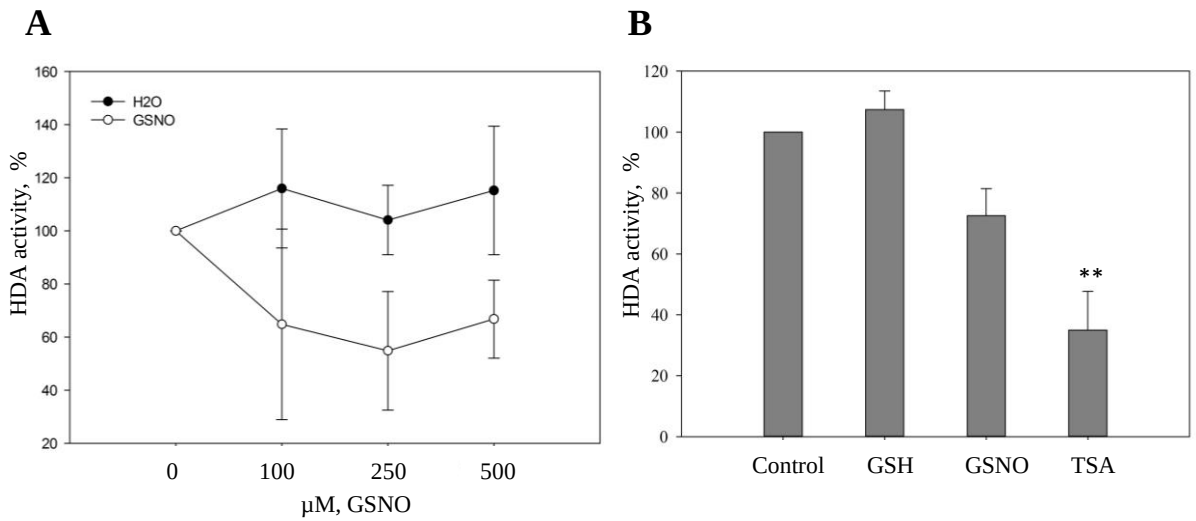

Supplemental Figure 2: 35S:Flag-HDA6 transgenic line.
A) Inhibition of 35S:Flag-HDA6 activity by GSNO. The recombinant plant HDA6 was incubated with 0 – 500 µM GSNO. B) Inhibition of 35S:Flag-HDA6 activity by GSNO and TSA. Recombinant protein was incubated in the presence of 500 µM GSH, 500 µM GSNO, 4 µM TSA and water. HDA activity was measured using Fluorometric HDA Activity Kit. Values are normalized to control treatment as 100%. Shown is a ±SE of three independent experiments. One-way ANOVA (Holm-Sidak Test) is performed, **p≤0.01.

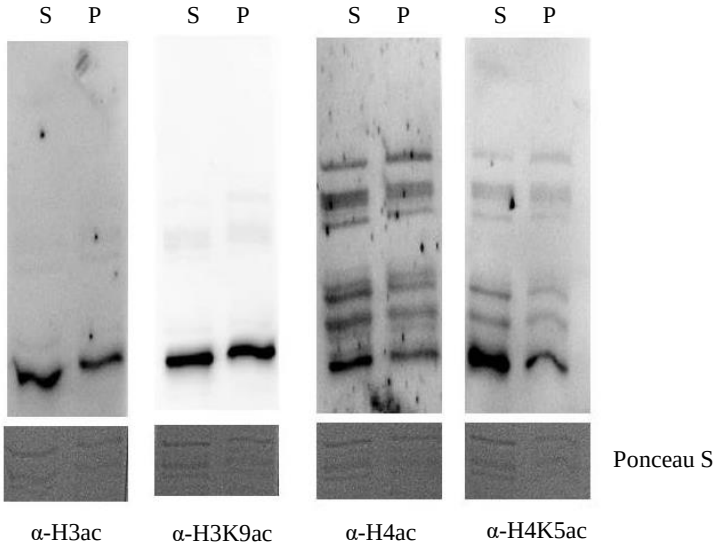

Supplemental Figure 3: Immunoblot analysis of acetylated H3 and H4 in 4 weeks old plants and 7 days old seedlings.
Histone proteins were separated on 12 % polyacrylamide gel followed by Western Blot. Proteins were transferred to nitrocellulose membrane and blocked in 5 % BSA. Antibodies used for analysis: acetylated-H3 (1:20000), acetylated-H3K9 (1:5000), acetylated-H4 (1:20000), and acetylated-H4K5 (1:10000). A second antibody was anti-rabbit HRP (1:2500). The bands detection was performed at Fusion Fx7. P, 4 weeks old plants. S, 7-days old seedlings.

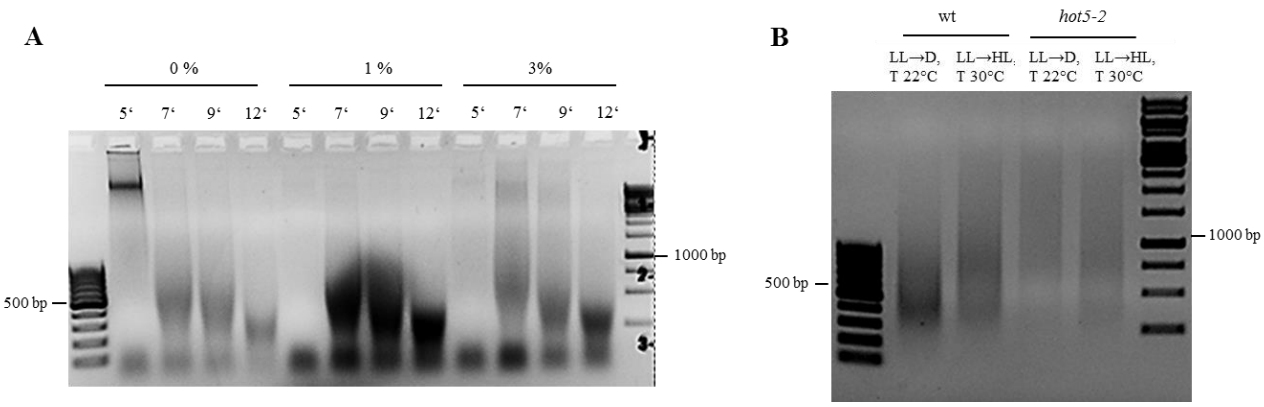

Supplemental Figure 4: Shearing efficiency of leaves chromatin using Bioruptor® Pico .
A) 4 weeks old plants were vacuum infiltrated either with 0 %, 1 % or 3 % formaldehyde. Aliquots of 100 µl chromatin were taken after 5-12 cycles. B) One representative example of shearing efficiency of wt and hot5-2 after exposure for 4 h to dark (D, T 22 °C) or high light (HL, T 30 °C). Aliquots separated on a 1.5% agarose gel followed by staining with ethidium bromide.

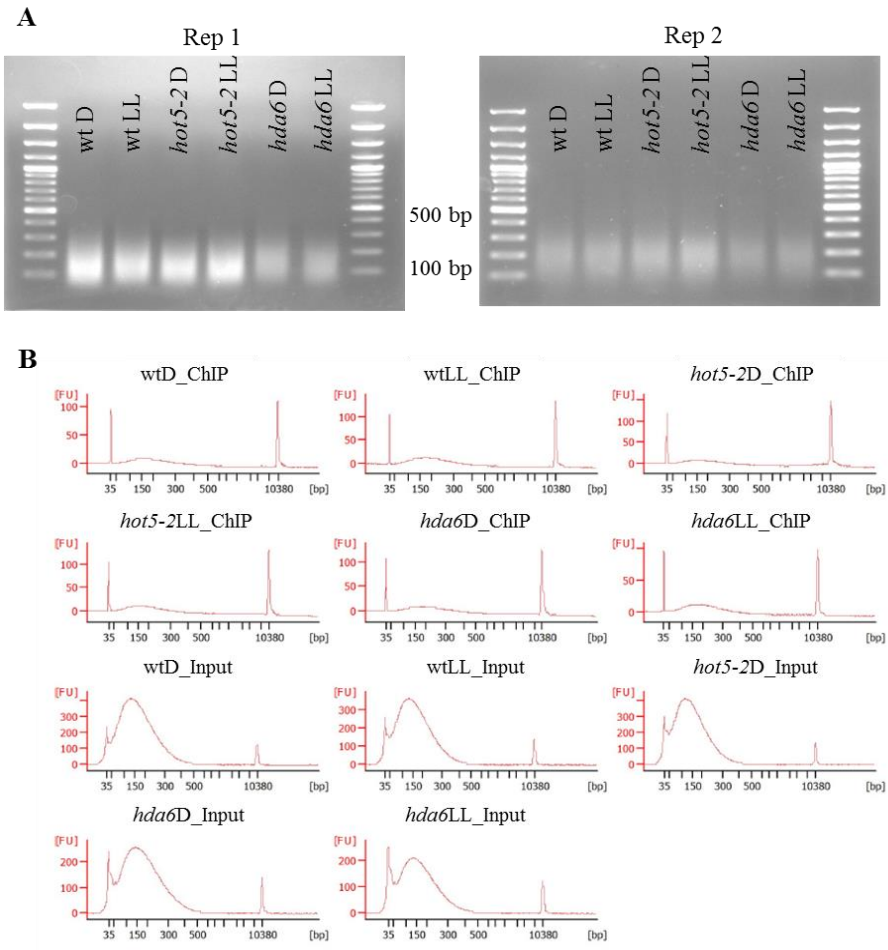

Supplemental Figure 5: Shearing efficiency of leaves chromatin using Covaris E220 evolution.
4 weeks old plants were vacuum infiltrated with 1 % formaldehyde. Nuclei were resuspended in 130 µl of sonication buffer and DNA was sheared using Covaris E220 evolution. A) 20 µl of each aliquot were decrosslinked followed by treatment with Proteinase K and RNase A. DNA was extracted by phenol-chlorophorm followed by ethanol precipitation. Aliquots separated on a 1.5% agarose gel followed by staining with ethidium bromide. B) The size of H3K9ac ChIPed and Input was analyzed by Agilent Sensitivity DNA Kit at Agilent 2100 Bioanalyzer following the manufacturing extractions. Shown is one reprehensive example.

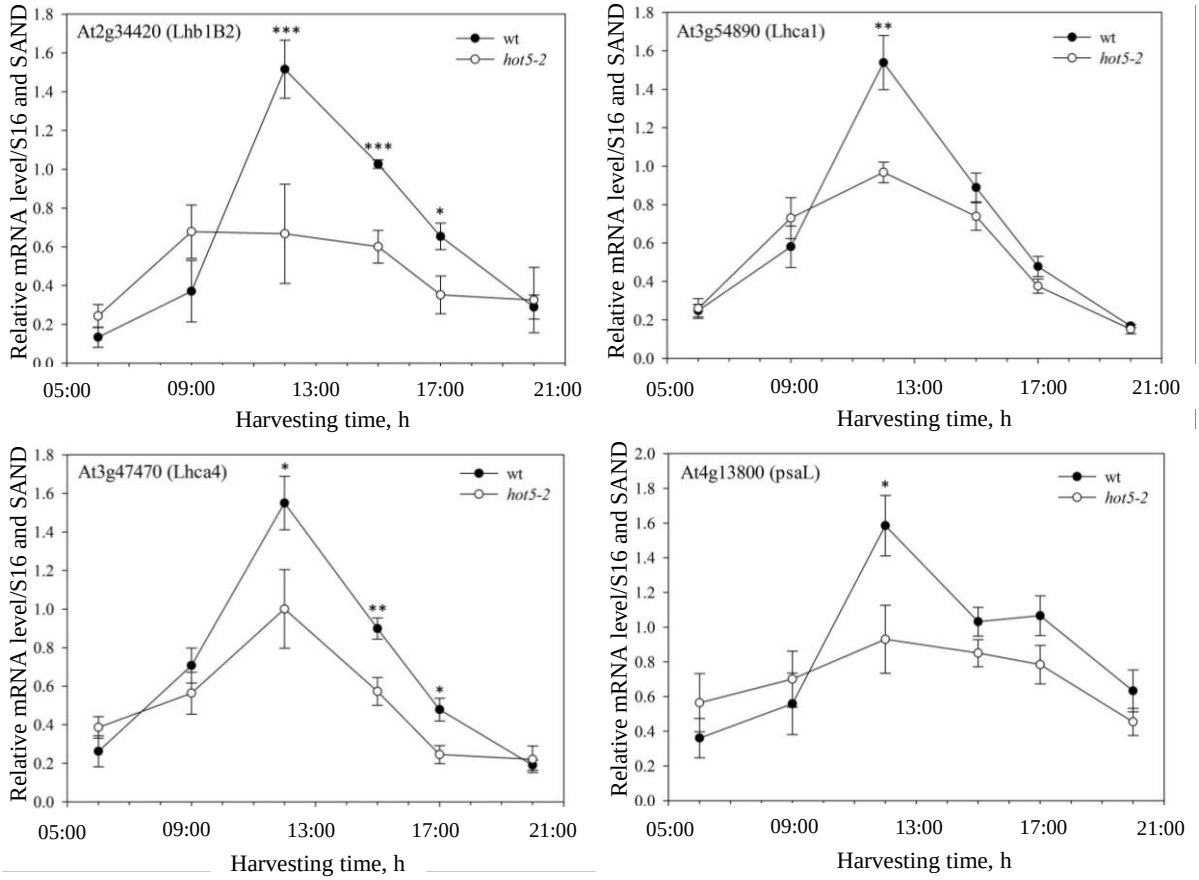

Supplemental Figure 6: Transcriptional level of photosynthesis related genes within a day.
4 weeks *Arabidopsis* plants grown on soil at a short day (10/14 h light/dark, 20/17 °C). Ca. 100 mg of leaves were pooled at 06:00, 09:00, 12:00, 14:00, 17:00 and 20:00 o'clock. Light in a chamber was switched on at 07:00 and switched off at 17:00 o'clock. RNA was extracted with Rneasy Plant Mini Kit. cDNA was synthetized using QuantiTect Reverse Transcription Kit and diluted for analysis 1:15. qPCR was performed on ABI 7500. mRNA level was normalized to S16 and SAND. Shown is a ±SE of at least three independent experiments. Student t-test was performed, *p≤0.05, **p≤0.01 and ***p≤0.001.

Supplemental Figure 7: Phenotype of *hda6* mutant plants (53 days after sowing).
Complementation line was obtained by transferring genomic HDA6 sequence with ca. 2000 bp of endogenous promoter into *hda6* knockout (*axe1*-5) plants. Cysteine mutants were generated by an exchanging of cysteines (C) to alanines (A) in the background of the complementation line.

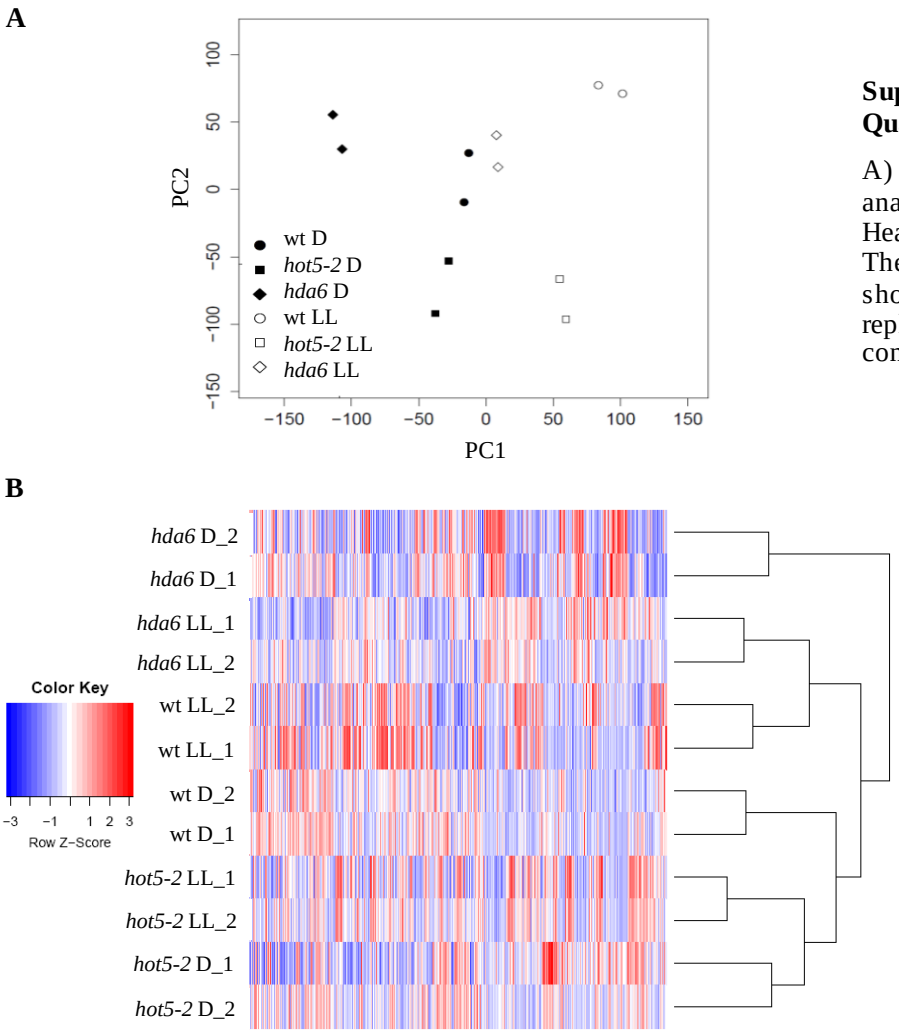

Supplemental Figure 8: Quality of ChIP-seq samples.

A) Principle component analysis of (PCA) plots and B) Heatmap of ChIP-seq samples. The plots and the heatmap show the clusters of all replicates with the same conditions.

Supplemental Table 1: Alignment of ChIP-seq results.

Sample / H3K9ac	Total reads	Aligned reads	% Aligned
# 1	34,199,863	33,850,292	98.98
# 2	32,220,897	32,009,032	99.34
# 3	41,628,968	40,949,279	98.37
# 4	29,472,823	29,255,852	99.26
# 5	37,107,389	35,368,288	95.31
# 6	41,615,811	41,043,716	98.63
# 7	30,642,389	30,149,906	98.39
# 8	38,307,883	37,789,082	98.65
# 9	31,514,260	31,025,656	98.45
# 10	32,189,165	31,922,537	99.17
# 11	40,197,196	39,418,429	98.06
# 12	31,646,176	31,131,291	98.37
# 13	36834625	36,473,528	99.02
# 14	33,323,404	32,984,252	98.98

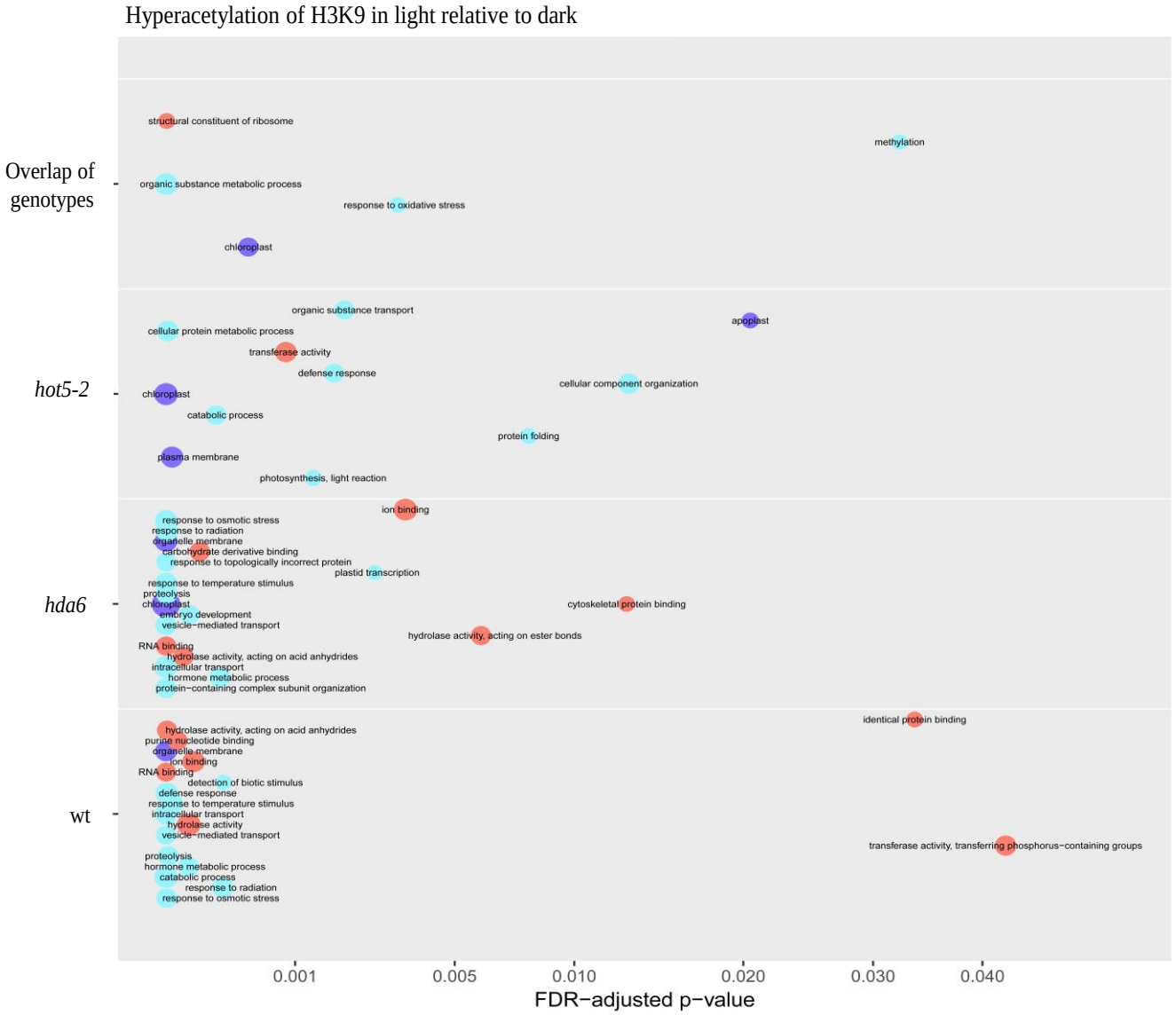

Supplemental Figure 9: GO enrichment analysis of H3K9 hyperacetylated loci depending on the condition effect.

Hyperacetylation was determined by comparison of light to dark conditions within each genotype (*hot5-2*LL vs. *hot5-2*D; *hda6*LL vs. *hda6*D; wtLL vs. wtD). Hyperacetylated are the genes which log2fold change ≥ 0 and FDR ≤ 0.05.

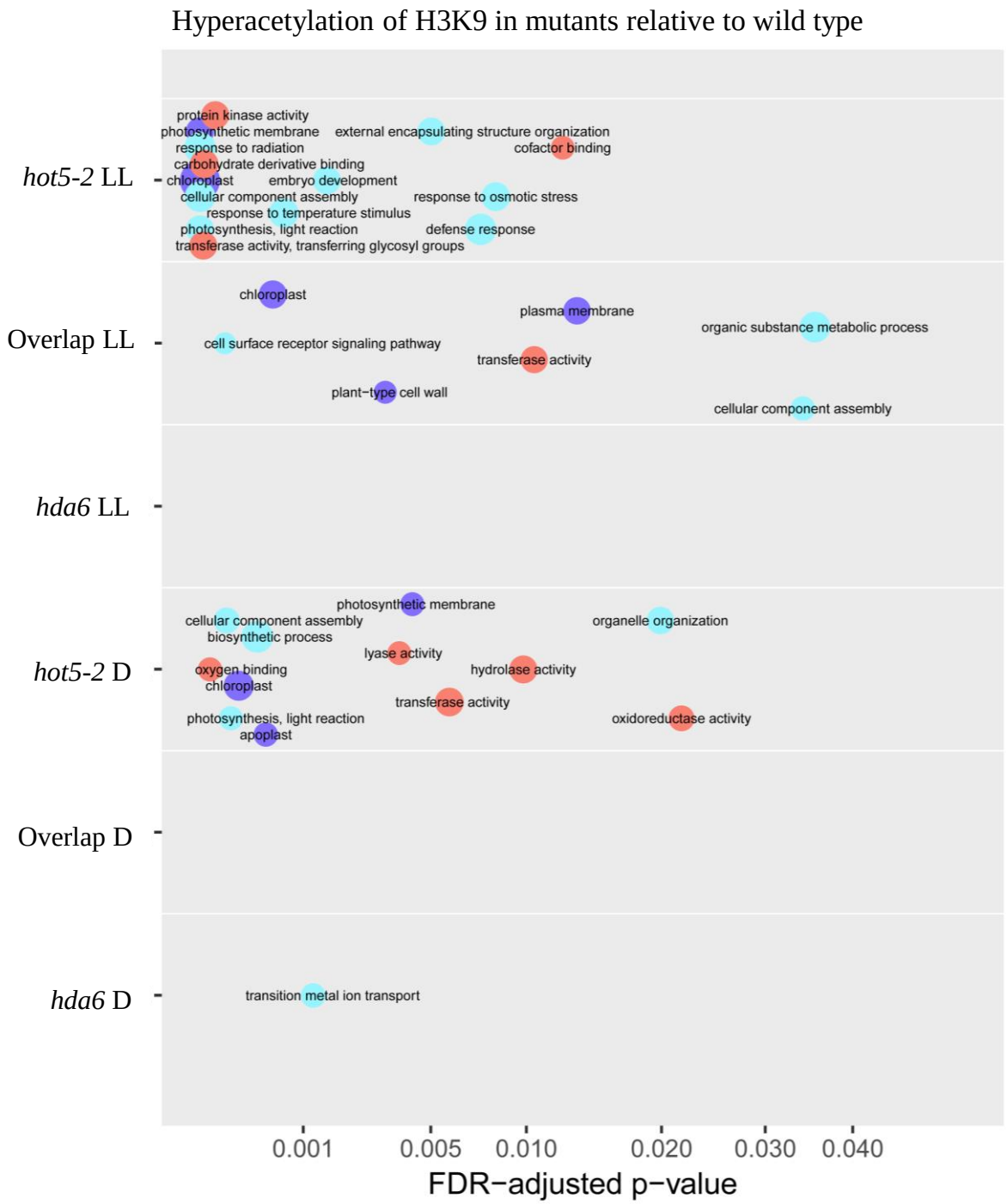

Supplemental Figure 10:GO enrichment analysis of H3K9 hyperacetylated loci depending on the genotyping effect.
Hyperacetylation was determined by comparison of peaks between mutants and wild type under light and dark conditions (*hot5-2*LL vs. wt LL; *hot5-2*D vs. wt D; *hda6*LL vs. wt LL; *hda6*D vs. wt D). Hyperacetylated are the genes which lo2fold change ≥ 0 and FDR ≤ 0.05.

Supplemental Table 2: List of significantly H3K9 hyperacetylated sites associated with chloroplast.

TAIR	Description	Symbol	Appeared H3K9ac in	
			left pathway	right pathway
AT4G08870	Arginase/deacetylase superfamily protein	ARGAH2	*hot5-2*	
AT3G57030	Calcium-dependent phosphotriesterase superfamily protein	n.a.	*hot5-2, hda6*	
AT5G43750	NAD(P)H dehydrogenase 18	PnsB5	*hot5-2*	*hot5-2*
AT2G42710	Ribosomal protein L1p/L10e family	n.a.	*hot5-2*	*hot5-2*
AT3G56710	Sigma factor binding protein 1	SIB1	*hot5-2*	*hot5-2*
AT2G31230	Ethylene-responsive element binding factor 15	ERF15	*hot5-2*	
AT2G31790	UDP-Glycosyltransferase superfamily protein	n.a.	*hot5-2*	hda6
AT5G04140	Glutamate synthase 1	GLU1	*hot5-2*	*hot5-2*
AT1G23740	Oxidoreductase zinc-binding dehydrogenase family protein	AOR	*hot5-2*	
AT5G43400	Plant/protein	n.a.	*hot5-2*	hda6
AT2G05310	Transmembrane protein	n.a.	*hot5-2*	
AT1G78930	Mitochondrial transcription termination factor family protein	n.a.	*hot5-2*	
AT1G62870	Hypothetical protein	n.a.	*hot5-2, hda6*	
AT1G67740	Photosystem II BY	PSBY	*hot5-2*	
AT2G26900	Sodium Bile acid symporter family	BASS2	*hot5-2*	*hot5-2*
AT1G32380	Phosphoribosyl pyrophosphate (PRPP) synthase 2	PRS2	*hot5-2*	*hot5-2*
AT5G44600	S-adenosyl-L-methionine-dependent methyltransferases superfamily protein	n.a.	*hot5-2*	
AT3G15360	Thioredoxin M-type 4	TRX-M4	*hot5-2*	
AT3G05625	Tetratricopeptide repeat (TPR)-like superfamily protein	n.a.	*hot5-2*	
AT3G19480	D-3-phosphoglycerate dehydrogenase	PGDH3	*hot5-2*	hda6
AT4G09650	F-type H+-transporting ATPase subunit delta	ATPD	*hot5-2*	
AT2G29180	Transmembrane protein	n.a.	*hot5-2, hda6*	*hot5-2, hda6*
AT5G38520	Alpha/beta-Hydrolases superfamily protein	n.a.	*hot5-2*	
AT4G04640	ATPase F1 complex gamma subunit protein	ATPC1	*hot5-2*	
AT5G21430	Chaperone DnaJ-domain superfamily protein	NdhU	*hot5-2*	

AT3G27020	YELLOW STRIPE like 6	YSL6	*hot5-2*	
AT1G64150	Uncharacterized protein family (UPF0016)	n.a.	*hot5-2*	
AT1G19150	PSI type II chlorophyll a/b-binding protein (Lhca2*1)	Lhca6	*hot5-2*	
AT5G62720	Integral membrane HPP family protein	n.a.	*hot5-2*	
AT4G27800	Thylakoid-associated phosphatase 38	TAP38	*hot5-2*	
AT5G66530	Galactose mutarotase-like superfamily protein	n.a.	*hot5-2*	
AT4G14970	Fanconi anemia group D2 protein	n.a.	*hot5-2*	
AT3G19180	Plastid division protein	PARC6	*hot5-2*	
AT3G28760	3-dehydroquinate synthase	n.a.	*hot5-2*	
AT5G54270	Light-harvesting chlorophyll B-binding protein 3	Lhcb3	*hot5-2, hda6*	
AT1G57770	FAD/NAD(P)-binding oxidoreductase family protein	n.a.	*hot5-2*	
AT1G64430	Pentatricopeptide repeat (PPR) superfamily protein	n.a.	*hot5-2*	
AT1G66970	SHV3-like 2	SHV3-like 2	*hot5-2*	*hot5-2*
AT5G44520	NagB/RpiA/CoA transferase-like superfamily protein	n.a.	*hot5-2*	
AT2G42210	Mitochondrial import inner membrane translocase subunit Tim17/Tim22/Tim23 family protein	OEP16-3	*hot5-2*	*hot5-2*
AT1G18440	Peptidyl-tRNA hydrolase family protein	n.a.	*hot5-2*	
AT5G18660	NAD(P)-binding Rossmann-fold superfamily protein	PCB2	*hot5-2*	
AT4G00630	K+ efflux antiporter 2	KEA2	*hot5-2*	
AT4G28660	Photosystem II reaction center PSB28 protein	PSB28	*hot5-2*	*hot5-2*
AT4G15110	Cytochrome P450 family 97 subfamily B polypeptide 3	CYP97B3	*hot5-2*	
AT1G77510	PDI-like 1-2	PDIL1-2	*hot5-2*	
AT1G65230	Transmembrane protein putative (DUF2358)	n.a.	*hot5-2*	
AT2G21710	Mitochondrial transcription termination factor family protein	EMB2219	*hot5-2*	
AT4G03200	Catalytics	n.a.	*hot5-2*	
AT2G34630	Geranyl diphosphate synthase 1	GPS1	*hot5-2*	
AT2G04030	Chaperone protein htpG family protein	CR88	*hot5-2*	
AT3G56300	Cysteinyl-tRNA synthetase%2C class Ia family protein	n.a.	*hot5-2*	
AT3G21055	Photosystem II subunit T	PSBTN	*hot5-2*	
AT3G13120	Ribosomal protein S10p/S20e family protein	n.a.	*hot5-2*	

AT1G67950	RNA-binding (RRM/RBD/RNP motifs) family protein	n.a.	*hot5-2*	
AT1G24280	Glucose-6-phosphate dehydrogenase 3	G6PD3	*hot5-2*	
AT3G54050	High cyclic electron flow 1	HCEF1	*hot5-2*	*hot5-2*
AT2G36160	Ribosomal protein S11 family protein	n.a.	*hot5-2*	
AT4G14100	Transferases transferring glycosyl groups	n.a.	*hot5-2*	
AT5G08050	Wiskott-aldrich syndrome family protein putative (DUF1118)	n.a.	*hot5-2*	
AT5G44785	Organellar single-stranded DNA binding protein 3	OSB3	*hot5-2*	
AT2G26500	Cytochrome b6f complex subunit (petM)	n.a.	*hot5-2*	
AT2G30570	Photosystem II reaction center W	PSBW	*hot5-2*	
AT1G07770	Ribosomal protein S15A	RPS15A	*hot5-2*	
AT1G13540	Hypothetical protein (DUF1262)	n.a.	*hda6*	*hda6*
AT1G18310	Glycosyl hydrolase family 81 protein	n.a.	*hda6*	
AT5G07280	Leucine-rich repeat transmembrane protein kinase	EMS1	*hda6*	*hda6*
AT3G28080	Nodulin MtN21 /EamA-like transporter family protein	UMAMIT47		*hot5-2*
AT1G55480	Protein containing PDZ domain a K-box domain and a TPR region	ZKT		*hot5-2*
AT3G51820	UbiA prenyltransferase family protein	G4		*hot5-2*
AT5G56600	Profilin	PRF3		*hot5-2*
AT3G28070	Nodulin MtN21 /EamA-like transporter family protein	UMAMIT46		*hot5-2*
AT3G51420	Strictosidine synthase-like 4	SSL4		*hot5-2*
AT4G22890	PGR5-LIKE A	n.a.		*hot5-2*
AT1G74880	NAD(P)H:plastoquinone dehydrogenase complex subunit O	NdhO		*hot5-2*
AT2G32650	RmlC-like cupins superfamily protein	n.a.		*hot5-2*
AT3G51510	Transmembrane protein	n.a.		*hot5-2*
AT5G62140	ATP-dependent Clp protease ATP-binding subunit	n.a.		*hot5-2*
AT2G15440	Polysaccharide biosynthesis protein (DUF579)	n.a.		*hot5-2*
AT1G23310	Glutamate:glyoxylate aminotransferase	GGT1		*hot5-2*
AT1G11290	Pentatricopeptide repeat (PPR) superfamily protein	CRR22		*hot5-2*
AT1G14345	NAD(P)-linked oxidoreductase superfamily protein	n.a.		*hot5-2*
AT3G25180	Cytochrome P450 family 82 subfamily G polypeptide 1	CYP82G1		*hda6*

AT3G57020	Calcium-dependent phosphotriesterase superfamily protein	n.a.	*hda6*
AT4G18350	Nine-cis-epoxycarotenoid dioxygenase 2	NCED2	*hda6*
AT3G46390	NAC domain protein	n.a.	*hda6*
AT5G20740	Plant invertase/pectin methylesterase inhibitor superfamily protein	n.a.	*hda6*
AT4G17470	Alpha/beta-Hydrolases superfamily protein	n.a.	*hda6*
AT3G42050	Vacuolar ATP synthase subunit H family protein	n.a.	*hda6*
AT4G33010	Glycine decarboxylase P-protein 1	GLDP1	*hda6*
AT2G32290	Beta-amylase 6	BAM6	*hda6*

Shown are only the genes that are more acetylated in the mutants in comparison to wild type under the light condition (left p athway) and genes that are more acetylated in the mutants under the light than under the dark condition (right pathway). Genes are significantly hyperacetylated if FDR ≤ 0.05 and log2FC ≥ 0.

Acknowledgements

First, I would like to thank my supervisor Dr. Christian Lindermayr for his support and many discussions provided during my studies. Under his supervision I learned how to define a scientific problem and find a creative solution to it. His optimistic view and collegial working style helped me to proceed with my research even through difficult times.

Second, I would like to express my sincere gratitude to Prof. Jörg Durner for the opportunity to work at the institute he leads and his continuous support of my PhD study. His guidance helped me in all the time of research and writing of this thesis. I appreciate a lot his contributions of time and the possibility to develop, implement and present my own ideas.

I would like to thank my thesis committee members, Prof. Aurélien Tellier and Prof. Martin Göttlicher, as well as my second examiner Prof. Frank Johannes for their invaluable advice and crucial remarks that formed my final dissertation.

Special thanks go to Dr. Jonatan Darr and Dr. Elisabeth Georgii, who helped me a lot with optimizing the protocol and analyzing the data of ChIP-seq experience.

I would also like to thank Dr. Ghirardo Andrea and Dr. Barbro Winkler for their help with measurements of photosynthetic performance and NO emissions.

Many thanks go to Dr. Albert Andreas whose technical skills enable me to stimulate different climate conditions for many experiments.

I appreciate a lot the contribution of Dr. Ignasi Forne. Thank you for the opportunity to work in your lab and the knowledge and experience to work with LC-MS/MS you provided to me and Eva.

I am also very grateful to all lab members and colleagues. This dissertation would not have been possible without the intellectual contribution of each of you. Thank you for a relaxing working atmosphere, spending lunch time together and support throughout different phases of PhD times.

Very special thanks go to my husband, Guntram. I feel very grateful for your belief in me and your help and support in many questions coming across every day. You are a great example for me how don’t throw up the hands and work towards the goals.

Last but not least, I would like to express my deepest gratitude to my family and friends. Your warm love, continued patience, endless support and advices shaped me as a person and made this thesis come true.